AIAA 2020-2021 Undergraduate Team RFP

Austere Field Light Attack Aircraft

Benjamin Bui, Steven Cantrell, Preston Daniels, Jessica Kong, Branden O'Brien, Sergio Torres, and Mark Wagner
Mechanical and Aerospace Engineering Department
University of Florida, Gainesville, Florida, 32611

UF-7 Sabretooth
EAS4710 Aerospace Design 2

Faculty Advisor: Dr. Ting Dong
Mechanical and Aerospace Engineering Department
University of Florida, Gainesville, Florida, 32611

Date of Submission: April 28, 2021

Table of Contents

Nomenclature

A = *Wing aspect ratio*
A_{wetted} = *Wetted wing area* (ft^2)
A_P = *Footprint area* (ft^2)
A_{side} = *Approximate area of the side of the fuselage* (ft^2)
A_{Top} = *Approximate area of the top of the fuselage* (ft^2)
AR = *Aspect Ratio*
a = *Speed of sound* $\left(\frac{ft}{s}\right)$
b = *Wingspan*
C = *Specific fuel consumption* $\left(\frac{lb}{bhp*hr}\right)$
c = *Mean aerodynamic chord (for stability analysis)*
$C_{avionics}$ = *Avionics cost* (\$)
C_{bhp} = *Propeller specific fuel consumption* $\left(\frac{lb}{bhp*hr}\right)$
C_D = *Development support cost (\$)*
C_{eng} = *Engine production Cost (\$)*
C_F = *Flight Test Cost (\$)*
C_M = *Manufacturing cost (\$)*
$C_{F\beta_v}$ = *Vertical tail airfoil lift slope*
$C_{n\beta}$ = *Yaw moment derivative*
$C_{n\beta v}$ = *Vertical tail yaw moment*
$C_{n\beta w}$ = *Wing yaw moment*
$C_{n\beta_{fus}}$ = *Fuselage yaw moment*
C_L = *Lift coefficient*
C_{L_α} = *Lift slope of the wing per angle of attack*
$C_{L_{\alpha_h}}$ = *Lift slope of horizontal stabilizer per angle of attack*
C_{l_β} = *Rolling moment due to sideslip*
$\left(C_{l_\beta}\right)\Gamma$ = *Rolling moment with respect to sideslip due to wing geometric dihedral*
$C_{l_{\beta_{wf}}}$ = *Rolling moment due to placement of the wing*
$C_{L\beta_w}$ = *Wing rolling moment due to sideslip*
$C_{L_{\beta_v}}$ = *Vertical tail rolling moment due to sideslip*
$C_{l_{\delta a}}$ = *Roll moment derivative due to aileron deflection*
$C_{n_{\delta a}}$ = *Yaw moment derivative due to aileron deflection*
C_M = *Moment coefficient*
$C_{m_{\alpha_{fus}}}$ = *Longitudinal static stability contribution from fuselage*
C_P = *Power coefficient*
C_{Root} = *Root chord*
C_T = *Thrust coefficient*
c_{HT} = *Horizontal tail volume coefficient*
c_{VT} = *Vertical tail volume coefficient*
$C_{T,static}$ = *Static thrust coefficient*
D = *Drag (lbs)*
D_f = *Fuselage depth* (ft)
D_P = *Propeller diameter (ft)*
D_T = *Tire diameter* (in)
E = *Endurance, or loiter time* (hr)
F_{p_α} = *Force produced by propeller with respect to angle of attack* (lbf)
$F_{p\beta}$ = *Force contribution by propeller with respect to* β
FTA = *Number of flight-test aircraft*
g = *Gravitational constant* $(\frac{ft}{s^2})$
h = *Cruising altitude* (ft)
H_E = *Engineering hours (hr)*
H_T = *Tooling hours (hr)*
H_Q = *Quality control hours (hr)*
H_M = *Manufacturing hours (hr)*
i = *Incidence angle*
J = *Advance ratio*
L_{ec} = *Wire routing distance from front of engine to front of cockpit (ft)*
KE_{abs} = *Kinetic energy absorbed by the tire (ft-lb)*
K_{LD} = *Lift to drag constant*
KE_{shock} = *Kinetic energy absorbed by the shock absorber (ft-lb)*
KE_{Vert} = *Kinetic energy absorbed by the tire (ft-lb)*
K_{fus} = *Empirical pitching moment factor*
K_{vsh} = *Hydraulic Constant*
L = *Lift (lbs)*
L_d = *Average total load during deflection* (lbs)
L_f = *Length of the fuselage* (ft)
L_{HT} = *Horizontal tail moment arm*
L_{VT} = *Vertical tail moment arm*
$\frac{L}{D_{max}}$ = *Maximum lift to drag of the aircraft*
M_{max} = *Engine maximum Mach Number*
MAC = *Mean Aerodynamic Chord*
N_{gear} = *Number of landing gear*
N = *Propeller rotation speed* $(\frac{rev}{sec})$
N_c = *Number of crew*

N_{en} = *Number of engines*
N_{eng} = *Total production quantity times number of engines per aircraft*
N_s = *Number of control surfaces*
N_u = *Number of hydraulic utility functions*
P = *Engine power* $\left(\frac{ft-lbf}{s}\right)$
P_t = *Tire pressure* (psi)
Q = *Number to be produced in 5 years*
q = *Dynamic pressure* $\left(\frac{lb_f}{ft^3}\right)$
R = *Range of cruise segment (nautical miles)*
R_e = *Reynold's number*
R_E = *Engineering rate* ($)
R_T = *Tooling rate* ($)
R_Q = *Quality control rate ($)*
R_M = *Manufacturing rate ($)*
R_r = *Rolling radius* (in)
S_{cs} = *Total Surface are of control surfaces* (ft^2)
$S_{exposed}$ = *Exposed surface area of the wings and tail* (ft^2)
$S_{flapped}$ = *Surface area of flaps* (ft^2)
S_{ref} = *Reference area of the wing* (ft^2)
S_{wet} = *Wetted surface area* (ft^2)
S_{HT} = *Area of horizontal tail* (ft^2)
S_h = *Area of horizontal stabilizer* (ft^2)
S_w = *Area of wing* (ft^2)
S_v = *Area of vertical tail* (ft^2)
S'_{vs} = *Area of vertical tail if bottom line is extended to aircraft centerline* (ft^2)
S_{VT} = *Area of vertical tail* (ft^2)
SF = *Scaling Factor*
S_1 = *Area of the strut of each flap strip* (ft^2)
T = *Thrust (lbs)*
T_{max} = *Max thrust* (lbs)
T_{static} = *Static thrust (lbs)*
$T_{turb_{in}}$ = *Turbine inlet temperature* $(°R)$
$\frac{T}{W_{cruise}}$ = *Thrust to weight at cruise ratio*
$\frac{T}{W_o}$ = *Thrust to weight at takeoff ratio*
U = *Cruising velocity* $\left(\frac{ft}{s}\right)$
V = *Volume of the fuselage* (ft^3)
$V_{tip,\ helical}$ = *Helical propeller tip velocity* $\left(\frac{ft}{s}\right)$
$V_{tip,\ static}$ = *Static propeller tip velocity* $\left(\frac{ft}{s}\right)$
W_{crew} = *Weight of the crew (lbs)*
W_{Cruise} = *Weight of aircraft at cruise (lbs)*
W_f = *Maximum width of the fuselage (ft)*
W_i = *Weight of aircraft at each mission profile segment (lbs)*
W_o = *Total weight of aircraft at takeoff*
W_e = *Empty weight* (lbs)
$W_{payload}$ = *Weight of the payload (lbs)*
$W_{Takeoff}$ = *Weight of aircraft at takeoff (lbs)*
$W_{landing}$ = *Weight of aircraft at landing* (lbs)
$\frac{W}{S}$ = *Wing loading* $\left(\frac{lb}{ft^2}\right)$
$\frac{W_e}{W_o}$ = *Empty weight to full weight ratio*
$\frac{W_f}{W_o}$ = *Fuel to full weight of aircraft ratio*
W_w = *Weight on each wheel* (lbs)
w = *Tire width* (in)
Y_1 = *Moment arm from the aircraft centerline to the flaps*
$\bar{X}_{acw}$ = *Aerodynamic center of wing from nose normalized by MAC*
$\bar{X}_{ach}$ = *Aerodynamic center of horizontal stabilizer normalized by MAC*
$\bar{X}_{cg}$ = *Center of gravity of aircraft from nose normalized by MAC*
$\bar{X}_p$ = *Distance of propeller from nose normalized by chord length*
$V_{vertical}$ = *Vertical velocity at landing* $(\frac{ft}{s})$
V = *Maximum velocity* $\left(\frac{ft}{s}\right)$
Z_{wf} = *Vertical height of the wing above the centerline* (ft)
ηp = *Propeller efficiency*
Λ = *Wing sweep (deg)*
Λ_{HL} = *Wing sweep at the hinge line of the airfoil*
$\Lambda_{\frac{c}{4}}$ = *Quarter chord wing-sweep angle (deg)*
λ = *Taper ratio (deg)*
Γ = *Dihedral angle (deg)*
ρ = *Air density* $\left(\frac{slugs}{ft^3}\right)$
μ = *Dynamic viscosity* $\left(\frac{slugs}{ft \times s}\right)$
ψ = *Characteristic length* (ft)
η_h = *Ratio between q at tail and freestream q*
η_S = *Oleopneumatic metered orifice efficiency value*
η_T = *Shock-absorbing efficiency of the tire*
$\frac{\partial \alpha_h}{\partial \alpha}$ = *Downwash due to the wing with respect to angle of attack*

$\frac{\partial \alpha_p}{\partial \alpha}$ = *Downwash from propeller normal force w.r.t. angle of attack*

$\frac{\partial \beta_p}{\partial \beta}$ = *Normal direction of the force exerted by the propeller*

$\frac{\partial \beta_v}{\partial \beta}\eta_v$ = *Normal direction of the force exerted by the vertical tail*

$\frac{\partial C_l}{\partial \delta f}$ = *Rolling moment due to flap deflection*

$\frac{\partial C_L}{\partial \delta f}$ = *Change in lift due to change in flap deflection*

I. Executive Summary

THE 2021 AIAA request for proposal calls for a new light attack aircraft that is ready for both close air support and ferry missions. The designed aircraft must be capable of taking off and landing over a 50-foot obstacle within 4,000 ft or less. Additionally, the aircraft must have built-in countermeasure systems, carry a payload of at least 3000 lbs. of a variety of weapons, have an integrated gun, have a service life of 15,000 hours over 25 years, have a service ceiling of at least 30,000 ft, and have space for two crew, both with ejection seats.

In response to the RFP, this team has developed the UF-7 Sabretooth, a single-engine aircraft which satisfies each AIAA requirement. The Sabretooth has an overall length of 34.1 ft, height of 11.6 ft, and a wingspan of 34.9 ft. It is powered by a Pratt and Whitney PT6A-68D 1,600-horsepower turboprop engine, which, when combined with a four-blade, 9.3-foot propeller, generates 1,398 lbs. of thrust. The empty and gross takeoff weights of the aircraft are 7,873.5 and 13,664.8 lbs., respectively. In its current configuration, the Sabretooth has a payload of 3,067.8 lbs. and is equipped with four, GBU-49 500-lb bombs, four AGM-114 Hellfire missiles, two pods containing seven, 2.75-″ GATR laser-guided rockets each, one NC621 20 mm cannon mounted at the center of the undercarriage, and two HMP-400 0.50-caliber gun pods, one mounted below each wing. Ammunition stores include 180 rounds of 20 mm and 1100 rounds of 0.50-caliber projectiles.

For performance, the Sabretooth exceeds mission requirements. It has a takeoff and landing velocity of 112 mph, cruising velocity of 245 mph, cruising altitude of 25,000 ft, service ceiling of 32,339.9 ft, cruising range of 1,502.2 nautical miles, and endurance of 6.12 hours. At austere fields with 50-ft obstacles at either end and altitude densities between 0 and 6,000 ft above sea level, the UF-7 has takeoff and landing distances of 2,901 and 3,789.8 ft, respectively. It is estimated that the Sabretooth will cost $13.5 million per unit, from initial research and development to first flight and will have an annual maintenance cost of $978,000 assuming 1,200 flight hours per year. Therefore, for an order of 50 aircraft, the UF-7 will cost $676.1 million for flyaway and an additional $54 million annually. Over its intended service life of 25 years, 50 UF-7 Sabretooth aircraft will cost a total of $2 billion.

II. Introduction

THE ever-shifting nature of the modern battlefield deems a new light attack aircraft necessary. According to the AIAA 2021 Aircraft Design RFP, this aircraft must be capable of providing close air support via a 3,000-lb payload and an integrated gun for ground targets. Additionally, the aircraft is required to be deployable from short, austere fields like those near the front lines [1].

The UF-7 Sabretooth has been designed to compete for defense funding from governments operating in hostile environments that require short-notice close air support. Mission requirements dictate that the aircraft must be more survivable than current attack helicopters, be flexible for a multitude of assignments, and be cost-effective in both acquisition and operation. As an aircraft for the United States military, the UF-7 Sabretooth has been designed to be certified for military standard airworthiness (MIL-STD-516C) and consistent with the Joint Service Specification Guides (JSSGs). The UF-7 Sabretooth can operate with two crew members and a payload weight of 3,000 lbs, including ammunition for the integrated gun and armaments mounted under the wings and fuselage.

III. Concept of Operations

The major design requirements as per AIAA Undergraduate Team Aircraft Design RFP 2021 are provided below in Table I [2]. The payload and range were the two main contributing factors for the initial estimations.

Table I: RFP Requirements

Type	Requirement
Takeoff	Over a 50ft obstacle, ≤ 4,000 ft from austere fields at density altitude up to 6,000ft with semi-prepared runaways with California Bearing Ratio of 5
Landing	Over a 50ft obstacle, ≤ 4,000 ft to austere fields at density altitude up to 6,000ft with semi-prepared runaways with California Bearing Ratio of 5
Payload	3,000 lbs of armament
Weapons	Integrated gun for ground targets
Service Life	15,000 hours over 25 years
Service Ceiling	≥ 30,000 ft
Crew	Two members, both with zero-zero ejection seats

Design and ferry mission profiles can be seen in Fig. 1. Flat segments in each profile detail no change in altitude, such as taxi/takeoff, and cruise. Alternatively, sloped segments indicate altitude changes such as climb and descent. The aircraft must also be able to loiter for a certain amount of time, at roughly 4 hours for the design mission indicated by segment 6.

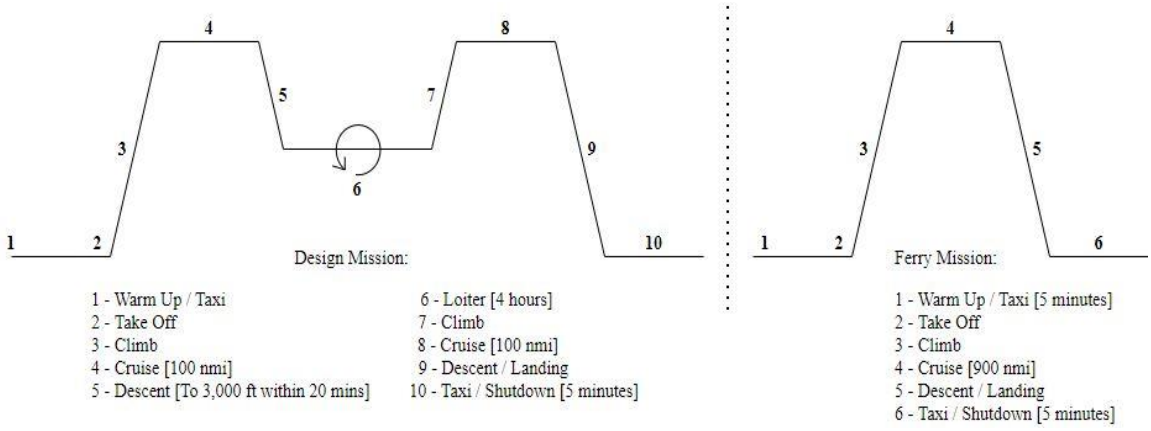

Fig. 1: Design and ferry mission profiles

IV. Initial Estimated Design Parameters

For an initial design basis, a simplified estimation and analysis of the takeoff weight, lift-to-drag ratio, thrust-to-weight, and mid-wing loading was developed and run according to Raymer [2]. This estimation served to provide us with an approximate model of the plane with which to iterate upon to arrive at a more true-to-life design.

Using the above-mentioned requirements and missions, the initial values of the design parameters were estimated. The values used for the sizing and constraint analysis were calculated using the known values of two seed aircraft, the 7075-T6 [4]. These aircraft were light attack aircraft that utilize a single turbopropeller engine. These aircraft were designed to complete missions such as the desired design and ferry missions while operating within similar design constraints.

Takeoff Weight and Lift to Drag Ratio

First, the takeoff weight was estimated from the known payload and crew weights, as well as estimations for the weight of the fuel and weight of the empty aircraft. This aircraft will utilize a two-person crew, with each person weighing approximately 200 lbs. The payload requirement for the design mission is the full 3,000 lbs. while the ferry mission requires 60% of the full payload. The unknown values for the aircraft, the weight of the fuel, and the empty aircraft were estimated using historical data. The weight fraction of the fuel needed for each mission over the total takeoff weight, $\frac{W_f}{W_0}$, and the weight fraction of the empty aircraft over the total takeoff weight, $\frac{W_e}{W_0}$ was used to find the total takeoff weight, such that:

$$W_0 = W_{payload} + W_{crew} + \left(\frac{W_f}{W_0}\right)W_0 + \left(\frac{W_e}{W_0}\right)W_0 \quad (1)$$

From historical data given by Raymer, it can be found that the approximate empty weight fraction for aircraft like the UF-7 Sabretooth will be $\frac{W_e}{W_0} \approx 0.55$ [2]. To compute the fuel weight fraction during the mission, the individual weight fraction for each segment of the mission profiles can be used, such that

$$\frac{W_f}{W_0} = \frac{W_1}{W_0} * \frac{W_2}{W_1} * \ldots * \frac{W_i}{W_{i-1}} \quad (2)$$

The weight fractions of startup/takeoff, climbing, and landing are known from historical data to be 0.970, 0.985, and 0.995, respectively. The weight fractions for the cruising and loitering segments of flight can be estimated using (3) and (4):

$$\text{Cruising: } \frac{W_i}{W_{i-1}} = \exp\left(-\frac{RC}{V(L/D)_{cruise}}\right)) \tag{3}$$

$$\text{Loitering: } \frac{W_i}{W_{i-1}} = \exp\left(-\frac{EC}{(L/D)_{loit}}\right) \tag{4}$$

where R is the range of the cruise segment, C is the specific fuel consumption of the turbopropeller, V is the velocity of the aircraft during the cruise, E is the endurance, or loiter time, of the loitering segment, and L/D is the lift to drag ratio of the aircraft during the segment. For a turbopropeller aircraft, the propeller-specific fuel consumption, C_{bhp}, during cruise is 0.5 $\frac{\text{lb}}{\text{bhp}*\text{hr}}$ and 0.6 $\frac{\text{lb}}{\text{bhp}*\text{hr}}$ during loiter. The specific fuel consumption, C, can be calculated such that

$$C = C_{bhp} \cdot \frac{V}{550\eta_p} \tag{5}$$

where V is the velocity of the aircraft and η_p is the propeller efficiency, which is typically 80%. Austere field light attack aircraft typically fly around 472 $\frac{\text{ft}}{\text{s}}$ during cruise and 130% of the stall speed during loiter, which is around 150 $\frac{\text{ft}}{\text{s}}$ [4].

The maximum cruising lift to drag ratio required various reference values and constants including K_{LD} and the wetted area ratio A_{wetted}. The value for K_{LD} is a constant value of 11 for retractable propeller aircraft [2]. To obtain A_{wetted}, historical data from the Raymer book was utilized [2]. Considering values for A_{wetted} cover a range from 1.0 to 2.3, an average was taken yielding a final value of 1.7. Now that both values were obtained, the value for $\frac{L}{D_m}$ was calculated.

$$\frac{L}{D_{max}} = K_{LD}\sqrt{A_{wetted}} \tag{6}$$

The value for the cruising lift to drag ratio was found to be approximately 14.34. Following this computation, the value for the lift to drag ratio during loiter ($\frac{L}{D_{loit}}$) was obtained. This value is directly based on the calculated value for the maximum lift to drag ratio during the cruising segments. It is accepted that "the most efficient loiter speed for

a propeller aircraft… yields an L/D of 86.6% of the maximum L/D" [2]. Therefore, the lift to drag ratio during loiter was computed (7) and is dependent on the value obtained for the lift to drag ratio during cruise.

$$\frac{L}{D_{loit}} = 0.866 \bullet \frac{L}{D_{\mathrm{m}}} \tag{7}$$

Using this equation, the value for the loitering lift to drag ratio was found to be approximately 12.42. These values were then utilized in computing the mission segment weight fractions provided in (2) and (3), where the maximum lift to drag ratio is utilized in the cruise equation, (2), and the loitering lift to drag ratio is utilized in the loitering equation, (3). Using this information, the fuel weight fraction for the design mission is 0.1883 and 0.1939 for the ferry mission. Using equation (2), this results in estimated total takeoff weights of 12,994 lbs and 8,591 lbs for the design and ferry mission, respectively.

Thrust to Weight Ratio

The thrust to weight ratio during cruise is the inverse of the lift to drag ratio during cruise. Using the previous information, the estimated thrust to weight ratio during cruise, $\frac{T}{W_{cruise}}$ is 0.0697. During takeoff, the thrust to weight ratio is expected to be greater than during cruise. This can be estimated from historical data, which shows that the thrust during cruise is about 45% of the takeoff thrust. Additionally, the weight of the aircraft during cruise was utilized, which was calculated using the previously described weight fractions [2]. Using this information, the thrust to weight of the Sabretooth during takeoff can be calculated by

$$\left(\frac{T}{W}\right)_{takeoff} = \left(\frac{T}{W}\right)_{cruise} \left(\frac{W_{cruise}}{W_{takeoff}}\right) \left(\frac{T_{takeoff}}{T_{cruise}}\right) \tag{8}$$

where $\left(\frac{W_{cruise}}{W_{takeoff}}\right)$ is a weight fraction calculated previously, and $\left(\frac{T_{takeoff}}{T_{cruise}}\right)$ is determined from the historical data as $\frac{1}{0.45}$. This results in a thrust to weight ratio during takeoff, $\frac{T}{W_0}$, of 0.1313.

Wing Loading

The analysis of the wing loading can be done using during cruise and during loitering, as each design mission calls for phases of each scenario. The wing loading during cruise can be calculated by

$$\frac{W}{S} = q\sqrt{\pi * AR * e * C_0} \tag{9}$$

where q is the dynamic pressure, AR is the aspect ratio of the wing, e is the Oswald span efficiency, and C_{D_0} is the estimated zero-lift drag coefficient. The wing loading during loiter can be similarly calculated by

$$\frac{W}{S} = q\sqrt{3\pi * AR * e * C_0} \tag{10}$$

because with a "propeller-powered aircraft, loiter is optimized when the induced drag is three times the parasitic drag" [2]. The dynamic pressures were calculated for altitudes between 0 and 30,000 ft in 5,000-foot increments. The dynamic pressure for the operating altitudes were found using (11):

$$q = \frac{\rho u^2}{2} \tag{11}$$

where q is the dynamic pressure, ρ is the density, and u is the speed of the aircraft. With density values based on the altitude, dynamic pressure for each altitude was found from standard atmosphere conditions [6]. For cruise, the altitude will be considered 25,000ft, while the altitude for loitering is 10,000ft.

Once the dynamic pressure was found, the aspect ratio, Oswald span efficiency, zero-lift drag coefficient, was determined using historical data and given in Table II [2]. The aspect ratio was taken as the average of the AT-6 Wolverine and the historical data for general aviation aircraft [2][3]. A clean propeller-powered aircraft, like the Sabretooth, typically has a zero-lift drag coefficient of 0.02 [2].

With these values, (9) and (10), and assuming the cruising and loiter altitudes were 25,000 and 10,000 ft respectively, the wing loading, W/S, during cruise and loiter were found to be 70.16 lb/ft^2 for cruise and 34.17 lb/ft^2 for loiter. A summary of all the initial estimations for the aircraft performance is included in Table III.

Table II: Aspect Ratio, Oswald Span Efficiency, and Zero-Lift Drag Coefficient

Parameter	Value
Aspect Ratio, AR	6.945
Oswald span efficiency, e	0.8
Zero-lift drag coefficient, C_0	0.02

Table III: Initial Estimations

Initial Estimations	Design Mission	Ferry Mission
Takeoff Weight (W_o)	12,994 lbs	8,591 lbs
$\frac{L}{D_{\mathrm{m}}}$	14.34	
$\frac{T}{W_{cruise}}$	0.0697	
$\frac{T}{W_o}$	0.1313	
Wing Loading (Cruise) $\frac{W}{S}_{cruise}$	70.16 $\frac{lb}{ft^2}$	
Wing Loading (Loiter) $\frac{W}{S}_{loiter}$	34.17 $\frac{lb}{ft^2}$	

V. Airfoil Design

Airfoil Lift Coefficient

To determine the desired airfoil lift coefficient, C_l, parameters and assumptions from the initial estimations were used. These estimations include 472 $\frac{ft}{s}$ for cruising speed and 195 $\frac{ft}{s}$ for loitering speed. The values for $\frac{W}{S}$ were found to be 70.16 $\frac{lb}{ft^2}$ for cruise and 34.17 $\frac{lb}{ft^2}$ for loiter from previous calculations. With the wing loading and dynamic pressure known, the values for the airfoil lift coefficients at cruise and loiter were found using (12).

$$C_l = \frac{1}{q} * \left(\frac{W}{S}\right) \tag{12}$$

At cruise, the airfoil lift coefficient was found to be 0.5908; similarly, at loiter, the airfoil lift coefficient was found to be 1.0234. At takeoff and landing, the aircraft is assumed to be at sea-level, using the landing speed of 195 $\frac{ft}{s}$, the coefficient of lift is 0.756.

Reynolds Number

Throughout the airfoil selection process, it was critical to determine the expected Reynolds number the aircraft will experience during cruise. This calculation was dependent on various properties surrounding the cruise conditions. These properties include air density at the cruise altitude ρ, the cruising velocity U, the characteristic length ψ (in this case, the aircraft wingspan b), and the dynamic viscosity at the cruising altitude μ, as noted in Table IV. Using these properties and their corresponding values, the Reynolds number was determined for the UF-7 Sabretooth under cruise conditions using (13). The values for air density, and dynamic viscosity were obtained based on their corresponding values at the aircraft's cruising altitude (25,000 ft or 7,620 m) [7]. Using each of the required values yields a Reynolds number of approximately 5.59 x 10^6. This value is reasonable due to the approximated cruising speed of the aircraft being 143.9 $\frac{m}{s}$.

Table IV: Aircraft Cruise Properties

Property	Value	Unit
Cruising altitude, h	25,000	ft
Air density, ρ	10.66 x10^{-4}	$\frac{slugs}{ft^3}$
Cruising velocity, U	472	$\frac{ft}{s}$
Characteristic length, ψ	33.01	ft
Dynamic viscosity, μ	3.217 x 10^{-7}	$\frac{slug}{ft\ s}$

$$\mathrm{Re} = \frac{\rho U \psi}{\mu} \tag{13}$$

Mach Number

Equation (14) was used to determine the Mach number at the cruise altitude.

$$M = \frac{U}{a} \tag{14}$$

where, a, is the speed of sound at the cruise altitude, 25,000 ft, and U is the airspeed velocity at the cruise altitude, 472 m/s. The Mach Number calculated using these estimations gives a Mach Number of 0.42. This value for Mach Number is essential in the determination of the airfoil shape and size.

Airfoil Geometry

Using the above calculations for airfoil characteristics, the geometry for the preferred airfoil was narrowed down. With emphasis on the airfoils being compared being able to reach the calculated airfoil lift coefficient, a trade study with the airfoils in Table V was conducted.

Table V: Airfoil Trade Study

Parameters	**Weight**	AH94-145	**Score**	NACA 63A415	**Score**	**WORTMANN FX 049-915**	**Score**	**EPPLER 715**	**Score**	**FX** 67-K-150/17	**Score**
$C_{l_{max}}$	25%	1.50	10.0	1.50	10.0	1.50	10.0	1.45	9.7	1.18	7.9
α_{max}	20%	7.00	4.4	15.00	9.4	10.00	6.3	16.00	10.0	12.60	8.4
C_l at $\alpha = 0°$	20%	0.75	10.0	0.40	5.3	0.48	6.4	0.25	3.3	0.51	6.8
C_D at $\alpha = 5°$	5%	0.008	10.0	0.009	8.9	0.009	8.9	0.009	8.9	0.008	10.0
C_D at $\alpha = 10°$	5%	0.022	4.5	0.019	5.3	0.010	10.0	0.015	6.7	0.035	2.9
C_D at $\alpha = 15°$	5%	0.062	7.3	0.045	10.0	0.080	5.6	0.050	9.0	0.054	8.3
Max Camber	10%	5.6%	3.9	2.2%	10.0	5.8%	3.8	5.3%	4.2	4.8%	4.6
Max Thickness	10%	14.6%	10	15.0%	9.7	14.7%	9.9	14.9%	9.8	15.0%	9.7
Total:	**100%**		**78.6**		**86.2**		**76.3**		**77.1**		**75.0**

From analysis, a NACA 63A415 airfoil was selected as the best option as shown in Fig. 2. This geometry most closely matches the lift required at operating speeds and altitudes while minimizing drag. The graphs in Fig. 3 display several parameters of this airfoil's performance and show that it is very useful for use in the aircraft.

To determine the ideal airfoil for the UF-7 Sabretooth, a trade study was performed with the results compiled in Table V. The coefficients of lift at both maximum and zero-degree angle of attack, coefficients of drag at various angles of attack, max angle of attack prior to stall, max camber, and max thickness were compared. Throughout the analysis, these parameters were assigned a "weight" based on relative importance in order to compute each airfoil's "score" in the trade study. Based on the airfoils that were analyzed, the NACA 63A415 obtained the greatest score with the AH94-145 being a close second. Although each of the airfoils that were analyzed would have proven sufficient for the UF-7 Sabretooth, the NACA 63A415 was ultimately utilized for the aircraft design.

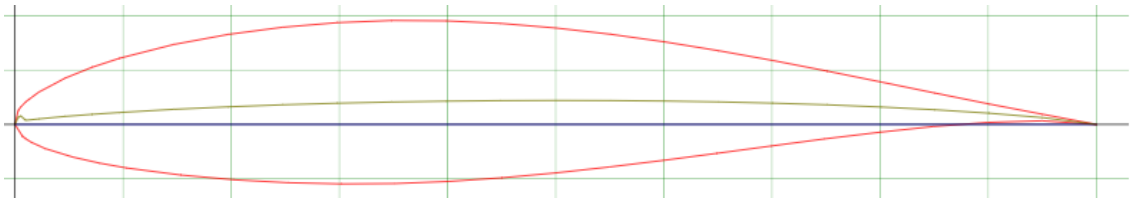

Fig. 2: Plot of the NACA 63A415 Cross Section [6]

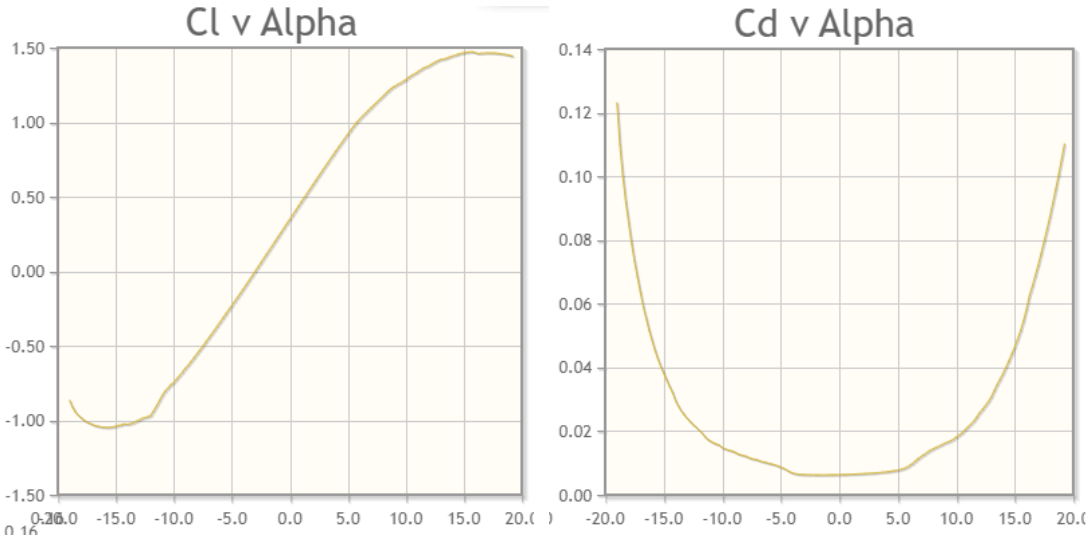

Fig. 3: Airfoil performance graphs for NACA 63A415 airfoil [6]

VI. Wing Design

Wing Sweep

To determine the wing sweep, Λ, for the design, it was first necessary to determine if it should be determined by leading edge sweep or the quarter-chord sweep. The Mach number during cruise of the Sabretooth indicates that the aircraft will always fly at a subsonic speed. Due to this, the wing sweep was identified as leading-edge sweep only. With a cruising Mach number of 0.42, the appropriate leading-edge wing sweep, Λ_{LE}, is 3 degrees according to historical trends. The quarter-chord sweep for the Sabretooth will be zero, since using no sweep will reduce the weight of the wing while providing increased stability at a high angle of attack. Since the Sabretooth will only be slightly in the transonic region, there is no need to include a sweep angle in order to reduce the velocity to reduce the chordwise air velocity to be lower than the critical Mach number, since it will already be well under the airfoil's critical Mach number.

Taper Ratio

Most wings have a taper ratio between 0.2-0.3, excluding planes that have a low wing sweep which have a taper ratio of about 0.4-0.5. The taper ratio of a wing affects the lift distribution along the span. To aid in achieving the ideal elliptical wing lift distribution, the taper ratio of a wing should be chosen based off the quarter-chord sweep angle. Historical data was used to find the corresponding taper ratio to the Sabretooth's quarter-chord sweep angle [2]. The line used is the one that accounts for twisted wings. The desired taper ratio on the Sabretooth was determined to be 0.55 for a leading-edge wing sweep of 2 degrees.

Wing Geometry

Using the weight estimation and wing loading estimation determined above for the aircraft during cruise, the design wing area, S, was determined to be 156.91 ft^2. Using the aspect ratio, AR, determined in the initial estimation, 6.9450, the span of the wing can be determined using (15).

$$b = \sqrt{AR * S} \tag{15}$$

The value calculated for the span, b, was found to be 33.01 ft.

The taper ratio, λ, of 0.55 was used to determine the chord length for the root and the tip of the wing. Equations (12) and (13) from Raymer [2] were used to determine these values:

$$C_{ROOT} = \frac{2S}{b(1+\lambda)} \quad (16)$$

$$C_{TIP} = \lambda C_{ROOT} \quad (17)$$

Using these equations and the values for wing area, span and the taper ratio, the chord at the root, C_{ROOT}, was calculated as 6.13 ft and the chord at the tip, C_{TIP}, as 3.37 ft.

Wing Twist

Wing twist is implemented in aircraft to improve stall performance by forcing the outboard section of the wing to retain lift. On a typical aircraft, one can see anywhere from 0 to -5 degrees of twist. An angle of -3 degrees was suggested by Raymer [2] for providing, "adequate stall characteristics" and is the angle of twist implemented on the Sabretooth. An incidence angle of 0 degrees was chosen to match historical data of previous light attack, military, aircraft. The wing of the Sabretooth will use a geometric twist of -3 degrees, as Raymer suggests.

Wing Tips

Wing tips are utilized to minimize drag losses and the presence of wing tip vortices. When designing the wing for the light-attack-aircraft, various wingtips were taken into consideration. A tip design with sufficient aerodynamic characteristics and lowest production cost were some of the most desirable characteristics during the selection process. Ultimately, cut-off wing tips were selected for the UF-7 Sabretooth.

Throughout the design process, a cost-efficient wingtip was one of the most important characteristics. This greatly narrowed down the selection process effectively between rounded and cut-off wingtips, where every other design (Hoerner, drooped, cut-off forward swept, etc.) would be more expensive and less efficient for mass production. Rounded wing tips are an inefficient design, making it easier for air to flow from the lower surface of the wing to the upper surface. On the other hand, "a simple cutoff tip offers less drag than a rounded-off tip, due to the sharp edges where the upper and lower surfaces end" [2] The UF-7 Sabretooth is intended to cruise at Mach 0.42 where effects from wing tip vortices should not be very strong. The use of cut-off wing tips improves the aerodynamic characteristics of the wing while minimizing the total weight of the aircraft through a lack of end plates and winglets.

Wing Vertical Location

For this aircraft, it is superior to use low mounted wings. A low wing position allows the landing gear to be more conveniently stored within the wings of the aircraft while still maintaining sufficient clearance for the aircraft's payload. During cruise, the landing gear will be stored within the wing structure of the aircraft, reducing drag. The landing gear will also be directly mounted to the wing box, improving the strength of the landing gear mechanism. The increased strength of the landing gear system is beneficial for landing on semi-prepared runways, such as those intended for the UF-7 Sabretooth. The low mounted wings will require the use of a dihedral to make the aircraft more stable in flight, as well as increasing the clearance between the wing tip and the ground, reducing the risk of it striking the ground during landing. Additionally, the low mounted wings will make it easier for crews to load payload onto aircraft and make deployment of the Sabretooth faster.

Wing Dihedral

Wing dihedral was chosen to aid in lateral stability and flight dynamics. Since the aircraft was chosen to have a low wing, historical data from Raymer in Table 4.2 suggests that a subsonic, swept, wing should have between 3 to 7 degrees of dihedral angle [2]. A middle ground of 5 degrees was chosen for the dihedral of the Sabretooth.

Wing Aerodynamic Characteristics

The wing was modeled in the aerodynamic analysis software XFLR5. The wing geometry, dihedral, and twist were included, along with the NACA 63A415 airfoil shape, which was obtained from Airfoil Tools [6]. The wing was analyzed at cruise speeds at 25,000 ft, at loiter speeds at 10,000 ft, and at takeoff and landing speeds at sea level. Cruise speed is taken to be 472 $\frac{\text{ft}}{\text{s}}$, while the loitering, takeoff, and landing speed is 130% of the stall speed, or 195 $\frac{\text{ft}}{\text{s}}$. Using these values, the plots displayed in Fig. 4 was created. The figure uses the blue line to show to conditions at cruise, the orange line to show conditions at loitering, and the green line to show conditions at takeoff and landing. From this analysis, we find that the coefficient of lift at $\alpha = 0°$ is 0.175. This is less than the maximum coefficient of lift needed, which occurs at loitering, so a high-lift device will be needed.

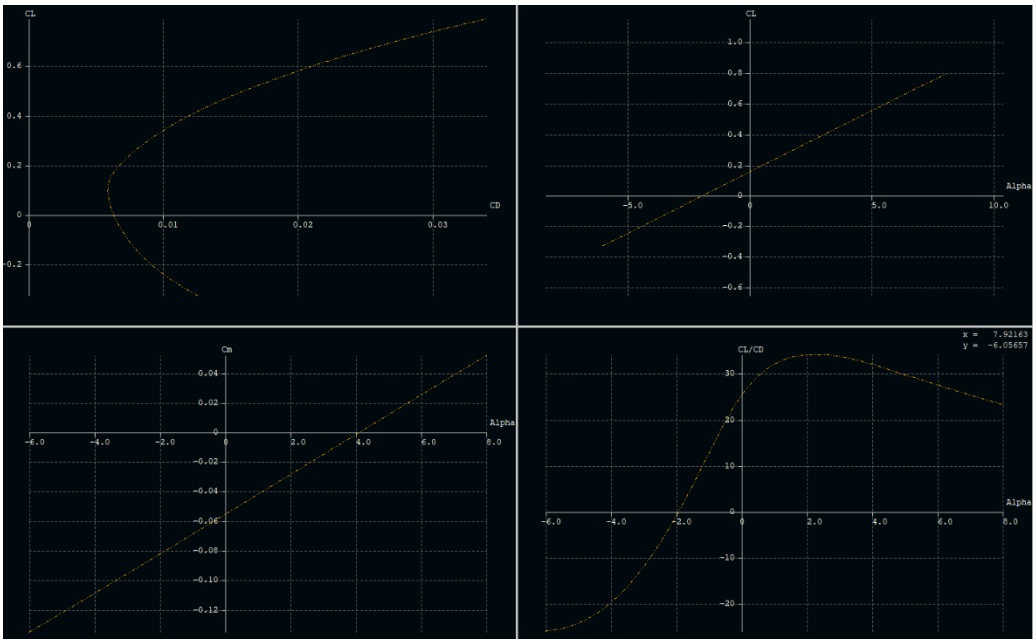

Fig. 4: XFLR5 Plots of Coefficient of Lift Vs. Drag and Angle of Attack, Coefficient of Moment Vs. Angle of Attack, and Coefficient of Lift over Drag Vs. Angle of Attack

High-Lift Devices

To determine if high-lift devices are required, the coefficient of lift for the cruise can be compared to the coefficient of lift for landing and for loitering, where more lift is desired. As noted previously, the estimated coefficient of lift for this aircraft during cruise is 0.6, while calculations show that the desired maximum coefficient of lift is 1.02 at loiter and 0.756 at takeoff and landing. To give some room for flexibility, it is preferable to use a factor of safety to determine what high-lift device to use. Using historical data from Raymer, with a quarter chord sweep angle of 0 degrees, the inclusion of a plain flap is ideal for this wing. The plain flap is able increase the camber of the airfoil by actuating the trailing edge when flaps are deployed, increasing the lift, and lowering the stall speed of the aircraft [2]. Using the XFLR5 analysis, it was determined that the wing with the NACA 63A415 is not able to reach the necessary coefficient for loitering. The plain flap will allow the Sabretooth to increase its coefficient of lift to as desired while reducing the necessary angle of attack. The plain flap will also be easier to implement than more complicated mechanisms like slotted flaps, helping reduce the overall cost of the aircraft. To determine the area of the flapped wing, (18) was used [2].

$$\Delta C_{L,max} = 0.9\Delta C_{l,max}\left(\frac{S_{flapped}}{Sref}\right)cos\Lambda_{H.L.} \quad (18)$$

Using 0.47 as $\Delta C_{L,max}$ which is the difference between the maximum desired coefficient of lift and the coefficient of lift that the airfoil produces at zero angle of attack at 10,000 ft, 0.9 as $\Delta C_{l,max}$, 156.91 ft^2 as S_{ref}, and 6.555 degrees as $\Lambda_{H.L.}$, (18) is manipulated to find the flapped area of the wing. It was found that, per wing, the flapped area was 45.82 ft^2. Using an estimate of 30% of the airfoil's chord length as the chord length of the flap, or 21.96 ″, the length required for the flap along the trailing edge of the wing was 104.65 ″. Multiplying these together leads to a total flap area of 2,298.11 in^2, or 15.96 ft^2 for each wing, or 31.92 ft^2 of flap for the total aircraft. A summary of all the values determined for the wing design are listed in Table VI.

Table VI: Values for Wing Design Calculations

Quantity	Value	Unit
AR	6.945	-
S	156.9	ft^2
b	33.0 ft	ft
C_L at $\alpha = 0°$	0.175	-
Λ_{LE}	3°	$degrees$
$\Lambda_{1/4c}$	0°	$degrees$
λ	0.55	-
C_{ROOT}	6.13 ft	ft
C_{TIP}	3.37 ft	ft
Γ	5°	$degrees$
Twist	-3°	$degrees$
i	0°	$degrees$

Wing CAD Model Rendering

To supplement the visualization of the design as well as confirm that the chosen design parameters resulted in a feasible wing shape, a CAD model was generated using SolidWorks. The basic wing was modeled without any control surfaces to simplify the initial render and begin doing additional calculations on it.

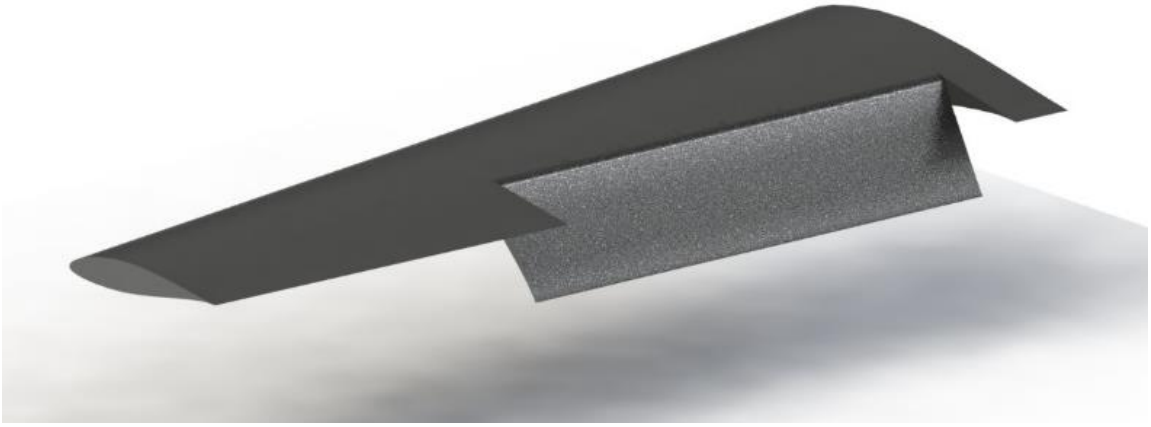

Fig. 5: Rendered model of designed wing isometric view. Flap Included

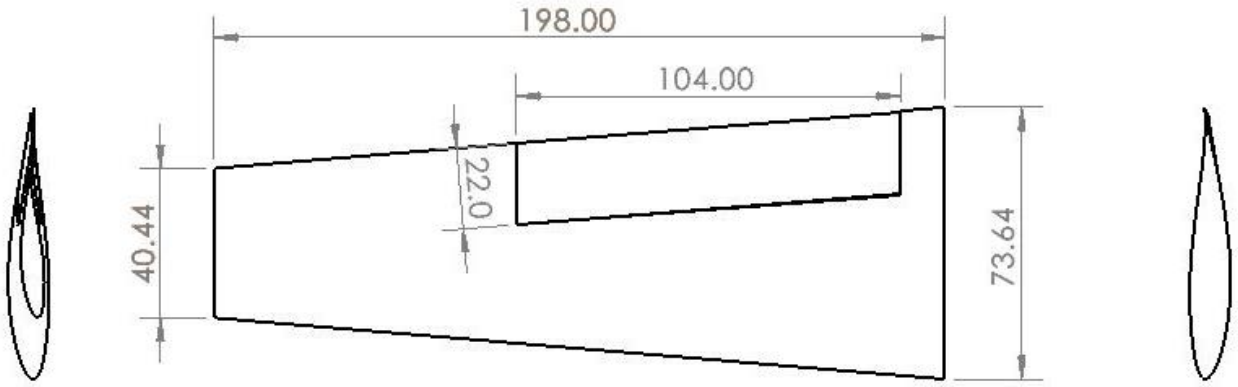

Fig. 6: Dimensioned drawing of model of designed wing. Top and side views. Units in inches.

VIII. Propulsion

Engine Selection

The UF-7 Sabretooth was loosely based on the AT-6 Wolverine and the Embraer EMB-314 Super Tucano. Each uses a variation of the Pratt and Whitney PT6A engine. The shaft horsepower for the PT6A-68, the engine used in the Super Tucano, is 1250 SHP whereas the PT6A-68D, the engine used in the Wolverine, produces 1600 SHP. Other engines were also investigated in a trade study for consideration in the UF-7 Sabretooth, including the General Electric Catalyst engine and the Pratt & Whitney PW118. These engines are newer than the PT6A-68D, potentially providing advantages over the PT6A derived engines.

Since shaft horsepower is the highest priority design parameter for engine selection, a scale factor was applied to the engines being analyzed in the trade study. This scale factor ensured all engines were evaluated for a design having the required 1500 SHP. The engines length, diameter, and weight were scaled using the following equations [2]. In this case, *L*, *D*, *W*, and *SF* are the length, diameter, weight, and scale factor, respectively.

$$L = L_{actual}(SF)^{0.4} \quad (19)$$

$$D = D_{actual}(SF)^{0.5} \quad (20)$$

$$W = W_{actual}(SF)^{1.1} \quad (21)$$

Each engine was set to an individual scale factor based on the difference in SHP. Other than SHP, the most significant factors for the Sabretooth were cost, fuel consumption, and technology readiness level. The other engine parameters were multiplied by this scale factor. Table VII details each engine's respective specifications alongside the weighing system used for the parameters.

In this table, the cells highlighted in green were the best values of the three engines investigated. The PT6A-68D, highlighted in blue, was the best overall pick and was selected as the engine for the UF-7 Sabretooth. The scaling factors for the PT6-68A, Catalyst and PW118 to produce the desired shaft horsepower are 0.9375, 1.2097, 0.8333, respectively. This engine has a relatively affordable cost while also meeting power requirements without modification, considering losses and a safety factor. This engine has also been in service, with numerous variants, since 1960 and has been tried and tested over many years.

Table VII: Engine Trade Study

Engine	Weight	PT6A-68D			GE Catalyst			PW118		
SHP (Original SHP)	0%	1500 (1600)	10.0	0.0	1500 (1240)	10.0	0.0	1500 (1800)	10.0	0.0
Cost	20%	$ 801,563	10.0	2.0	$967,760	8.3	1.7	$1,083,290	7.4	1.5
Weight (***lbs***)	30%	253.36	10.0	3.0	739.75	3.4	1.0	319.13	7.9	2.4
Diameter (***in***)	10%	18.4	10.0	1.0	20.9	8.8	0.9	24.65	7.5	0.7
Length (***in***)	10%	60.42	10.0	1.0	66.91	9.0	0.9	78.09	7.7	0.8
Specific fuel consumption ($\frac{lb}{hp \cdot hr}$)	20%	0.628125	6.5	1.3	0.648399	6.3	1.3	0.408317	10.0	2.0
TRL	10%	9	10.0	1.0	7	7.8	0.8	9	10.0	1.0
Total:	**100%**			**9.3**			**6.5**			**8.4**
*Note: Price and specific fuel consumption for GE Catalyst derived from estimates [3, 8, and 9].										
*Note: All engine values scaled around the required SHP of 1500.										

Propeller Design

With the engine selected, the diameter for the propeller was determined. Based on historical data, it was found that using either four or five blades was optimal for transferring the most power to the propeller for the selected engine [3][4]. Since there is no numerical difference between four and five blades for blade diameter, four blades were assumed, which yields a K_p value of 1.5 [2]. The power provided by the PT6A-68D engine is 1600 horsepower, or 880,000 $\frac{\text{ft}\cdot\text{lb}_\text{f}}{\text{s}}$ [3]. Using equation (22), it was found that the propeller's diameter is 9.468 ft.

$$D_P = K_p \sqrt[4]{Power} \tag{22}$$

The result is a propeller diameter of 9.468 ft. It is good to note that this propeller diameter is similar in size to the propeller of the AT-6 Wolverine with a diameter of 8.08 ft [10].

Tip Velocities

To validate the propeller diameter previously calculated, the tip velocities of the propeller were determined. Tip velocities are an important measurement to ensure the propeller does not exceed the critical Mach number for the airfoil of the propeller. If this velocity were exceeded, the tip of the propeller would become supersonic, which would cause dangerous shockwaves and stresses on the propeller. From research, a metal propeller, like the one on the Sabretooth, must not exceed about 950 $\frac{\text{ft}}{\text{s}}$ at sea level [2]. With this constraint known, the velocity of the propeller tip can be calculated from the known size and rotational speed of the propeller and the cruise speed. The static velocity of the propeller can be determined using:

$$(V_{tip})_{static} = \pi n D_p \tag{23}$$

where n is the revolutions per second of the propeller and D_p is the diameter of the propeller. It was determined that the propeller will reach 591.1 $\frac{\text{ft}}{\text{s}}$ at cruise, using 70% of the maximum rotational speed and 844.4 $\frac{\text{ft}}{\text{s}}$ at 100% of the maximum rotational speed.

The helical propeller speed can be determined using the static tip velocity and the known cruise speed, using (24).

$$(V_{tip})_{helical} = \sqrt{V_{tip}^2 + V^2} \tag{24}$$

where V is the cruise speed of the aircraft. This equation was used to determine that the propeller will reach 756.4 $\frac{\text{ft}}{\text{s}}$ at cruise, and 967.4 $\frac{\text{ft}}{\text{s}}$ at full throttle and full cruise speed. Since the calculated propeller diameter allows the propeller to exceed the 950 $\frac{\text{ft}}{\text{s}}$ limit for metal propellers, the diameter must be reduced. Solving for the maximum helical tip speed to be 950 $\frac{\text{ft}}{\text{s}}$, the allowable propeller diameter, D_p, is 9.2622 ft. Using this propeller diameter, the propeller will reach 745.6 $\frac{\text{ft}}{\text{s}}$ at cruise with and 950.0 $\frac{\text{ft}}{\text{s}}$ using full throttle and full cruise speed.

Advance Ratio

Propeller design for the UF-7 Sabretooth began with the calculation of various parameters. Values such as the advance ratio, power coefficient, thrust, and thrust coefficients were computed to determine the effectiveness of the propeller design concerning the RFP requirements [1].

The advance ratio is a nondimensional velocity related to the propeller tip speed. This corresponds to, “the distance the aircraft moves with one turn of the propeller” [2]. To compute this ratio, values such as the cruising velocity of the aircraft U, the rotation speed of the propeller n, and the propeller diameter D_P were needed alongside the appropriate equation (25). The resulting advance ratio for the Sabretooth is 2.57 at cruise and 1.80 at full throttle.

$$J = \frac{U}{nD_P} \tag{25}$$

Power Coefficient

Following the advance ratio calculation, the power coefficient was determined. Utilizing the Pratt and Whitney PT6A-68D, the UF-7 Sabretooth can produce a maximum of 1,500 SHP. To properly nondimensionalize the power coefficient calculation, the value for shaft horsepower must be converted to standard horsepower using (26).

$$\text{HP } [\frac{lb-ft}{s}] = \text{SHP} * 550\text{bhp} \tag{26}$$

After performing the proper conversion, various propeller parameters are needed to compute the power coefficient. Values such as the engine power P, air density at cruise ρ, rotation speed n, and the propeller diameter D were needed. Using these, the power coefficient was computed using (27). The resulting power coefficient for the Sabretooth is 1.46 at cruise and 0.50 at full throttle.

$$C_p = \frac{P}{\rho n^3 {D_P}^5} \tag{27}$$

Thrust, Thrust Coefficient, and Static Thrust

After the power coefficient was computed, the thrust production of the engine was approximated. This calculation utilizes the engine power P, the propeller efficiency [2] η_P, and the aircraft velocity V. These values were used to approximate the thrust of the engine under cruise conditions (28), noting that a propeller efficiency of 80% was utilized.

$$T = \frac{P\eta_p}{V} \tag{28}$$

Just as the power coefficient was calculated earlier, the thrust coefficient was computed similarly. Utilizing the same parameters, alongside aircraft thrust, the coefficient of thrust was computed (29).

$$C_T = \frac{T}{\rho n^2 {D_P}^4} \tag{29}$$

Previously, the thrust of the engine at cruise was computed. To continue the analysis of the engine for comparison purposes, the static thrust of the engine was also determined (30). This is the thrust that is generated by a propeller under static conditions when the aircraft is not moving. Typical parameters were utilized including, coefficient of thrust C_T, coefficient of power C_p, engine power P, rotation speed n, and propeller diameter D_P.

$$T_{static} = \frac{C_T P}{C_P n D_P} \quad (30)$$

The resulting thrust of the Sabretooth is 1398.3051 lb. for cruise and while static. The thrust coefficient for the Sabretooth is 0.45 at cruise and 0.22 at full throttle.

Table VIII: Summary Propeller Design Values

Property	Value(s)		Unit
Propeller Diameter, $\boldsymbol{D_P}$	9.2622		ft
Power, P	880,000		$\frac{ft-lb}{s}$
Thrust, T	1398.3051		lbs
Static Thrust, $\boldsymbol{T_{static}}$	1398.3051		lbs
Propeller Rotation Speed, n	1190 (70% of max)	1700 (100% of max)	RPM
Advance Ratio, J	2.5694	1.7986	-
Coefficient of Power, C_P	1.4552	0.4991	-
Coefficient of Thrust, $\boldsymbol{C_T}$	0.4531	0.2220	-
Static Propeller Velocity, $\boldsymbol{(V_{tip})_{static}}$	577.1142	824.4488	$\frac{ft}{s}$
Helical Propeller Velocity, $\boldsymbol{(V_{tip})_{helical}}$	745.5500	950.0000	$\frac{ft}{s}$

Location of Powerplant

The powerplant location for the Sabretooth will be a single powerplant in the front of the fuselage. This is called a "tractor "configuration and has several advantages over a tail-mounted, or "pusher," configuration. Placing the powerplant at the nose of the aircraft allows the propellers to fly through clean, undisturbed air, which increases the efficiency compared to the pusher configuration. The stability of the aircraft is also improved by using a tractor configuration, due to the center of gravity being shifted forwards. Since the propellers used on the Sabretooth are 9.5 ft in diameter, using the tractor configuration will also be helpful with ground clearance, as shorter landing gear will be needed relative to the pusher configuration.

Fuel System

The fuel for the Sabretooth will be stored in bladder tanks, which are best suited for retaining fuel in the event of a bullet entering the fuel tanks, due to their self-healing properties. The total amount of fuel required will depend on the type of mission the aircraft is to execute. For the design mission, with a 5% increase in volume considered, a maximum of 2,569 lbs. of fuel is required. Likewise, for the ferry mission, a maximum of 1,750 lbs. of fuel is required.

The fuel volume will also vary slightly with temperature. For every volume of required fuel calculated, a 5% increase was considered [2]. The constraints for total fuel capacity were calculated using the volume of the wings. In conjunction with the bladder tanks, the total useable volume for fuel storage within the wings was calculated to be 60.53 ft^3. Multiplying by the density of jet A fuel, this translates to a maximum of 5,069 lbs. of fuel available for the aircraft. Therefore, the wings will provide enough space for fuel storage.

Table IX: Fuel System Values

Property	Value	Unit
Fuel Storage Volume	60.53	ft^3
Jet A Fuel Density	50.1	$\frac{lb}{ft^3}$
Design Mission Fuel Weight	2569	lbs
Ferry Mission Fuel Weight	1750	lbs
Maximum Fuel Weight	3023	lbs

CAD Model

To supplement the visualization of the design as well as confirm that the chosen design parameters resulted in an acceptable size, a CAD model was generated using SolidWorks. Renders of the SolidWorks model are shown below with an approximate fuselage body shown to show where the fuel system will be stored. A CAD model of the PT6A-68D was available on the CAD-sharing platform GrabCAD, which was used for these models [11]. Note that this propeller has a spinner at the front to reduce drag and smooth the airflow to allow it to enter the intake more efficiently. This spinner covers about 25% of the radius.

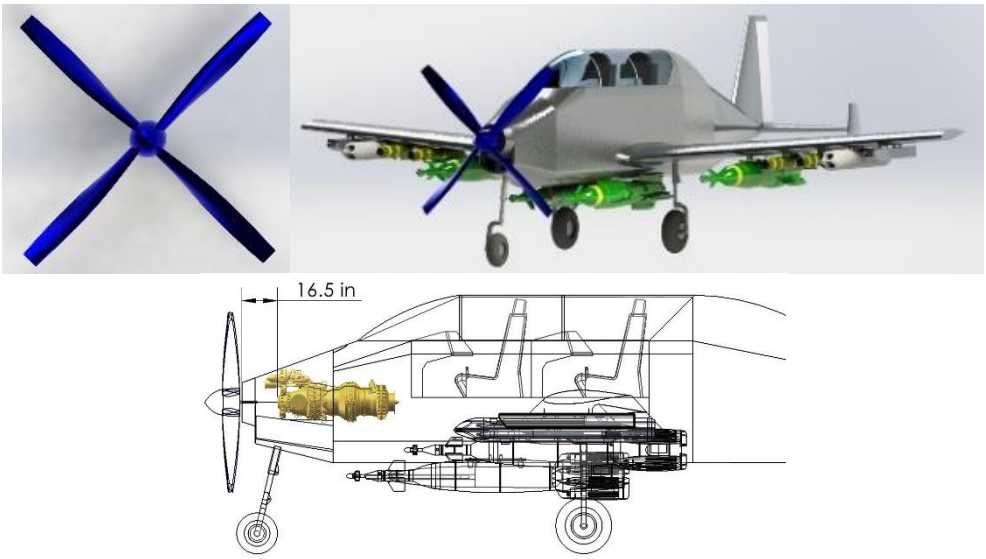

Fig. 7: SolidWorks CAD model of propeller. Powerplant location is also shown [2].

IX. Landing Gear

The tricycle landing gear configuration was chosen for the UF-7 Sabretooth for a variety of reasons. It is the most used arrangement today according to Raymer [2]. The center of gravity is ahead of the main two wheels, and thus, helps ground stability when the nose of the aircraft is not aligned with the runway. The final wheel is located towards the nose of the aircraft. Tricycle landing gear was also chosen because it improves forward visibility on the ground for the pilots. The landing gear is set to be retractable to reduce the drag coefficient of the aircraft.

Center of Gravity Estimation

The center of gravity of the aircraft can be estimated via a series of relations that give the approximate weights and locations of the main components of the aircraft [2]. The mean aerodynamic chord, MAC, was calculated using (31).

$$MAC = \frac{2}{3} C_{ROOT} \frac{1 + \lambda + \lambda^2}{1 + \lambda} \tag{31}$$

To calculate the exposed surface area of the tails, the surface area of the tails was first estimated using (32) and (33) with tail moment arms, L_{VT} and L_{HT}, estimated as 60% of the fuselage length [2] and tail volume coefficients, c_{VT} and c_{HT}, taken from Raymer [2].

$$S_{VT} = \frac{c_{VT} b_W S_W}{L_{VT}} \tag{32}$$

$$S_{HT} = \frac{c_{HT} MAC S_W}{L_{HT}} \tag{33}$$

The exposed surface area of the wings and tails, $S_{exposed}$, was estimated with the following (34).

$$S_{exposed} = \frac{S_{wet}}{1.977 + 0.52\left(\frac{t}{c}\right)} \tag{34}$$

The wetted surface area of the fuselage, S_{wet}, was estimated with the following (35).

$$S_{wet} = 3.4 \frac{A_{top} + A_{side}}{2} \tag{35}$$

It was assumed that the MAC occurs around 30% of the fuselage length from the nose of the aircraft. The centroid of the aircraft was assumed to be about 55% of the fuselage length from the nose of the aircraft. The resulting

center of gravity is 10.39 ft from the nose of the aircraft. Using this estimation of the center of gravity, the absolute locations of the wheels can be determined.

Tire Sizing

Preliminary tire sizing for the Sabretooth was completed using statistical data. As an austere field aircraft, the Sabretooth does not fit neatly in any of the categories of aircraft variants [2], but for preliminary sizing, the values used for the Sabretooth will be the mean of the general aviation and jet trainer aircraft. This results in a tire with an estimated diameter of 24.4″ and a width of 5.1″. The nose gear can be 60% to 100% of the main gear size, so preliminary estimates will use 75% of the size of the main gear [2]. This results in a nose diameter of 18.3″ and width of 3.8″.

Using these values, a standard-sized tire can be selected that will be a good fit for the Sabretooth. A manufacturer's tire book lists the available tires for a given type. The tires on the Sabretooth will be chosen as type III since these are typically for lower inflation pressures, which the Sabretooth will require. The tubeless, 10-ply, 8.50-10 tire is rated for 160 MPH speed, 5,500 lbs static load, and inflation to 70 psi. These tires have a diameter between 24.7″ and 25.65″ and a width between 8.2″ and 8.7″. The rolling radius of the main tires are 10.19″ [12]. The nose gear tires can use the 7.00-6 tubeless, 6 ply tire that is rated for 160 MPH, 3,600 lbs static load, and inflation to 73 psi. The 7.00-6 tire has a diameter between 18″ and 18.75″ and a width of 6.45″ and 7″. This tire is also rated for 5,225 lbs for dynamic braking load, which is well above the calculated maximum of 3,793 lbs [12].

Tire Pressure

The UF-7 Sabretooth is designed to operate from austere landing fields. In the current geopolitical sphere, this means operation primarily from temporary airstrips in the sandy and mountainous regions of the Middle East. However, any unpaved runway could be considered austere, including grass, dirt, snow, and lakebed-based fields. Therefore, adequate tire pressure must be selected for the Sabretooth to operate in a variety of ground conditions. To prevent the tires from being punctured by debris or terrain roughness, aircraft operating from unpaved landing strips typically have low tire pressures relative to those operating from paved landing strips [2].

The tire pressure can be determined by the weight on each wheel and using the estimated contact area of the tire, also known as the footprint area. Under load, each wheel will deform from its initial radius to that of a rolling

radius, which can be estimated to be two-thirds of the initial radius but can be more accurately calculated using the 10.19" rolling radius of the 8.50-10 tire being examined [2]. The footprint area, A_P can be determined using:

$$A_P = 2.3\sqrt{wd}\left(\frac{D_T}{2} - R_r\right) \tag{36}$$

where w is the tire width, D_T is the tire diameter, and R_r is the rolling radius. Using equation (36), the calculated footprint area for the main tire used on the Sabretooth is 120.4 in^2 and 40.7 in^2 for the nose gear.

The main tires of an aircraft typically support 90% of the total vehicle weight, which is estimated to be 10,858 lbs at landing using the weight fractions from earlier. This results in 4,886.2 lbs on each main wheel. The tire pressure can now be determined using (37), where W_w is the weight on each wheel.

$$P_t = \frac{W_w}{A_P} \tag{37}$$

Therefore, the main tire pressure needed at landing is at least 49 psi and at least 32 psi for the nose gear. Taking this information into account, the UF-7 Sabretooth will utilize a main tire pressure of 54 psi which is within the desired range for hard-packed sand, dry grass on hard soil, and temporary metal runways [2]. Additionally, it is 9 psi above the desired pressure for wet grass on soft soil, making it operable in those environments if necessary. Using this information, the Goodyear 8.50-10 tires selected previously for the main gears are valid for use on the Sabretooth and provides a good safety margin between the rated load and the expected load on the tires.

Shock Absorber

The shock absorber type chosen for the UF-7 Sabretooth is the oleo-pneumatic shock strut. This was chosen for its versatility and high efficiency in shock absorption. To calculate the "stroke" or required deflection it is necessary to consider the vertical kinetic energy of the aircraft as well as the kinetic energy absorbed by the tire. Using the shock efficiency for a fixed orifice oleo-pneumatic strut as 0.65 [2], a vertical velocity of 10 m/s, and Gear Load factor of 3 [2].

Utilizing these two parameters, the stroke size of the strut can be computed. To begin, the vertical kinetic energy of the aircraft was calculated. This parameter was dependent on the weight of the aircraft at landing, $W_{landing}$, as well as the vertical velocity of the aircraft at touchdown, $V_{vertical}$. The weight of the aircraft at landing was taken

from the initial weight estimations outlined at the beginning of the report. Initially, this weight was found to be 10,858.37 lbs. The vertical velocity is more commonly referred to as "sink speed" and varies for different types of aircraft. For initial design computations, the vertical velocity of the UF-7 Sabretooth was arbitrarily selected as 10 $\frac{ft}{s}$, a value typical of most aircraft [2]. Using these values alongside the gravitational constant, g, with a value of 32.2 $\frac{ft}{s^2}$, the vertical kinetic energy of the aircraft was computed (35). Using these values, the vertical kinetic energy was found to be approximately 16,861 ft-lbs.

$$KE_{Vert} = \left(\frac{1}{2}\right)\left(\frac{W_{landing}}{g}\right)V_{vertical}^2 KE_{Vertical} = \left(\frac{1}{2}\right)\left(\frac{W_{landing}}{g}\right)V_{vertical}^2 \quad (38)$$

Next, the kinetic energy absorbed by the tire was determined. To do so, the average total load during deflection L_d, needed to be computed. This parameter was dependent on the gear load factor $N_{gear,}$ and the weight of the aircraft at landing. The landing weight of the aircraft is the same value used earlier, and the gear load factor was arbitrarily taken to be 3, a value typical of general aviation aircraft [2]. Using these values, the average total load during deflection was calculated as 32,575 lbs.

$$L_D = N_{gear} \cdot W_{landing} \quad (39)$$

Additionally, prior to computing the kinetic energy absorbed by the tire, the tire stroke, S_T, was computed. Based upon the tire parameters listed earlier, the stroke of the tire is found as "half the diameter minus the rolling radius." [2] (37). In this case, the diameter of the tire is labeled as D_T and the rolling radius is denoted by R_r. Using a tire diameter of 25.65 ″ and a rolling radius of 10.2 ″, the tire stroke was calculated as 0.22 ft. Furthermore, the shock-absorbing efficiency of the tire, η_T, was needed to calculate the kinetic energy absorbed by the tire and was found to be 0.47 [2]. Using each of the outlined parameters, the kinetic energy absorbed by the tire was calculated as 3,349.1 ft-lbs (38).

$$S_t = \left(\frac{1}{2}\right)D_T - R_r \quad (40)$$

$$KE_{abs} = (\eta_T)(L)(S_T)KE_{absorbed} = (\eta_T)(L)(S_T) \quad (41)$$

Finally, one last step was necessary in the computation of the stroke size for the This step was composed of calculating the kinetic energy absorbed by the shock absorber, KE_{shock}. This value was found simply as the difference between the vertical kinetic energy of the aircraft and the kinetic energy absorbed by the tire of the aircraft (39). Using

the appropriate values, the kinetic energy absorbed by the shock was calculated to be 13,512 ft-lbs. Additionally, the only parameter needed to compute the stroke size that was undetermined to this point was the metered orifice efficiency value, η_s. The efficiency ranges from 0.75 to 0.90 and was taken as 0.75 for the initial design computations.

$$KE_{shock} = KE_{Vert} - KE_{abs} KE_{shock} = KE_{Vertical} - KE_{absorbed} \quad (42)$$

Using each of these calculations, the stroke required was calculated to be 8.66 ″, which is within the range for acceptable stroke values.

Oleo Sizing

After the oleo stroke size was determined, the external oleo diameter was approximated. The external diameter of the oleo strut was dependent on two parameters, the internal pressure of the strut, P_{oleo} and the load on the oleo, L_{oleo}. The internal pressure of the oleo strut was assumed to be 1800 psi, a typically accepted value [2]. The load on the oleo strut varied based on whether the oleo strut was for one of the two main wheels (43) or the nose wheel (44). The main wheel load was dependent on the max static load (40) whereas the nose wheel load was dependent on both the max static load of the nose (41) and dynamic braking load of the nose (42).

$$\text{Maximum static load} = W \frac{N_a}{B} \quad (43)$$

$$\text{Maximum static load (nose)} = W \frac{M_f}{B} \quad (44)$$

$$\text{Dynamic braking load (nose)} = \frac{10HW}{gB} \quad (45)$$

$$L_{oleo} = \frac{Max\ static\ load}{2} \quad (46)$$

$$L_{oleo} = \text{Max static load (nose)} + \text{Dynamic braking load (nose)} \quad (47)$$

$$D_{oleo} = 1.3\sqrt{\frac{4L_{oleo}}{P_{oleo}\pi}} \quad (48)$$

It is important to note, some of the sizing parameters are dependent on the location of the aircraft center of gravity in relation to the landing gear. As such, these parameters were assumed to be of the preferred values [2]. Parameters such as $\frac{M_a}{B}$ and $\frac{M_f}{B}$ were assumed to be 0.08 and 0.15, respectively. Additionally, based on historical value, the wheelbase *B*, was found to be approximately 12.5 ft. These values were critical in determining estimations for the oleo strut diameters.

Finally, the total length of the oleo strut was determined. This length is typically approximated as, "2.5 times the stroke" [2]. In this case, the oleo strut is 8.66 ″, therefore the total length of the oleo strut can be approximated as 21.65 ″. This approximation includes the computed strut distance as well as the fixed portion of the aircraft strut.

Landing Gear Retraction

A good landing gear retraction design is crucial for the success of the aircraft. Choosing the retraction method poorly can lead to unnecessarily increased weight, lowered fuel volume, and potentially increased drag. Using fixed landing gear for this aircraft will make the aircraft more vulnerable to external damage during the mission and will produce a significant amount of drag, which is undesirable. Most low-wing fighters, like the Sabretooth, retract the landing gear into the wing of the aircraft. This retraction method reduces drag but sacrifices some of the volume of the wing that would otherwise be used for carrying fuel. As calculated previously, the Sabretooth has plenty of volume in the wings to store fuel, so this makes the gear in wing retraction method ideal for the Sabretooth. For these reasons, the Sabretooth will store the main landing gear in the wing. The nose gear will be stored at the front of the aircraft, so it must remain stored in the front of the fuselage. Note that during deployment, the nose gear will use a strut-travel angle of approximately 7° forward from vertical. Raymer specifies that using "angle allows the tire to move upward and backward when a large bump is encountered, thus tending to smooth out the ride" [12].

The landing gear will be retracted into the body using variations of a four-bar linkage, which are the most common mechanisms for landing gear retraction. The four-bar linkages typically use one member called a drag brace, which connects the gear to a point behind the vertical strut. This drag brace withstands aerodynamic and braking loads applied during landing [2]. The nose gear will retract backwards along the centerline of the Sabretooth body, which is typical for nose gear and "breaks" the drag brace. This will reduce the length of the retracted gear, which is optimal for storing the gear in the wing but will result in a heavier mechanism than some other linkages [2].

Table X: Landing Gear Summary

Parameter	Value	Unit
Landing Gear Arrangement	Tricycle	-
Main Tire	8.50-10 Goodyear (850T06-3)	-
Main Tire Diameter, Width	25.65, 8.7	in
Nose Tire	7.00-6 Goodyear (706T01-1)	-
Nose Tire Diameter, Width	18.75, 7	in
Main Tire Rolling Radius	10.2	in
Nose Tire Rolling Radius	7.3	in
Main Tire Inflation Pressure	54	psi
Nose Tire Inflation Pressure	32	psi
Oleo Shock Stroke	8.66	in
Oleo Shock Diameter	2.39 (mainwheels) 2.32 (nosewheel)	in
Oleo Strut Total Length	21.65	in
Landing Gear Retraction Method	Gear in Wing	-

Landing Gear Location

The determination of the landing gear location requires several calculations and adjustments for the tricycle configuration. This can be difficult to analyze, compared to the other landing gear configurations, and requires further refinement later. These considerations include ensuring the tip back angle allows the wingtip remains at least 6" from the ground during a 5-degree roll and that the overturn angle remains at less than 63 degrees. Since several sections of the aircraft have not been designed yet, these landing gear locations will be estimates and will be refined later. It is also be noted that, for tricycle designs, the main wheels are ideally 8% to 15% of the wheelbase length, B, aft of the center of gravity. In turn, the nose gear will be located 85% to 92% the size of the wheelbase in front of the center of gravity.

For this analysis, an approximate wheelbase, B, of 12.5 ft will be used. An estimated fuselage diameter of 3.24 ft can be used, since this is the dimension of similar aircraft such as the AT-6 Wolverine and the Super Tucano. Using the ideal locations of the main gear, they will be located 11.5% the size of the wheelbase aft of the center of gravity. This results in the main gear being 17.25″ aft and the nose gear being 132.75″ forward of the center of gravity. Note that these locations show that it is appropriate to use gear-in-wing retraction, as these will be valid locations to mount the landing gear on the wing. The engine and propeller clearance were also accounted for, with the minimum clearance between the landing gear and the engine being about 12.32″ and between the landing gear and propeller of 13.96″.

Using the main gear tire rolling radius, oleo shock total length, and assuming the center of gravity acts along the centerline of the fuselage, the approximate center of gravity height from the ground can be determined to be 70.3″. Using an overturn angle of 55°, which is desired for the aircraft stability, the main landing gear will be located 49.2″ from the center of gravity along the span. These resulting landing gear locations relative to the center of gravity are listed in Table XI.

Table XI: Landing Gear Locations

Wheel	Spanwise Location	Forward / Aft Location	Unit
Nose Gear	0	132.75	*in*
Left Main Gear	-49.2	-17.25	*in*
Right Main Gear	49.2	-17.25	*in*

As noted in the shock absorber section, the loads on the shocks are dependent on the locations of the landing gear. Using these locations and (40) to (45), it can be shown that the tires selected are suitable for use in the Sabretooth. The maximum static load applied to each of the main tires is 4,615 lbs., while the maximum static load applied to the nose tire is 1,629 lbs. The dynamic braking load, using the center of gravity height as 70.3” from the ground, is 1,580 lbs. The maximum static load supported by each tire is greater than these loads, so the tires will be acceptable for use on the Sabretooth.

CAD Model

To supplement the visualization of the design as well as confirm that the chosen design parameters resulted in an acceptable size, a CAD model was generated using SolidWorks. Renders of the SolidWorks model are shown below with an approximate fuselage body shown to show how the landing gear will be located. Drawings of the two sets of landing gears and important dimensions are also included.

Fig. 8: SolidWorks CAD model renders of tricycle landing gear configuration.

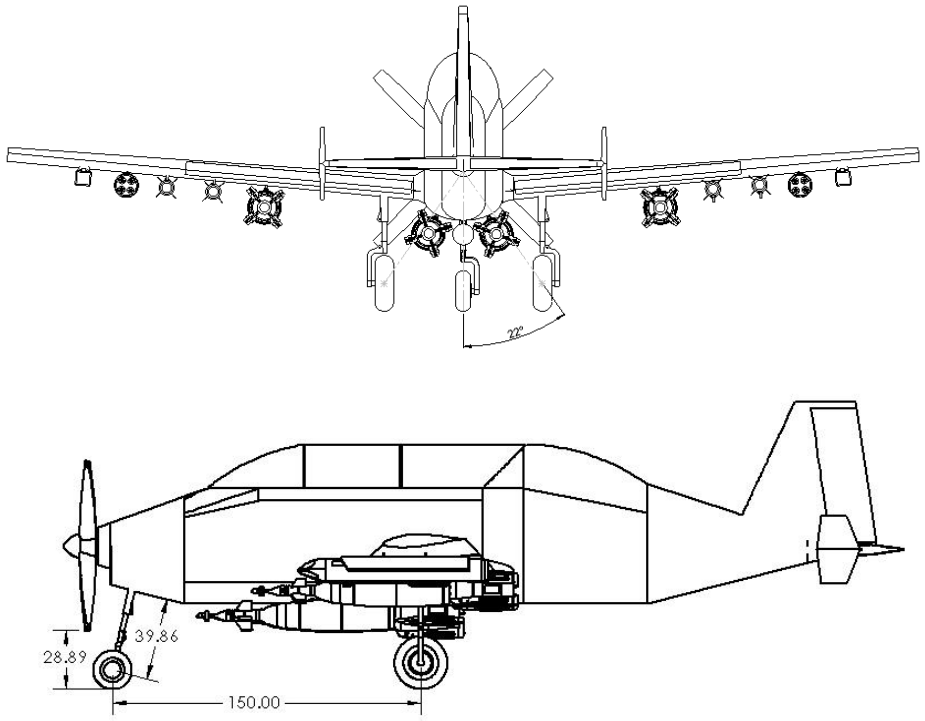

Fig. 9: SolidWorks drawings of landing gear spacing and engine clearance. Dimensions in inches.

Fig. 10: SolidWorks drawings of the main landing gear (left) and nose landing gear (right). Dimensions in inches.

X. Main Body Structures and Armaments

Fuselage

The length of the fuselage was determined from the Raymer textbook using Table 6.3 [2]. The initial constant from the table was chosen based on general aviation – single engine. This value came out to be 4.37. The exponential value was then given as 0.23. Table 6.3 considers the initial takeoff weight for the aircraft in the calculations; however, the empty weight of the aircraft was used as a basis for the UF-7 Sabretooth. The final length of the fuselage was calculated to be 33.6 ft. The fuselage fineness ratio is the ratio between the length of the fuselage and its maximum diameter. Raymer states that a fineness ratio of three is ideal to reduce drag on the aircraft, however, according to Roskin in Airplane Aerodynamics and Performance [44], the theoretical fineness ratios in subsonic aircraft fuselages are typically around 6:1 [13]. In order to reduce the surface area of the tail and take into account considerations such as seating height, this ratio can practically be set to 8:1. Thus, a fuselage fineness ratio of 8:1 was chosen for the Sabretooth making the largest effective diameter for the fuselage 4.2 ft.

Crew Station

The Sabretooth is required to carry two crew members, both with zero-zero ejection seats. Zero-zero ejections seats are an important feature for any fighter to have, as they allow the pilots to safely escape the aircraft at any altitude and airspeed. The Sabretooth will use Martin-Baker Mk16-US16LA ejection seats, as these will fulfill the requirements of the aircraft while being proven flight hardware. The Mk16 zero-zero ejection seats can support crew members up to 270 lbs., have a flight ceiling of 50,000 ft, and will deploy safely up to 620 ft/s. The ejection seats also support canopy fracture, which is a process by which the canopy will be broken directly above the ejection seat [14]. This is preferred for slower aircraft compared to a canopy jettison system in which the entire canopy is blown upwards and moved away by the relative wind. In slower moving aircraft, like the Sabretooth, it is important to make sure the canopy will not provide a threat to the escaping crew, so using a canopy fracturing system works best, while also being less complex and more lightweight [15].

Using the Mk16 Ejection seats, the crew station can be further developed. The crew members will be seated in tandem configuration, with the pilot in front and a weapons specialist in the rear. A typical fighter crew station can be used to provide a basis to create the Sabretooth's crew station. Pilot feedback is key during the development of the

crew station, so using historical data is important in this application [16]. A fighter aircraft usually allows 50 ″ from the front of the control panel to the ejection seat reference point [2].

With two crew members, each with Mk16 ejection seats, and controls, the Sabretooth crew station will be 145 ″ long, with 33 ″ between the two edges of the canopy. This provides ample room for the ejection seats, controls, and other equipment in the crew station. The crew station is configured to give the pilots optimal viewing angles, including having a canopy with a grazing angle of 30.25 degrees. This is an important measurement because a grazing angle of less than 30° will cause the canopy transparency to become significantly reduced, leading to the pilot having difficulty seeing ahead of the aircraft.

The Sabretooth must also meet vison requirements out the for the sides of the crew station and to the tail. The canopy was designed to provide clearance for the pilot to have good vision without moving their head. The look down angle, which is the angle from the pilot's eye line without moving their eyes, is 40.3 degrees, as shown in Fig. 11. The canopy was also designed to give the pilot a clear line of sight all the way from their seat to the tail to allow a pilot to see if a hostile aircraft is behind them. Due to the tail and the fact that there are two crew members, the Sabretooth will also feature a camera array in the rear of the crew station that will feed information to the pilot's display. This will allow the pilot to have a clear view behind them without turning their entire head around. A simplified version of the crew station was modeled in CAD software to better display how the Sabretooth functions.

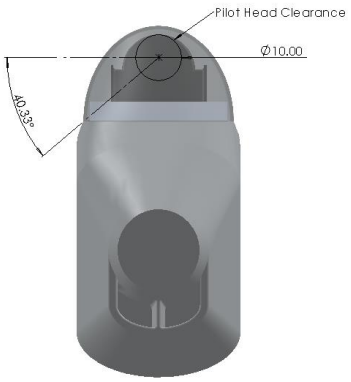

Fig. 11: Pilot side view considerations

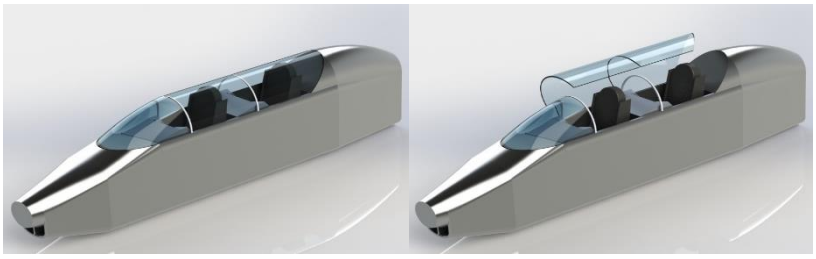

Fig. 12: Detailed view of the Sabretooth Crew Station

Integrated Gun

The aircraft request for proposal calls for an integrated gun intended to be used against ground targets. In missions typical for light attack aircraft, such as close air support, is it expected that the crew will face a variety of both armored and unarmored targets. Therefore, the Sabretooth is designed with two, relatively small caliber guns on either wing and the ability to accept one large cannon in the modular hardpoint under the fuselage. To determine exactly which weapon systems, the Sabretooth uses, a trade study was conducted for both the wing and fuselage guns. Both studies use the same parameters with slight variations.

Weight (the parameter, measured in lbs.) was the largest concern for meeting the mission requirements, so it was given the highest weight of 25%; weight for the main cannon was counted as the weight of the gun only, whereas weight of the wing guns was for the entire pod, including the gun and ammunition. This was done because the cannon is set on a hardpoint, making it easy to replace with another weapons system while the wing pods are permanent parts of the Sabretooth. The weapons system with the lowest weight won the category. The recoil force parameter (measured in lbs.) compared the force applied to the aircraft by each weapons system; it is important for this to be minimized for the best performance of the aircraft, so it was given a weight of 20%, where the system with the lowest recoil won the category. Muzzle energy (measured in ft-lbs) gave insight to the stopping power of each weapon system and was calculated as the weight times the muzzle velocity of the projectile. Muzzle energy was given a weight of 15%, where the winner was the design that had the highest energy. Capacity compared the number of rounds each system could carry and was weighted at 15%. Having a higher capacity was desirable for mission effectiveness, so the system with the highest capacity won the category. Frontal area (measured in square ″) was used to quantify the amount of drag each system would induce, so a lower frontal area was desirable for better aircraft performance. Frontal area was weighted at 15%. Fire rate (measured in rounds per minute, or RPM) was also used to measure effect on target, as

putting more rounds into the target tends to neutralize it quicker. This parameter was weighted at 10% and the system with the highest fire rate won the category.

Table XII: Main Cannon Trade Study

Parameter	Weight	NC621 (M621)			SUU-16 (M61)			GAU-8		
Weight (lbs) (gun only)	25%	100	10.00	2.50	248	4.03	1.01	620	1.61	0.40
Recoil Force (lbs)	20%	275	10.00	2.00	3200	0.86	0.17	10000	0.28	0.06
Muzzle Energy (ft-lbs) (AP)	15%	756	2.84	0.43	760	2.86	0.43	2659	10.00	1.50
Capacity (rounds)	15%	180	1.57	0.23	940	8.17	1.23	1150	10.00	1.50
Frontal Area (in^2)	15%	116	9.74	1.46	113	10.00	1.50	254	4.45	0.67
Fire Rate (RPM)	10%	800	1.33	0.13	6000	10.00	1.00	3900	6.50	0.65
Total	**100%**			6.76			5.33			4.78
Other Info Caliber Other Vehicles		20 mm Super Tucano			20 mm AH-1 Cobra			30 mm A-10 Thunderbolt		

Table XIII: Wing Guns Trade Study

Parameter	Weight	HMP-400 (M3P)			SUU-11A (M134)		
Weight (lbs) (pod + ammunition)	25%	345.5	3.76	0.94	130	10.00	2.50
Recoil Force (lbs)	20%	0	10.00	2.00	190	0.00	0.00
Muzzle Energy (ft-lbs)	15%	267	10.00	1.50	157	5.88	0.88
Capacity (rounds)	15%	550	10.00	1.50	260	4.73	0.71
Frontal Area (in^2)	15%	230	4.39	0.66	101	10.00	1.50
Fire Rate (RPM)	10%	1100	1.83	0.18	6000	10.00	1.00
Total	**100%**			6.78			6.59
Other Info Caliber Other Vehicles		0.50 caliber AT-6 Wolverine and Super Tucano			7.62x51 mm AH-1 Cobra		

Payload Selection

The UF-7 Sabretooth is a purpose built, light attack aircraft that is intended "to provide close air support to ground forces at short notice and complete some missions currently only feasible with attack helicopters" [1]. As such,

the aircraft must be able to carry a payload capable of supporting ground forces in a variety of ways. Outlined in the RFP, the required payload of the Sabretooth is at least 3,000 lbs. To meet this criterion, the Sabretooth will be supplied with a combination of missiles, rockets, and bombs. While meeting the minimum payload requirements, the aircraft will be very capable of providing close air support to friendly forces located on the ground.

The payload for the Sabretooth is designed to provide sufficient ground support for friendly forces while maintaining a total payload weight of at least 3,000 lbs. To begin, historical research was performed to determine the armament that light attack aircraft like the Sabretooth were capable of utilizing. The aircraft researched were those most like the Sabretooth; mainly, the AT-6 Wolverine and the A-29 Super Tucano. Each of these aircraft could carry a variety of missiles, rockets, and bombs with the AT-6 supporting the ability to be equipped with any combination of eleven different weapon types. Additionally, it was important to research the maximum payload each of the historical aircraft could carry. These results yielded a maximum supported payload of 4,109 lbs. for the AT-6 and 3,306 lbs. for the A-29 Super Tucano.

The payload for the Sabretooth will total 3,067.8 lbs., just above the minimum required payload. This payload includes a total explosives weight of 2,909.8 lbs. and a weight of 158 lbs. for the aircraft's ammunition. The exact weapon payload, including weapon quantity and weight per unit is tabulated in Table XIV.

Table XIV: Weapon Quantities and Weights

Weapon:	Quantity	Weight Per Unit	Unit
GBU-49 Enhanced Paveway II Laser-Guided Bomb [25]	4	500	lb
AGM-114 Hellfire Missile [26]	4	102.5	lb
GATR 2.75" Laser-Guided Rocket [27]	14	35.7	lb
Total Weapon Weight	**22**	**2,909.8**	lb

To begin, the loadout will consist of four GBU-49 Enhanced Paveway II laser-guided bombs weighing 500 lbs. per unit. This bomb features advanced GPS and laser-guidance technology making it the perfect fit to provide ground support to friendly troops. Additionally, the Sabretooth will utilize four AGM-114 Hellfire Missiles weighing 102.5 lbs. per unit. This missile is intended for air-to-ground support, specifically as anti-armor. The utilization of this missile will allow the Sabretooth to neutralize powerful, armored threats on the ground. Finally, the Sabretooth will employ a total of 14, GATR 2.75 inch laser-guided rockets, each weighing 35.7 lbs. These rockets are also intended

for air-to-ground support, fulfilling a role capable of neutralizing both stationary and moving lightly armored targets. Together, these three distinct weapon types will provide the UF-7 Sabretooth more than enough firepower to provide air-to-ground support for friendly forces when needed.

Payload Mounting

Another important consideration is how the desired payload will be carried by the aircraft. Typically, aircraft possess hardpoints "under the wing and fuselage to which weapons pylons can be attached" [2]. When not being utilized, the pylons and hardpoints can be removed to enhance the aerodynamic performance of the aircraft. The Sabretooth will utilize this same method for mounting the payload to the aircraft frame.

Typically, light attack aircraft contain multiple hardpoints. Aircraft such as the AT-6 Wolverine and the M-346 Master contain as many as seven hardpoints, whereas other aircraft like the A-29 Super Tucano and the Textron Airland Scorpion contain as few as five and six hardpoints, respectively. In order to maximize payload potential while maintaining a symmetric layout, the Sabretooth will utilize a total of seven hardpoints. Three hardpoints will be positioned under each wing to carry the distributed payload while the seventh hardpoint is mounted under the centerline of the aircraft fuselage. Pylons can then be mounted on the hardpoints to accommodate various objects such as an external fuel tank or perhaps another 250 lbs. bomb which would increase the total payload to 2,954.8 lbs.

Payload Positioning

The final consideration in terms of the aircraft payload, is the placement of each weapon. Being placed under the wing, each weapon will affect the aerodynamic stability of the aircraft. To minimize the negative effects, each weapon needs to be placed relatively close to the centerline of the aircraft. The GBU-49 bombs will be placed at the weapons pylon closest to the centerline of the aircraft, with two being mounted on each pylon. This is due to the substantial weight of the bombs, totaling 2,000 lbs. If only one of the bombs is launched, the payload becomes asymmetric, and the stability of the aircraft is negatively affected.

Moving further away from the centerline of the aircraft to the middle weapons pylon, the AGM-114 hellfire missiles will be rail mounted with one under each wing. Finally, the GATR rockets will be mounted on the outermost weapons pylon with seven being mounted under each wing. These rockets are contained within a seven-rocket smart

launcher which will be mounted directly to the pylon underneath the wing. Each missile and rocket launched from the aircraft weigh significantly less than the bombs and can therefore be mounted further away from the aircraft centerline.

Gun Systems

For the undercarriage system, the 20 mm NC621 gun pod (based off the M621 automatic cannon), the 20 mm SUU-16-gun pod (based off the M61 rotary cannon), and the GAU-8 rotary cannon were compared. These weapons are currently found on the Embraer Super Tucano, Boeing AH-6 Cobra, and Fairchild A-10 Thunderbolt, respectively. For the wing-mounted small arms, the 0.50 caliber HMP-400-gun pod (based off the M3P machine gun) and 7.62x51 mm SUU-11A gun pod (based off the M134 rotary gun) were compared. The HMP-400-gun pod is currently used on both the Embraer Super Tucano and Beechcraft AT-6 Wolverine while the M134 is found on the Boeing AH-6 Cobra's chin turret [17-24].

The NC621 cannon pod won as the undercarriage weapon system. This is not surprising, as one of the Sabretooth's closest competitors, the Embraer Super Tucano, also uses this system. This is due primarily due to the pod's low weight, recoil force, and frontal area. Despite the relatively low ammunition capacity of the pod, the low fire rate of the cannon allows for a total burst time slightly longer than that of the SUU-16 and slightly shorter than that of the GAU-8, at 9.4 seconds for the SUU-16, 13.5 seconds for the NC621, and 17.7 seconds for the GAU-8.

The HMP-400 gun pod narrowly won as the wing-mounted weapon system. This is mostly due to three parameters: recoilless design, high muzzle energy, and high capacity. FN generated a unique design for the gun pod that completely negated the recoil of the machine gun, which gave it an edge over the SUU-11A. Additionally, the larger 0.50 caliber round used by the HMP-400 compared to the 7.62x51 mm round employed by the SUU-11A drives its muzzle energy much higher than its competitor. The total burst time of the HMP-400 is 30.0 seconds while the SUU-11A gun pod had an incredibly low total burst time of 2.6 seconds.

Weapon Dimensions

As seen from figure 29, the 20 mm main cannon is located along the centerline of the Sabretooth, the GBU-49 bombs are centered at 1.33 and 7.5 ft from the centerline, the AGM-114 missiles are 10 ft from the centerline, the GATR pod is 12 ft from the centerline, and the HMP-400-gun pod is 14.5 ft from the centerline. The dimensions for each weapon are given in Table XV.

Table XV: Weapon Dimensions

Weapon	Length (in)	Width (in)	Height (in)	Diameter (in)	Distance from Centerline (ft)
NC621	86.9	8.0	9.6	n/a	0.0
GBU-49	128.4	n/a	n/a	10.7	1.33 and 7.5
AGM-114	64	n/a	n/a	7	10.0
GATR 2.75" Rocket Pod	76.5	n/a	n/a	16.3	12.0
HMP-400	17.1	n/a	n/a	17.1	14.5

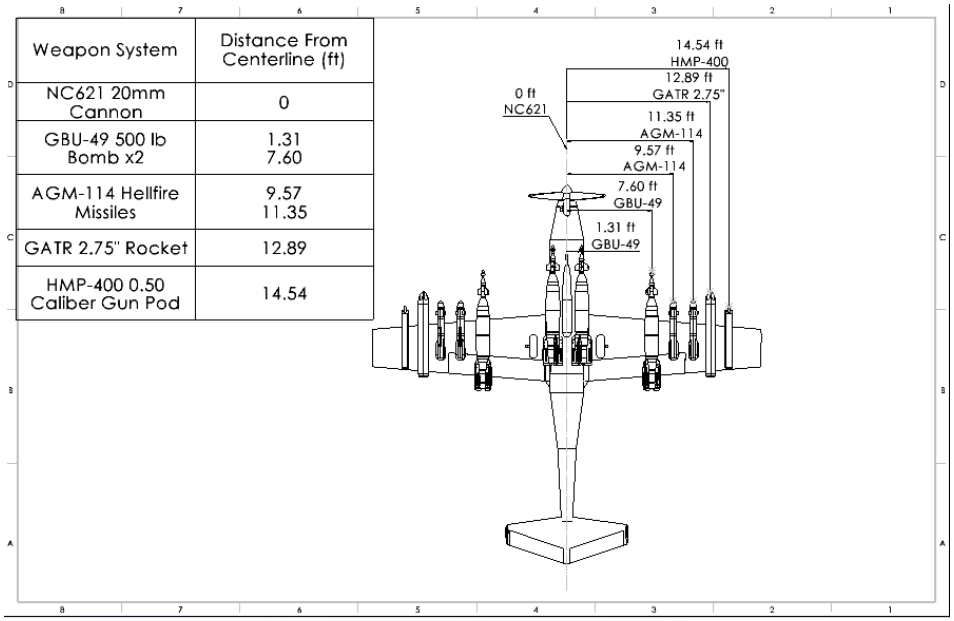

Fig. 13: Weapon System Positioning Drawing. Only one side dimensioned due to symmetry.

Fig. 14: Render of Sabretooth with payload

XI. Stealth Considerations

Radar Detectability

Due to the nature of a military aircraft, radar detectability must be considered for successful missions. To counteract radar in the cockpit, the canopy will be thinly cloaked in gold. Another way that the Sabretooth reduces radar detectability is by using radar absorbing materials (RAM). This radar absorbing material will be painted on to the body of the plane, which is a composite binder of urethane with ferrite particles embed in it. There is also a bandpass radome used to reduce the effect of the radar antenna to detection [2].

Infrared Detectability

As many short range air-to-air and ground-to-air missile rely on IR seekers to find aircraft. As these sensors are sophisticated enough to sense radiation from the engines and solar radiation bouncing off the cockpit windows and skin of the aircraft, it is important to reduce these issues as much as possible. Due to the aircraft only flying at subsonic speeds, the impact of the engines is much less than that of a faster aircraft. The aircraft will also use flares that can be sent out from the aircraft to create an IR signature that is like the aircraft's signature to confuse IR sensors [2].

Visual Detectability

An aircraft going at subsonic speeds like the Sabretooth would be easy to spot. A way to counteract this is by using camouflage. The underbelly of the aircraft would be painted a blue-gray color to have camouflage below and the top of the aircraft would be painted a green-brown color. These colors would be blended on the sides so that there is not an abrupt change of color. By using a mottled camouflage paint, the aircraft would look less like an aircraft up in the sky and could confuse a person who is giving it a passing glance [2].

Acoustic Detectability

Noise is primarily caused by the engine, so the usage of a turbofan instead of a turbojet for the Sabretooth comes to that advantage. A turbojet is much louder than a turboprop, because of the jet noise from high exhaust velocities. Propeller noise makes up the bulk of the aircraft noise, but there is not a way to reduce propeller noise without altering the propeller design, so this will not be changed to ensure that the aircraft performs at its peak efficiency [2].

Vulnerability Considerations

As a light attack aircraft, the Sabretooth may be subject to enemy fire. A stray bullet has the potential to cause a fire within the aircraft and endanger both the pilot and the mission. An uncontained fire can spread to other subsystems and further threaten the integrity of the aircraft. To avoid the ease at which a fire may spread, vulnerable components of the aircraft should be separated from each other as much and as logically as possible. Fuel is highly flammable and therefore will not be located directly adjacent to any engines or inlet ducts in the event of a leak. The Sabretooth has 'self-healing' bladder tanks for extra protection. In case a fire does start, all bays of the aircraft will be designed to a fire suppression system capable of either containing the fire or completely extinguishing it, depending on the ferocity of the fire. In the event a propeller snaps during an explosion or any other type of impact, the crew compartment will be located sufficiently aft – at the very least out of the 5° arc of the propeller disk. Electrical systems that aid with the control of the aircraft shall be strongly considered for redundancy. The total vulnerable area is tabulated in Table XVI.

Table XVI: Vulnerable Areas of UF7-Sabertooth

Component	Estimated area (ft^2)	P_k given hit	Vulnerable area (ft^2)
Fuel	60.53	0.3	18.16
Pilot	5	1	5
Engine	8.18	0.5	4.09
Total vulnerable area: 27.25 ft^2			

XII. Structures

V-n Diagram

A V-n diagram outlines the load factor of an aircraft as a function of airspeed. The load factor is dependent on a variety of factors such as the maneuverability of the aircraft as well as the environmental conditions under which the aircraft operates. As each of these factors increase, or become more "intense", the load the aircraft undergoes increases as well.

To begin initially generating the diagram, the bounds for the aircraft load factor were selected. The upper and lower load factors are dependent upon the classification of the aircraft being analyzed. Since the UF-7 Sabretooth is a light attack aircraft, the load factors were selected to correspond to the general aviation aircraft instead of a fighter. This is simply because the maneuverability loads the Sabretooth experiences will not be as great as those observed by a typical fighter. As such, the bounds for the load factor range from -1.5 to 3.8 [2].

Various points along the V-n diagram carry significance related to the general operation of the aircraft. Metrics such as the maneuver speed V_P, cruise speed V_L, dive speed V_D, and stall speed V_S, can be observed directly on the diagram. Having already known factors such as the cruise speed and dive speed, the other parameters were computed. To begin, the maneuver speed was calculated. This computation was dependent on a constant factor, K_P which was determined utilizing the maximum weight of the aircraft (49).

$$K_P = 0.15 + \frac{5400}{\mathrm{W} + 3300} \tag{49}$$

This constant was then utilized to calculate the maneuver speed which indicates a significant point on the V-n diagram. The maneuver speed was calculated using the constant as well as the cruise and stall speeds.

$$V_P = V_S + K_P(V_L - V_S) \tag{50}$$

Following the computation of these parameters, the speeds alongside their corresponding load factors were plotted (Fig. 15). It is important to note, when plotting the speeds for the V-n diagram, each speed was converted to equivalent airspeed. In other words, the equivalent airspeed is "based upon the dynamic pressure at the aircraft's velocity and altitude and not the actual velocity". A simple equation is utilized to converted actual velocity to

equivalent velocity (51). At the cruising altitude of 25,000 ft, values for density included 0.0011 $\frac{slug}{ft^3}$ at the cruising altitude ρ_c and 0.0024 $\frac{slug}{ft^3}$ at sea level ρ_{sl}.

$$V_e = \sqrt{\frac{\rho_c}{\rho_{sl}}}\,(V_{actual}) \tag{51}$$

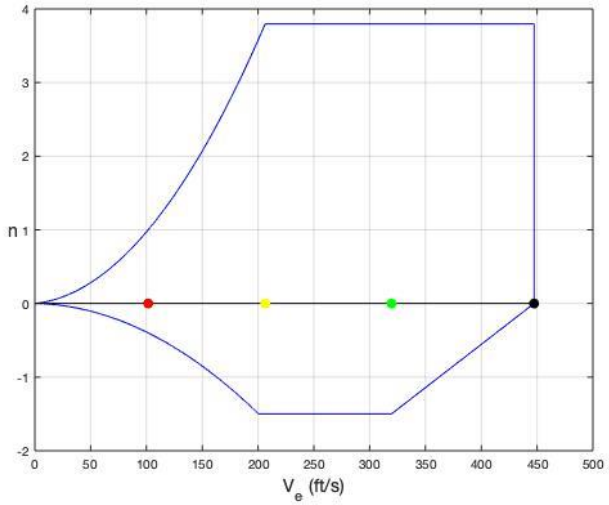

Fig. 15: V-n diagram outlining aircraft load factors and equivalent airspeeds.

Table XVII: Airspeeds for V-n Diagram

Type	Indicator	Actual Airspeed $(\frac{ft}{s})$	Equivalent Airspeed $\left(\frac{ft}{s}\right)$
Stall Speed	•	150.0	101.6
Maneuver Speed	•	305.0	206.5
Cruise Speed	•	472.0	319.6
Dive Speed	•	660.8	447.4

Wing structure type

As stated before, the wings of the Sabretooth will be low mounted. The wing will be attached to the fuselage via a wing box. The wing box will span the width of the fuselage. The wing box will be securely bolted to the fuselage. Likewise, the wing will be secure bolted to the wing box. This should ensure effective transfer of the aerodynamic forces experienced by the wing. It should be noted that the bladder tank shall be fitted to the shape of the wing box where it will be appropriately stored. Typical of most fighter aircrafts, it is most appropriate to use a multi-spar box

structure wing [28]. The ribs, which will run perpendicular to the spars, will create the shape of the airfoil. Additional ribs will take on the role of bearing the initial weight of the of the lift of the aircraft. Most of the weight will then be transferred to the spars of the of the wing. The spars of the wing will run parallel to each other and match the swept angle to the lateral axis of the plane. The spars will also span the entire length of the wing. The front spar will be located towards the leading edge of the wing (about 15% of the chord length). The subsequent main spar should be two-thirds from the trailing edge of the wing (about 60% of the chord length). This is a typical design choice for a reasonable balance of structural integrity and minimization of weight [28]. For security, the spars of the wing shall have a fail-safe mechanism built into their infrastructure. The upper and lower portions of the cross section of the spar will be spliced together. This will ensure that, should one half of the section fail, the weight of the aircraft can still be carried with little compromise.

The main support structure for the wing will be a box beam. This is an extruded beam that allows for a stiff structure with room for the fuel system internal to the wing structure. The selection of the box beam size is dependent on the airfoil geometry. The wing box beam size was determined from the geometry to allow for the semi-monocoque design previously discussed (Fig. 16). The thickness of the box beam was determined from structural analysis discussed later.

Fuselage structure type

Most modern aircraft use semi-monocoque construction for fuselage structure as it is especially useful for withstanding the changes in air pressure experienced by the aircraft [29]. The semi-monocoque is attached to the skin of the fuselage via longerons which will span across the length of several frame members. This will help redistribute the stress experienced by the skin of the fuselage during flight while also staying lightweight [30]. Stringers, which will be shorter than the longerons, will also be attached to the skin of the fuselage. In conjunction with the longerons, these two structures will aid in the prevention of the disfigurement of the fuselage from forces of compression and tension [31]. The longerons will transfer the forces from the skin to the bulkheads and frames throughout the semi-monocoque structure. A pair of frames will sandwich the wing box to help with the transfer of the forces experienced by the wings to the rest of the aircraft. A CAD model of the fuselage structure is shown in Fig. 20.

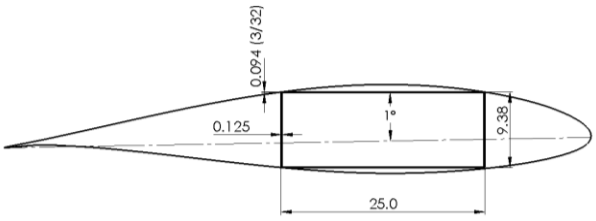

Fig. 16: Wing Box Diagram

Material Selection

Various Materials were considered for the UF-7 Sabretooth ranging from composites to alloys. Ultimately, it was decided that the Sabretooth would be comprised of more alloy than composite material. Although composite materials are being used more commonly in modern aircraft, the difficulty to repair is a strong deterrent for a light-attack military aircraft that may sustain damage during missions. Raymer states that composites are difficult to repair "because we need to match strength and stiffness characteristics" [2]. Patching the aircraft becomes an issue because "a patch that is weak is obviously undesirable, but one that is overly strong can cause excessive deflection on adjoining areas" [2]. This can lead to fracture and long lead times to run computer programs to match portions of the aircraft that may need to be repaired.

Aluminum is the most widely used aircraft material and the Sabretooth will be utilizing a few different alloys for its body and wing structure [2]. 7075-T6 is widely used for high-strength applications, and such, will be used for the main structural components of the plane: the wing box, adjoining section between wing and fuselage, and the frame for the fuselage. For the skin of the Sabretooth, 2024-T3 will be used. 2024 is relatively soft and easily manufacturable. It has a high fatigue resistance; however, welding is not recommended for this alloy [32].

Titanium is a highly desirable material for its strength-to-weight ratio and stiffness compared to aluminum alloy and because of its capability to resist high temperatures. It is also corrosion-resistant [2]. However, these properties also make it difficult to forge and form which is why aluminum is much more common on aircraft. Despite this, titanium's high temperature resistance makes it ideal for areas on the aircraft that must withstand high temperatures. Ti-6A1 will be used on the Sabretooth around the structure holding the engine on the fuselage.

The propeller of the Sabretooth will be made out of a carbon fiber composite. Carbon fiber holds a few benefits over aluminum alloys when it comes to implementation within the propeller. The composite can be designed to save weight compared to an alloy of similar strength. It can also be designed to reduce noise and vibrations that the

pilots encounter during flight. A foam core can be used instead of a wood or an aluminum one to help dampen vibrational effects. Unlike the downsides of repair on the main fuselage or wing, the propeller holds a much smaller surface area and has a reduced chance of becoming damaged in combat. Hartzell propeller designed a full carbon fiber composite propeller with a nickel-cobalt leading edge to act as an erosion shield [33] and the Sabretooth will follow a similar design to help protect against wear.

Table XVIII shows common materials used in aircraft and their various properties used for consideration on the UF-7 Sabretooth:

Table XVIII: Common Aircraft Materials and Properties

Material	2024-T3	6061-T6	5052-T6	7075/ 7050/ 7010	Ti-6A1 Titanium	Carbon Fiber Composite	Unit
Young's Modulus	10.6	9.9	10	10.3	16	75.4	MSI
Ultimate strength (tensile)	62	45	33	72	160	550	KSI
Shearing Strength	37	30	20	43	100	85.6	KSI
Yield Strength (tensile)	45	35	28	64	145	467	KSI

Structural Analysis

The wing box of the Sabretooth was analyzed to validate the material choice and geometry. The finite element analysis software, ABAQUS, was used to model the wing box. An extruded shell was generated that matched the dimensions of the wing box structure. The boundary conditions used fixed the edges of the shell at the root in all 3 axes and restricted rotation along the chord axis. The material properties were set to match that of the 7075-T6 aluminum alloy. The loading condition was modeled to represent a line load acting at the quarter-chord of the wing. The loading used an elliptical lift distribution to better model the spanwise lift load acting on the wing. The equation of the elliptical line is

$$F = A\sqrt{1 - \left(\frac{y}{b/2}\right)^2} \tag{52}$$

where F is the spanwise lift distribution load, A is the magnitude input for the initial distributed force in $\frac{\text{lbf}}{\text{in}}$, y is the spanwise axis location from the center of the aircraft, and b is the wingspan.

During cruise, the wing is assumed to be generating a lift equal to the takeoff weight of the entire aircraft. Since the stress analysis models half of the wing, the magnitude of the line load was calculated such that the entire

force acting on the wing was equal to half the total estimated takeoff weight. To find the correct magnitude, A, the integral of F over the entire wingspan was set to equal the lift being modeled, such that

$$\frac{W}{2} = \int_0^{\frac{b}{2}} A\sqrt{1-\left(\frac{y}{b/2}\right)^2}\,dy \tag{53}$$

where $\frac{W}{2}$ is half of the takeoff weight, equal to the desired lift generated by the wing. Solving this equation for A results in an initial magnitude of $A = \frac{4W}{\pi b}$, or 41.78 $\frac{\text{lbf}}{\text{in}}$. One third of this line load acts on the bottom surface of the wing box, while two thirds of this line load acts on the top surface, similar to a typical airfoil lift distribution [2]. Using the lifting load as the only load acting on the wing also provides a conservative analysis, since in reality the wing will have lift and its own weight acting on the wing box. Using this analysis ensures that the forces seen on the wing will not be expected to exceed this analysis, generating a strong structure.

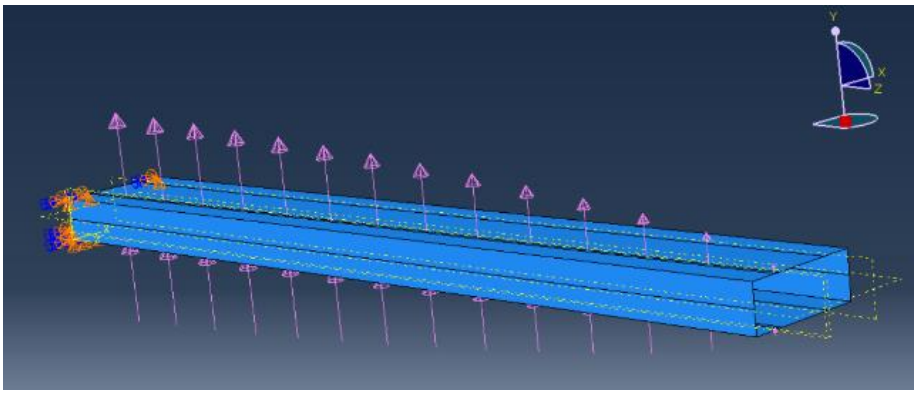

Fig. 17: Wing box loading in ABAQUS FEA software″

It was found that the wing box is strong enough to support the aircraft with a side thickness of 0.125 ″ and a top and bottom thickness of 3/32 (0.09375) ″. The total tip deflection of the wing box is 6.32 ″ and the maximum stress in the wing box is 42.1 ksi. This was determined using Von Mises' stress analysis and is much lower than 7075-T6's yield strength of 64 ksi. This results in a factor of safety of 1.52, which is acceptable for wing structures. Most components on the wing box have stress levels around 19.8 ksi. A model of the wing box with scaled deformations is shown in Fig. 18.

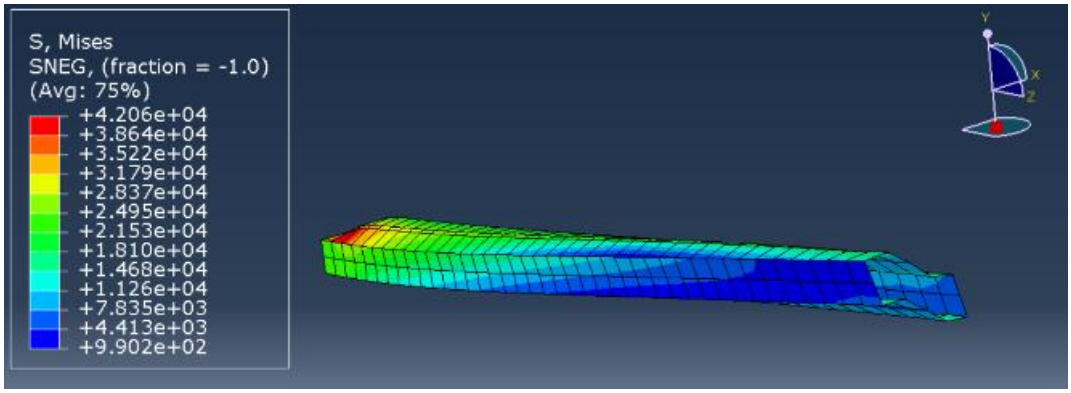

Fig. 18: Deformed Wing Box under Line load

To verify the analysis and provide more information on the wing box strength, a MATLAB analysis was completed. The analysis calculated the shear flow around the wing box, then calculated the stresses at various points on the wing. The analysis also calculated the allowable crack lengths and the fatigue life of the wing, using Soderberg's theory. The fatigue life was found to be 5×10^6 cycles to failure using Fig. 37, with a stress amplitude of 26.8 ksi. The maximum allowable crack length was found to be 0.686″, which occurs at the bottom aft section of the root. Fig. 19 shows plain fatigue and power (plain fatigue). For the purposes of the figure, plain fatigue represents actual data points from testing whereas power represents a trendline that can be used to predict future tests.

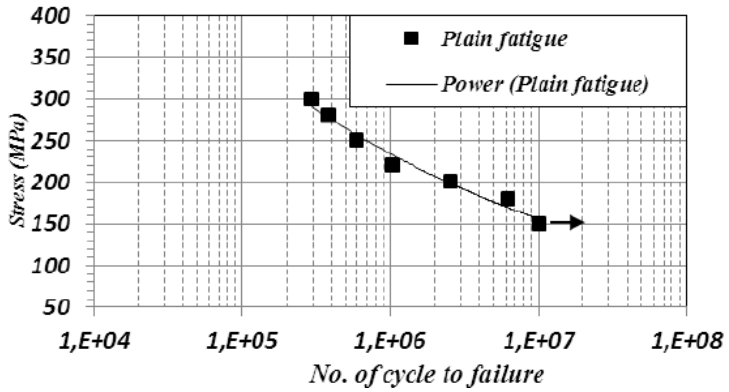

Fig. 19: S/N Curve of fatigue for 7075-T6 [34]

CAD Render

To supplement the visualization of the design as well as confirm that the chosen design parameters resulted in an acceptable size, a CAD model was generated using SolidWorks. Renders of the SolidWorks model are shown below with the designed fuselage structure, which is shows the semi-monocoque structure used. The CAD model of the wingbox was previously shown in Fig. 17.

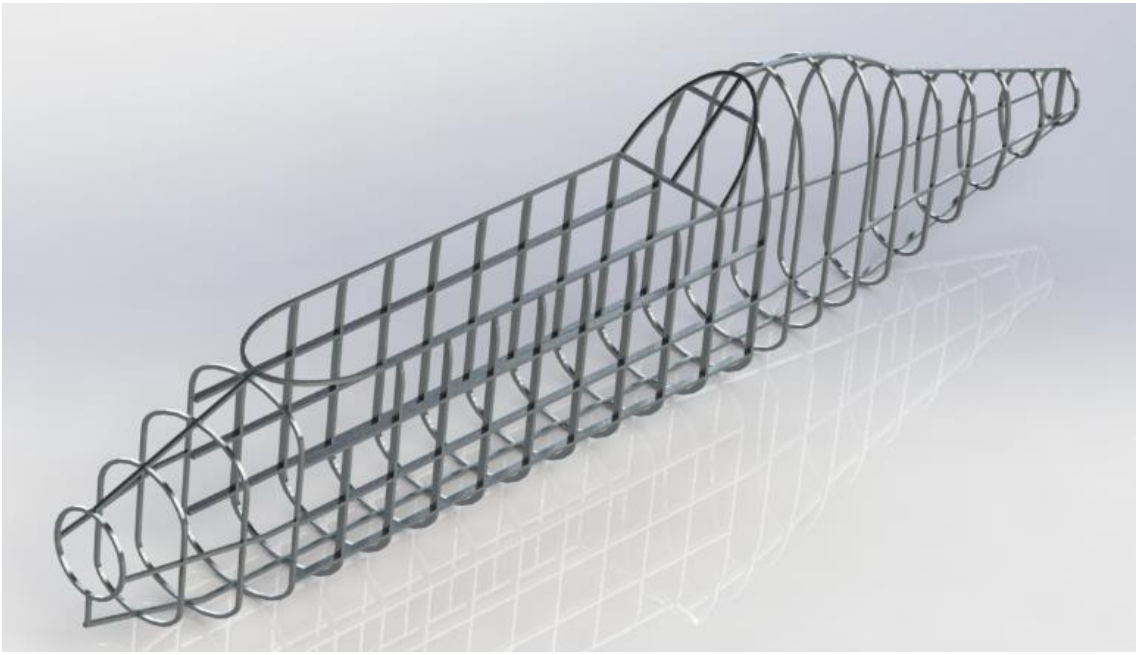

Fig. 20: CAD model of fuselage structure

XIII. Tail Design, Systems, Weight, and CG

Tail Design

A conventional tail design was chosen simply because it is the most common and that "it works" [2]. This design provides good stability and control while maintaining a relatively lower weight than the other options available. The horizontal stabilizer will see smooth airflow and will have a strong foothold on the fuselage.

The location of the horizontal stabilizer for the Sabretooth will be slightly above the main wing based on information from Raymer [2]. The best location for the horizontal tail would be below the wing to improve stall characteristics, however, since the Sabretooth has a low-mounted wing, the best location for the tail is just above the wing. The tail arm is located nearly 2.75 wing chord lengths from the quarter chord of the main wing and will be located about 0.25 wing chord lengths, or 1.5 ft, above the centerline of the wing.

The tail aspect ratio and taper ratio was chosen based off historical data [2]. The horizontal tail will have an aspect ratio of 3 with a taper ratio of 0.3. The vertical tail will have an aspect ratio of 1 with a taper ratio of 0.3.

Leading-edge sweep of the horizontal tail is suggested to be about 5° more than the wing sweep [2]. The Sabretooth has a leading-edge sweep of 3°, and thus, the horizontal tail will have a leading-edge sweep of 8°. With this leading-edge sweep angle, the tail will stall after the wing and will provide the tail with a higher critical Mach number, something not as important for a subsonic aircraft. Vertical tail sweep is historically varying from 35° to 55°. However, for subsonic aircraft, Raymer states that "there is little reason for vertical-tail sweep beyond about 20 deg other than aesthetics" [2]. The Sabretooth will use a vertical wing sweep of 25°.

The tail thickness ratio was chosen to be 12% thinner than that of the wing even though the aircraft is not a high-speed aircraft to reduce weight. The airfoil selected was the GOE 411, a symmetric airfoil. Symmetric airfoils are required for stabilizers since having any bias from cambered airfoils will make it unfit for stability. The vertical tail will also use the GOE 411 airfoil but will be offset a few degrees to suppress the "p-effect" from the propeller wash. The "p-effect" has several causes, one of which is the propeller wash, which generates a yawing moment from the relative motion of the washed air against the vertical stabilizer [2]. Offsetting the vertical stabilizer a few degrees will counter the p-effect and testing will be done to determine the appropriate offset.

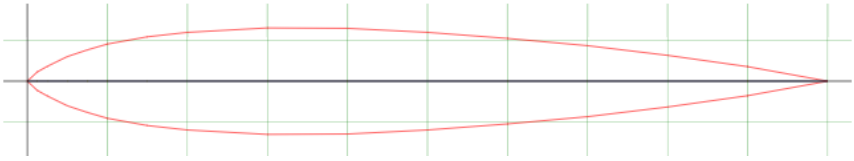

Fig. 21: GOE 411 airfoil diagram [35]

To calculate the span of the vertical tail and the span of the horizontal tail, equations (32) and (33) were revisited to first recalculate the surface area of each respective tail. The horizontal tail volume coefficient was taken to be 0.7 whereas that of the tail was taken to be 0.04. The area of the vertical tail was found to be $10.27\ ft^2$ and the area of the horizontal tail was found to be $26.61\ ft^2$. Equation (54) was then used to find the span of each tail, where b is the span, S is the area, and AR is the aspect ratio found previously.

$$AR = \frac{b^2}{S} \tag{54}$$

The span of the horizontal tail was found to be $9.65\ ft$ whereas the span of the vertical tail was found to be $3.79\ ft$. Using the calculated wing area, sweep angle, and span, the root chord can be determined for the vertical and horizontal tail using geometry. Each stabilizer can be broken into two triangular portions, one forward and one aft, and a central rectangular portion. Knowing the area of the wing must be the cumulative area of these sections, a formula can be developed to solve for the root chord. This equation is

$$C = \frac{2S}{b(\lambda + 1)} \tag{55}$$

where S is the stabilizer area, b is the stabilizer span, and λ is the taper ratio. Using this equation, the root chord of the horizontal stabilizer was found to be 3.94 ft and the root chord of the vertical stabilizer was found to be 3.87 ft

Control Surface Sizing

The elevator is the control surface that acts on the trailing edge of the horizontal tail. The elevator for the Sabretooth makes up 30% of the horizontal tail, with a length of 1.182 ft. The elevator spans 90% of the horizontal stabilizer, with 5% of the fixed horizontal tail on each side.

The rudder is the control surface that acts on the trailing edge of the vertical tail. The rudder for the Sabretooth makes up 30% of the vertical tail, with a length of 1.161 ft. The rudder also spans 90% of the length of the vertical stabilizer, with 5% of the fixed vertical tail on each side. Having the elevator and rudder in this configuration allows

the tail to use an overhung aerodynamic balance for the hinge lines on the tail control surfaces. The overhung aerodynamic balance reduces the effect of flutter from the actuation of the control surfaces. The vertical stabilizer is also positioned forward of the horizontal stabilizer, to allow at least 1/3 of the control surface to be unblanketed, which is important for spin recovery.

Table XIX: Tail Geometry Summary

Parameter	Value	Units
Stabilizer location	2.75 $\bar{C}_{wing}$ behind, 0.25 $\bar{C}_{wing}$ above	-
Horizontal tail leading-edge sweep	8°	$degree$
Vertical tail sweep	25°	$degree$
Horizontal Tail AR	3	-
Vertical Tail AR	1	-
Horizontal Tail Taper Ratio	0.4	-
Vertical Tail Taper Ratio	0.4	-
Max Tail thickness ratio	88% of main wing	-
Area of Vertical Tail	10.28	ft^2
Area of Horizontal Tail	26.61	ft^2
Span of Vertical Tail	3.79	ft
Span of Horizontal Tail	9.65	ft
Root Chord of Vertical Tail	3.87	ft
Root Chord of Horizontal Tail	3.94	ft
Span of Elevator	90% of horizontal tail	-
Span of Rudder	90% of vertical tail	-
Length of Elevator	1.182	ft
Length of Rudder	1.161	ft

A CAD model of the tail was generated to supplement the visualization of the design as well as confirm that the chosen design parameters resulted in an acceptable size.

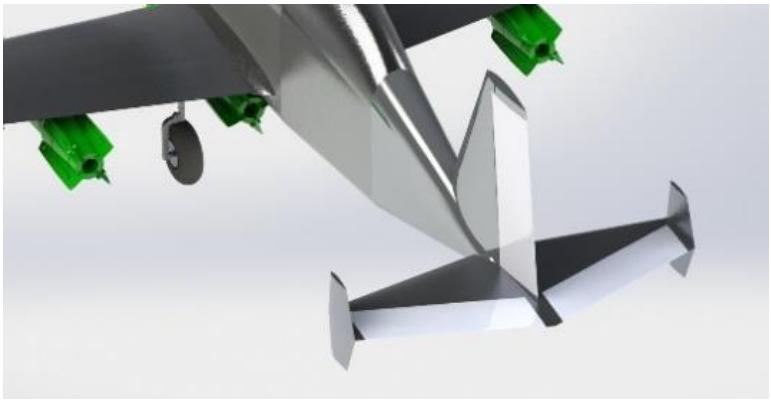

Fig. 22: Render of the Sabretooth tail section

Flight Control System

Various methods can be employed to control subsystems within the aircraft as well as the aircraft's control surfaces. Methods such as fly-by-wire, utilizing electronic components and signals, or a standard hydraulic and mechanical system may be utilized. The fly-by-wire control system is a far more modern approach to aircraft control. Using this system, as the pilot adjusts the control stick, a series of electronic signals are sent to the computers within the aircraft. These computers then interpret the signals and adjust the aircraft's control surfaces as needed [37]. These factors alone are compelling reasons for employing a fly-by-wire control system within the UF-7 Sabretooth. Aside from the factors previously stated, this system allows for improved fuel efficiency during flight as well as improved safety. For redundancy, standard hydraulic actuators will be present for the landing gear and control surfaces in case complications arise during flight.

A. Flight Controls Weight Estimation

In order to determine an estimation of the weight contribution of the fly-by-wire control system to the total weight of the aircraft, (56) was utilized. This equation requires various parameters including cruise Mach number M, total surface area of the control surfaces S_{cs}, number of control surfaces N_s, and the number of crew within the aircraft N_c.

$$W_{flight\ controls} = 36.28(M^{0.003})(S_{cs}^{0.489})(N_s^{0.484})(N_c^{0.127}) \quad (56)$$

Utilizing the appropriate values corresponding to these parameters, a value of 213.98 lbs resulted. This value corresponds to an approximate total weight of the fly-by-wire system including the computers and electronic components necessary for electronic signal interpretation.

B. Engine Controls

Aside from the flight control system, the total weight of the aircraft's engine controls were calculated. This weight estimation composes of a rough approximation of the weight for the components of the aircraft's engine control system, including the engine control unit (ECU) and any actuators and sensors necessary for operation. This calculation requires parameters such as the number of engines within the aircraft N_{en}, and the wire routing distance between the front of the engine to the front of the cockpit L_{ec}. Using these parameters, the weight of the aircraft's engine controls was calculated (57).

$$W_{engine\ controls} = 10.5(N_{en}^{1.008})(L_{ec}^{0.222}) \quad (57)$$

It is important to note, to simplify the calculations, the wire routing distance was approximated as the distance between the engine front and the cockpit front in a straight line totaling 8.3 ft. Using this value, alongside a value of one for N_{en}, yielded an engine controls weight estimation of 16.8 lbs.

C. Hydraulics and Wiring

Hydraulic systems on aircraft are present in order to manipulate control surfaces on the aircraft as well as other moveable subsystems. Subsystems such as the aircraft's landing gear, high-lift devices, and flight controls are powered via hydraulic systems. As such, an approximation regarding the weight of the aircraft's hydraulic system is needed. This approximation requires parameters such as a hydraulic constant K_{vsh}, and the number of hydraulic utility functions Nu. In the case of the Sabretooth, the hydraulic constant is equal to one, and the number of hydraulic utility functions is approximated as 10. Aircraft contain varying hydraulic utility functions from 5 to 15, so an average of 10 utility functions was assumed for the Sabretooth. Using these parameters, the hydraulic weight estimation was calculated, yielding a value of 171.75 lbs.

$$W_{hydraulics} = 37.23(K_{vsh})(N_u^{0.664}) \quad (58)$$

Aside from the hydraulics and other subsystems listed earlier, a weight estimation was performed for general wiring throughout the entire aircraft. In this case, the weight estimation is primarily referring to wiring for electrical systems throughout the Sabretooth. Although no equations were found to approximate this value, research has yielded that electrical wiring typically composes of one to two percent of an aircraft's empty weight, W_{empty} [38]. Knowing that the empty weight of the Sabretooth is 7,146.70 lbs, the weight of the electrical wiring was computed (59). These parameters yield a wiring weight of approximately 107.2 lbs.

$$W_{wiring} = 0.015(W_{empty}) \quad (59)$$

The hydraulics system of this aircraft will be used for wheel braking, wheel steering, flight control, and wing flap control. There is one central hydraulic reservoir and one standby hydraulic reservoir. These hydraulic reservoirs are located behind the cockpit in the fuselage. The central hydraulic reservoir runs off the power generated by the turboprop and the standby system runs off the electrical system in the airplane. The hydraulics system is powered by a generator attached to the engine as well as the APU. The standby system is there as a redundancy in case the central hydraulic system fails. The standby system is powered by the APU. Each control surface is operated by the central

hydraulic system and contains smaller backup actuators at each control surface location in the case of total failure of both the central system and the backup standby system.

Subsystems

A. Electrical System

The electrical system generates power for the main systems and subsystems of the aircraft. These electrical systems include the standby hydraulic system, the avionics controls, flight controls, and the various sensors around the aircraft. This power comes from power generated by the jet-fuel APU and a generator connected to the engine.

B. Pneumatic/ECS system

The pneumatic system provides air pressure to the different systems of the aircraft. The pneumatic system bleeds air from the engine's compressor and supplies it to the various systems, such as the environmental control system, pressurization of the cockpit, engine starting, and anti-icing. The air bled from the engine is run through a heat exchanger to be cooled and used in the environmental control system (ECS). The environmental control system is used to keep the pilots comfortable and to keep the cargo/weapons a safe temperature. The environmental control system mainly uses air bled from the pneumatic system and will be used to keep the cockpit pressurized and at a safe/comfortable temperature for the pilots. For anti-icing, the compressed bleed air is directed through ducts to the wing leading edge, inlet cowls, and the windshield.

C. Auxiliary/Emergency Power

A jet-fuel Auxiliary Power Unit (APU) was chosen for the Sabretooth. This APU is in the fuselage of the aircraft near the hydraulic pumps. Fighters usually have the APU in the fuselage, near the hydraulic pumps and generators [2]. The inlet to the APU is normal to the top of the fuselage and the outlet is normal to the top of the fuselage aft of the inlet and the APU.

D. Accessory Drives

The airframe mounted accessory drive (AMAD) is mounted to the engine and is used to convert power from the engine to other systems that require the use of the engine's mechanical power. This power can then be used to power the electrical systems, the heat exchanger from the pneumatic system, and the central hydraulic system. During

engine maintenance, the AMAD makes the separation of different subsystems from the main engine much more efficient.

E. Avionics

The avionics required in the UF7-Sabertooth includes communication, navigation, and sensor information routing modules. The systems are planned to be routed as an Integrated Modular Avionics (IMA) system as its flight management system, allowing for greater customization of the avionics systems and reducing overall weight of control systems, compared to a federated system architecture. This is due to the IMA having a central processing unit that connects to all other modules. The IMA will allow greater intercommunication and lessen the overall need for individual units to process information from sensors, so long as modules are compatible. This will include flight and data management modules, navigation and guidance modules, communication systems, and warning systems. In addition, flight data instruments and indicators will be integrated to provide basic flight data to the pilot and IMA. The main processor will be the Lockheed Martin Special Mission Processor (SMP) [35]. The avionics system is located in the fuselage, behind the cockpit. Since the wiring for the aircraft systems tends to be very heavy, the overall weight can be minimized by locating the control units near the APU.

Weight Estimation

The weight of the Sabretooth was assessed using a weight statement. This method takes the approximate weights and distances of all the subsystems in the aircraft and compiles them into a total. Using the weight and distance from the nose, the moment about the nose for each component was found. Each component can be modified for different flight conditions and payload usage.

CG Estimation

The center of gravity of the aircraft is essential in determining flight stability and handling characteristics. To calculate the center of gravity, the moment about the nose (in ft-lbs) was divided by the overall weight. The empty center of gravity (measured without the crew, fuel, oil, and ammunition) was found to be 14.200 ft from the nose and the loaded center of gravity was found to be 14.085 ft from the nose. This is primarily due to the fact that the wings carry most of the armaments, resulting in most of the load being applied along the ¼ chord line of the wing. Using

this same process about the landing gear and left wing respectively, the center of gravity in the z-direction is 5.203 ft and, in the y-direction is 17.444 ft, directly along the centerline of the aircraft.

The forward and aft center of gravity limits are the acceptable boundaries that the center of gravity can shift about without significantly changing the flight characteristics. These limits were estimated as 8% of the mean aerodynamic chord of the wing [2]. Since the Sabretooth's wing has an M.A.C. of 73.64 ″, the center of gravity was shifted 5.89 ″ in either direction, between 13.59 and 14.56 ft as seen by the center-of-gravity envelope, the maximum center of gravity that the airplane experiences after using all its fuel and payload occurs at 14.54 ft and the minimum center of gravity experienced on a fully loaded aircraft occurs at 14.09 ft. Both values are within the desired range.

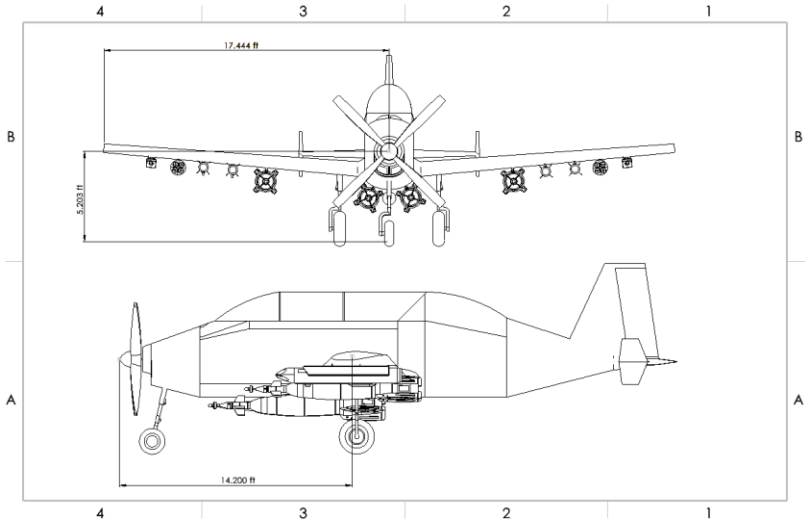

Fig. 23: Top view Position of Center of Gravity

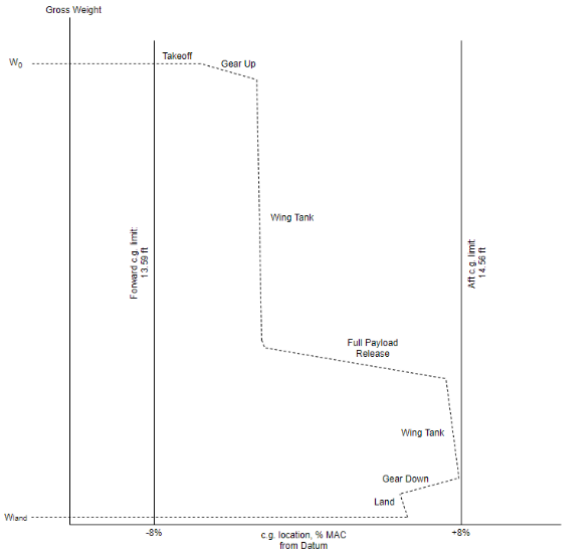

Fig. 24: Weight vs Relative Location to C.G.

Table XX: Weight Estimation Summary

System	Weight (lbs)	Distance of Centroid from Nose (ft)	Moment about Nose (ft*lbs)
Propulsion			
Engine	253.360	5.018	1271.234
Propeller	325.310	1.000	325.310
Gearbox	202.690	2.250	456.048
Housing	25.000	5.018	125.438
Structure			
Wings - Structure	287.860	13.410	3860.203
Wings - Skin	277.640	13.410	3723.152
Horizontal Tail	77.040	31.550	2430.612
Vertical Tail	21.690	31.264	678.116
Fuselage	833.610	18.800	15671.868
Main Landing Gear	497.020	13.073	6497.549
Nose Landing Gear	87.710	4.616	404.889
Firewall	9.820	5.518	54.187
Equipment			
Flight Controls	213.980	14.079	3012.624
APU	258.500	25.083	6483.956
Instruments	40.000	14.079	563.160
Hydraulics	171.780	25.083	4308.758
Electrical/Wiring	107.200	18.800	2015.360
Avionics	16.810	7.000	117.670
Seats	434.000	16.938	7351.092
Pneumatics	67.690	25.083	1697.868
Miscellaneous Equipment	250.000	18.800	4700.000
Armament			
Main Cannon	100.000	16.000	1600.000
Wing Guns	610.000	13.410	8180.100
Bombs	2000.000	13.410	26820.000
Missiles	410.000	13.410	2749.050
Rockets	499.800	13.410	6702.318
Empty Weight Totals:	8078.510	-	111800.561
Useful Load			
Crew	400.000	16.938	6775.200
Fuel	5069.000	13.410	67975.290
Oil	40.000	5.018	200.720
Ammunition	158.000	14.729	2327.180
Takeoff Totals:	13745.510	-	189078.951
Initial Estimation:	12994.000		
Difference:	751.510		

XIV. Stability and Control

Longitudinal Static Stability

To determine if the Sabretooth will be stable during flight, the coefficient of the pitch moment must be calculated. If the derivative of the pitch moment concerning angle of attack, C_{m_α}, is less than zero, the aircraft will pitch down due to a nose-up disturbance, which is desired for the aircraft to be stable. The pitch moment can be calculated from the contributions of all the effects on the aircraft [2].

The moment arm for all of these calculations will act from the center of gravity to the contributing member of the aircraft. In this analysis, the x-axis is out of the rear of the plane, y-axis is out the left-wing, and z-axis is up. To determine the derivative of the coefficient of the pitch moment with respect to the angle of attack, C_{m_α}, the following equation was used (60). Supplementary equations required are also listed below (60-62). Since the Sabretooth's propeller and power plant are at the front of the aircraft, the term $\frac{\delta\alpha_p}{\delta\alpha}$ was assumed to be unity as there would be no difference between the angle of attack that the propeller sees and the angle of attack that the aircraft sees. Likewise, a small angle approximation was made for $\frac{\delta\alpha_h}{\delta\alpha}$ in (61) for the downwash effect and was assumed to be unity. The following equations were used to determine if the Sabretooth achieves longitudinal static stability.

$$C_{m_\alpha} = C_{L_\alpha}\left(\bar{X}_{cg} - \bar{X}_{acw}\right) + C_{m_{\alpha_{fus}}} - \eta_h \frac{S_h}{S_w} C L_{\alpha_h} \frac{\partial\alpha_h}{\partial\alpha}\left(\bar{X}_{ach} - \bar{X}_{cg}\right) + \frac{F_{p_\alpha}}{qS_w}\frac{\partial\alpha_p}{\partial\alpha}\left(\bar{X}_{cg} - \bar{X}_p\right) \quad (60)$$

$$\frac{\partial\alpha_h}{\partial\alpha} = 1 - \frac{\partial\epsilon}{\partial\alpha} \quad (61)$$

$$C_{m_{\alpha_{fus}}} = \frac{K_{fus} W_f^2 L_f}{cS_w}\ per\ deg \quad (62)$$

To aid in finding the influence of the fuselage on longitudinal static stability, the coefficient K_{fus} must be found. Historical data from Raymer was used to determine it based on the root quarter-chord position as a percent of fuselage length [2]. A K_{fus} value of 0.01 was determined based on a 30% position.

The following equation solves for an empirical method for estimation of the propeller normal force with respect to angle of attack, F_{p_α}. N_B is the number of blades per propeller, and A_p is the area of one propellor disk. The derivative term was found using historical data [2]. The advance ratio of the Sabretooth is 1.8 (as shown in Table VIII), thus, the derivative term was found to be 0.09 [2]. The final $f(t)$ term adjusts for nonzero thrust and was found

using information from the Raymer book [2]. The value in the x-axis was found to be close to 0, causing the function term to be unity.

$$F_{p_\alpha} = qN_B A_p \frac{\partial C_{N_{blade}}}{\partial \alpha} f(T) \quad per\ rad \tag{63}$$

Using this analysis, the derivative of the coefficient of the pitch moment with respect to the angle of attack for the Sabretooth was determined. The Sabretooth has a C_{m_α} value of -0.1345 when empty, and -0.2676 when full after a few corrections were made to the design of the aircraft. The horizontal stabilizer's area was increased by 25% for a total area of 33.2625 ft^2. It was also moved back a total of 1 ft aft. This changed the C_{m_α} at full from 0.350042 and at empty from 0.479882 to their current values. The design changes were made to ensure the aircraft was stable.

The following equation solves for the neutral point on the aircraft, or the point where $C_{m_\alpha} = 0$. The neutral point for the Sabretooth was found to be 14.33 ft aft of the nose of the aircraft, with the neutral point normalized by the mean aerodynamic chord of the wing, $\bar{X}_{np}$, of 3.015.

$$\bar{X}_{np} = \frac{C_{L_\alpha}\bar{X}_{acw} - C_{m_{\alpha_{fus}}} + \eta_h \frac{S_h}{S_w} CL_{\alpha_h} \frac{\partial \alpha_h}{\partial \alpha} \bar{X}_{ach} + \frac{F_{p_\alpha}}{qS_w} \frac{\partial \alpha_p}{\partial \alpha} \bar{X}_p}{C_{L_\alpha} + \eta_h \frac{S_h}{S_w} C_{L_{\alpha_h}} \frac{\partial \alpha_h}{\partial \alpha} + \frac{F_{p_\alpha}}{qS_w} \frac{\partial \alpha_p}{\partial \alpha}} \tag{64}$$

The difference between the neutral point and the center of gravity is known as the static margin and was calculated using the following equation. The empty static margin was found to be 0.025062 ft using eq (65), and the full weight static margin was found to be 0.049887 ft using the same equation.

$$SM = \bar{X}_{np} - \bar{X}_{cg} = \frac{-C_{m_\alpha}}{C_{L_\alpha}} \tag{65}$$

To determine the flap deflection required for trim during cruise, landing, and takeoff, (66) was used. The coefficient of the moment about the center of gravity, $C_{m_{cg}}$, was set equal to 0 for trim, while solving for the flap deflection angle that generates zero moment about the center of gravity. It was determined that at 0 degrees angle of attack, which occurs during cruise, the flap deflection, δ_f, was found to be 0.4 degrees, which can be eliminated with the inclusion of an incidence angle of the same magnitude. During landing and takeoff, the Sabretooth can be assumed to fly at an angle of attack at takeoff and landing of 3 degrees and at a velocity of 150 $\frac{\text{ft}}{\text{s}}$. It was determined that during

takeoff and landing, a flap deflection of 7.94 degrees is required for landing and 7.71 degrees is required for landing. It should be noted that these are the minimum values needed for stability, but can be increased during flight, especially during landing where large drag forces are beneficial for slowing down the aircraft. Table XXI summarizes the important findings for the longitudinal stability of the Sabretooth.

$$C_{m_{cg}} = C_L(\bar{X}_{cg} - \bar{X}_{acw}) + C_{m_w} + C_{m_{w\delta f}}\delta f + C_{m_{fus}} - \eta_h \frac{S_h}{S_w} C_{L_h}(\bar{X}_{ach} - \bar{X}_{cg}) - \frac{T}{qS_w}\bar{Z}_t + \frac{F_p}{qS_w}(\bar{X}_{cg} - \bar{X}_p) \quad (66)$$

$$F_p = \dot{m}V tan\,\alpha_p \cong \dot{m}V\alpha_p = \rho V^2 A_{inlet}\alpha_p \quad (67)$$

$$\dot{m} \cong \rho V A_{inlet} \quad (68)$$

Table XXI: Longitudinal Static Stability Results

Parameter	Value	Units
C_{m_α} (empty)	-0.134	-
C_{m_α} (full)	-0.268	-
$\bar{X}_{np}$	3.015	-
SM (empty)	0.0251	ft
SM (full)	0.0499	ft
δ_f at cruise	~0	$degree$
δ_f at Takeoff	7.94	$degree$
δ_f at Landing	7.71	$degree$

Lateral-Directional Static Stability

The lateral-directional static stability relies on the yaw and roll the aircraft experiences. Both the yaw moment (N) and rolling moment (L) rely on the sideslip angle, β. If the derivative of the yaw moment with respect to the sideslip angle is positive, the aircraft is stable. Additionally, if the derivative of the roll moment with respect to the sideslip angle is negative, the aircraft is also stable. Yaw and rolling moment derivatives with respect to the sideslip angle may be calculated using the following equations.

Lateral Stability

To determine the lateral stability of the Sabretooth, the roll moment derivative with respect to sideslip, C_{l_β}, was determined using (69). As stated previously, if the calculated value is negative, the aircraft is stable. In this case, the lateral stability of the aircraft is purely dependent on the wing rolling moment due to sideslip $C_{l_{\beta_w}}$, as well as the

vertical tail rolling moment due to sideslip $C_{l_{\beta_v}}$. Using equation 69, the roll moment derivative with respect to sideslip was computed.

$$C_{l_\beta} = C_{l_{\beta_w}} + C_{l_{\beta_v}} \tag{69}$$

To obtain the lateral stability value calculated above, the individual lateral stability contributions from the wing and vertical tail were computed. As such, the lateral stability of the wing was dependent on many factors. These factors included the roll moment derivative with respect to sideslip due to the wing geometric dihedral $(C_{l_\beta})\Gamma$, the roll moment derivative with respect to sideslip due to the placement of the wing relative to the aircraft fuselage $C_{l_{\beta_{wf}}}$, as well as a general term regarding the wing dihedral effect $\frac{C_{l_{\beta_{wing}}}}{C_L}$. Combining these factors, the wing rolling moment due to sideslip was computed and found to be -0.1339 (70). This value was computed utilizing equation 71 for $(C_{l_\beta})\Gamma$ as well as (72) for $C_{l_{\beta_{wf}}}$.

$$C_{l_{\beta_w}} = \left(\frac{C_{l_{\beta_{wing}}}}{C_L}\right) C_L + \left(C_{l_\beta}\right)\Gamma + C_{l_{\beta_{wf}}} \tag{70}$$

$$(C_{l_\beta})\Gamma = \frac{C_{L_\alpha}\Gamma}{4}\left[\frac{2(1+2\lambda)}{3(1+\lambda)}\right] \tag{71}$$

$$C_{l_{\beta_{wf}}} = -1.2\frac{\sqrt{A}Z_{wf}\left(D_f + W_f\right)}{b^2} \tag{72}$$

$$C_{l_{\beta_v}} = -C_{F_{\beta_v}}\frac{\partial\beta_v}{\partial\beta}\eta_v\frac{S_v}{S_W}\overline{Z}_v \tag{73}$$

Various parameters were needed to compute $\left(C_{l_\beta}\right)\Gamma$, such as the slope of the lift curve C_{L_α}, the wing dihedral angle Γ, and the wing taper ratio λ. Additional values were needed to compute $C_{l_{\beta_{wf}}}$ as well, such as the aspect ratio of the wing A, the vertical height of the wing above the fuselage Z_{wf}, fuselage width W_f, fuselage depth D_f, and wing span b. Each of the intermittent values necessary for the lateral stability computations are found in Table XXII. The roll moment derivative due to sideslip was found to be -0.139. Since the roll moment with respect to sideslip is a negative value, and of small magnitude, the UF-7 Sabretooth was found to be laterally stable.

Table XXII: Lateral Stability Intermediate Values and Results

Parameter	Value	Unit
A	6.945	-
b	33	ft
C_{L_α}	4.519	-
C_{l_β}	-0.138	-
$\left(C_{l_\beta}\right)\Gamma$	-0.089	-
$C_{l_{\beta_{wf}}}$	-0.0269	-
$C_{l_{\beta_v}}$	-0.0036	-
$C_{l_{\beta_{wl}}}$	-0.139	-
D_f	3.83	ft
Γ	5	degrees
λ	0.55	-
W_f	3	ft
Z_{wf}	1.3628	ft

Directional Stability

The yaw-moment derivative, $C_{n\beta}$, defines the directional stability of the aircraft. Its value typically ranges between 0.05 and 0.3, with higher values indicating more directional stability [2]. "More" directional stability means that it takes more force to put an aircraft off its original direction because the aircraft creates a large moment when perturbed. Since the UF-7 Sabretooth is a military light attack aircraft, it is desired that the aircraft is not "too stable," or it will not be as nimble as the pilot may want it. Therefore, it is preferable that a low C_{n_β} value is obtained. C_{n_β} is calculated as (74):

$$C_{n\beta} = C_{n\beta wl} + C_{n\beta w} + C_{n\beta fus} + C_{n\beta v} - \frac{F_{p\beta}}{qS_w} * \frac{\delta\beta_p}{\delta\beta}\left(\bar{X}_{cg} - \bar{X}_p\right) \quad (74)$$

where $C_{n\beta w}$ (75), $C_{n\beta fus}$ (76), and $C_{n\beta v}$ (76) are the contributions to directional stability from the wings, fuselage, and vertical tail, respectively. $\frac{F_{p\beta}}{qS_w}$ is the force contribution from the propeller, $\frac{\delta\beta_p}{\delta\beta}$ is the direction normal to the force exerted by one propeller blade, and $\left(\bar{X}_{cg} - \bar{X}_p\right)$ is the location of aircraft's center of gravity minus the location of the propeller, both normalized by the chord of the aircraft's wings. The contributions were calculated as follows [2].

$$C_{n\beta w} = C_L^2\left\{\frac{1}{4\pi A} - \left[\frac{tan\Lambda}{\pi A(A + 4cos\Lambda)}\right] * \left[cos\Lambda - \frac{A}{2} - \frac{A^2}{8cos\Lambda} + \frac{6\left(\bar{X}_{acw} - \bar{X}_{cg}\right) * sin\Lambda}{A}\right]\right\} \quad (75)$$

$$C_{n\beta fus} = -1.3\frac{V}{S_w b}\left(\frac{D_f}{W_f}\right) \quad (76)$$

$$C_{n\beta v} = C_{F\beta v} \frac{\delta\beta_v}{\delta\beta} \eta_v \frac{S_v}{S_w} (\bar{X}_{acv} - \bar{X}_{cg}) \quad (77)$$

$$C_{n\beta wl} = C_{F\beta wl} \frac{\delta\beta_{wl}}{\delta\beta} \eta_{wl} \frac{S_{wl}}{S_w} (\bar{X}_{acv} - \bar{X}_{cg}) \quad (78)$$

Out of these three equations, the parameter $\frac{\delta\beta_v}{\delta\beta}\eta_v$ (76) is unknown. It was calculated using the following equation [2]:

$$\frac{\delta\beta_v}{\delta\beta}\eta_v = 0.724 + \frac{3.06 * \frac{S'_{vs}}{S_w}}{1 + cos\Lambda} - 0.4 \frac{Z_{wf}}{D_f} + 0.009A_{wing} \quad (79)$$

The winglets', wing's, fuselage's, and vertical tail's contributions to directional stability were found to be 0.1242, 0.0048, -0.0435, and 0.0364, respectively. Subtracting the propeller's contribution 0.0219, the overall yaw moment derivative was found to be 0.1, well within the bounds of directional stability. This would make our aircraft directionally stable. The definitions and final values for the lateral-directional stability of the UF-7 Sabretooth are given in Table XXIII.

Table XXIII: Directional Static Stability Results

Symbol	Definition	Value	Unit
A	Wing aspect ratio	6.4950	-
b	Wingspan	33	ft
c	Chord of the wing	4.7534	ft
C_L	Wing lift coefficient	0.6	-
$C_{F\beta v}$	Vertical tail airfoil lift slope	0.12	-
$C_{n\beta}$	Yaw moment derivative	0.1	-
$C_{n\beta fus}$	Fuselage yaw moment	-0.0435	-
$C_{n\beta v}$	Vertical tail yaw moment	0.0364	-
$C_{n\beta w}$	Wing yaw moment	0.0048	-
$C_{n\beta_{wl}}$	Yaw moment of winglets	0.1242	-
D_f	Fuselage depth	3.83	ft
$F_{p\beta}$	Force contribution from the propeller	3200.2	lbs
q	Dynamic pressure at 25000 ft	118.74	$\frac{lbs}{ft^3}$
S_v	Area of the vertical tail	25.7	ft^2
S'_{vs}	Area of the vertical tail if bottom line is extended to the centerline of the aircraft	25.7	ft^2
S_w	Area of the wings	156.9	ft^2
V	Volume of the fuselage	238.65	ft^3
W_f	Width of fuselage	3	ft
$\bar{X}_{acw}$	Wing aerodynamic center location normalized by the wingspan	0.3704	-
$\bar{X}_{cg}$	Aircraft center of gravity location normalized by the wingspan	0.4268	-
$\bar{X}_p$	Location of the propeller	0.1649	-
Z_{wf}	Vertical height of the wing above the centerline	1.3628	ft
Λ	Wing sweep	3	$degrees$
$\frac{\delta\beta_p}{\delta\beta}$	Normal direction of the force exerted by the propeller	1	-
$\frac{\delta\beta_v}{\delta\beta}\eta_v$	Normal direction of the force exerted by the vertical tail	1.153	-

Lateral Trim Analysis

The main static lateral-trim condition that needs to be checked is that of a crosswind-landing case. According to Raymer, the aircraft must be able to operate in crosswinds equal to 20% of takeoff speed or 11.5 degrees of sideslip, β [2]. This was checked by determining the deflection angle of the aileron that is required to allow $C_n, C_l = 0$ in landing at that angle of sideslip. The equations used to determine the deflection, (80) and (81), of the aileron, δ_a, are 16.38 and 16.40 in the Raymer book [2].

$$C_n = C_{n_{\beta_w}}\beta + C_{n_{\beta_{wl}}}\beta + C_{n_{\delta_a}}\delta_a + C_{n_{\beta_{fus}}}\beta + C_{n_{\beta_v}}\beta - \frac{T\bar{Y}_p}{qS_w} - \frac{D\bar{Y}_p}{qS_w} - \frac{F_p}{qS_w}\left(\bar{X}_{cg} - \bar{X}_p\right) \quad (80)$$

$$C_l = C_{l_{\beta_w}}\beta + C_{l_{\delta_a}}\delta_a + C_{l_{\beta_v}}\beta \quad (81)$$

Most of these values are already known, but $C_{n_{\delta_a}}$ and $C_{l_{\delta_a}}$ must be calculated to determine the deflection of the aileron for both cases. $\bar{Y}_p$ is zero for our design, because the propellor is at the nose of the aircraft so those two terms are not necessary to determine the aileron deflection for lateral trim in a crosswind-landing case. These necessary equations are 16.49 and 16.48 in the Raymer book [2], respectively.

$$C_{l_{\delta_a}} = \frac{2\Sigma K_f \left(\frac{\partial C_L}{\partial \delta_f}\right)' Y_i S_i cos\Lambda_{H.L.}}{S_w b} \quad (82)$$

$$C_{n_{\delta_a}} = -0.2 C_L C_{l_{\delta_a}} \quad (83)$$

K_f and the lift derivative, $\left(\frac{\partial C_l}{\partial \delta_f}\right)$, are found from the Raymer book [2]. Y_i, S_i, and $\Lambda_{H.L.}$ are determined based on the location of the aileron flaps. Y_i is the moment arm from the centerline of the aircraft to each strip of the flap, S_i is the area of each flap strip, and $\Lambda_{H.L.}$ is the wing sweep at the hinge line of the flap on the wing. $\left(\frac{\partial C_L}{\partial \delta_f}\right)'$ was found using equation (84). This equation comes from equation 16.17 in the Raymer book [2].

$$\left(\frac{\partial C_L}{\partial \delta_f}\right) = 0.9 K_f \left(\frac{\partial C_l}{\partial \delta_f}\right)_{airfoil} \frac{S_{flapped}}{Sref} \quad (84)$$

The values determined for δ_a for roll were found to be -8 degrees and 10 degrees for yaw to maintain lateral trim in the crosswind-landing case. The intermittent values found to do this analysis are tabulated in Table XXIV.

Table XXIV: Lateral Trim Analysis Intermittent Values and Results

Symbol	Definition	Value	Unit
β	Angle of Sideslip	11.5	$degrees$
$C_{n_{\beta_w}}$	Wing Yaw Moment	0.0048	-
$C_{n_{\beta_{fus}}}$	Fuselage Yaw Moment	-0.0435	-
$C_{n_{\beta_v}}$	Vertical Tail Yaw Moment	0.0364	-
$\bar{X}_{cg}$	Aircraft center of gravity location normalized by the wingspan	2.9632	-
$\bar{X}_p$	Location of the propeller normalized by the wingspan	0.1649	-
F_p	Force Contribution from the Propeller	.43	lbs
S_w	Area of the wings	156.9	ft^2
q	Dynamic Pressure at 25000 ft	118.74	$\frac{lb}{ft^3}$
$C_{l_{\beta_w}}$	Wing Roll Moment	-0.1339	-
$C_{l_{\beta_v}}$	Vertical Tail Roll Moment	-0.0036	-
K_f	Empirical Correction value for plain flap lift increment	1	-
$S_{flapped}$	Surface area of the flaps	10.2671	ft^2
$Sref$	Reference area of the wing	63.8531	ft^2
$\left(\frac{\partial C_l}{\partial \delta_f}\right)$	Rolling moment due to flap deflection	4.6	-
$\left(\frac{\partial C_L}{\partial \delta_f}\right)'$	Change in lift due to change in flap deflection	0.6613	-
$\Lambda_{H.L.}$	Wing sweep at the hinge-line of the airfoil	6.55	$degrees$
Y_1	Moment arm from the centerline to the flaps	6.28	ft
S_1	Area of strut of each flap strip	10.2663	ft^2
$C_{l_{\delta_a}}$	Roll Moment due to aileron deflection	0.0164	-
$C_{n_{\delta_a}}$	Yaw Moment due to aileron deflection	-0.0020	-
δ_{a_n}	Aileron deflection necessary to maintain directional trim	10	$degrees$
δ_{a_l}	Aileron deflection necessary to maintain lateral trim	-8	$degrees$

XV. Performance Analysis

Range

The range of the Sabretooth was recalculated using the modified Breguet range equation for propeller aircraft [2] (85). The total range during cruise was found to be 1502.2 nautical miles, where C_{bhp} was 0.628 $\frac{lb}{bhp \times hr}$, η_p was 75%, $\frac{L}{D}$ was found to be 7.2 during cruise, and $\frac{Wi}{Wf}$, the weight fraction of the mission segment, was 3.0648. This range surpasses the requirement for the design mission.

$$R = \frac{550\eta_p}{C_{bhp}} \frac{L}{D} \ln \frac{W_i}{W_f} \tag{85}$$

Endurance

The loiter time of the Sabretooth was recalculated using the endurance equation for propeller aircraft [2] (86).

$$\mathrm{E} = \left(\frac{L}{D}\right)\left(\frac{550\eta_p}{C_{bhp} V_{min}}\right) \ln\left(\frac{W_i}{W_f}\right) \tag{86}$$

V_{min} in the above equation was the velocity condition for the minimum power required, as this would provide the maximum endurance. This can be calculated from equation 17.33 in the Raymer book [2] (87).

$$\mathrm{V} = \sqrt{\frac{2\mathrm{W}}{\rho \mathrm{S}} \sqrt{\frac{K}{3C_{D_0}}}} \tag{87}$$

This equation can be solved symbolically to be 76% of the velocity for the max lift-to-drag ratio and this the lift-to-drag ratio became about 86.6% of the max. The maximum endurance for cruise during the design mission was found to be 6.12 hours, where C_{bhp} was 0.628 $\frac{lb}{bhp \times hr}$, η_p was 75%, $\frac{L}{D}$ was 6.24, V was 358.72 $\frac{ft}{s}$, and $\frac{Wi}{Wf}$, the weight fraction of the mission segment, was 1.7095.

Takeoff Analysis

The requirements for the Sabretooth limit the total takeoff distance to 4,000 ft while requiring the Sabretooth to clear a 50 ft obstacle at the runway. To determine how long of a runway the Sabretooth will need to takeoff, the takeoff sequence can be split into segments: ground roll, transition to climb, and climb [2].

The ground roll is the segment in which the aircraft accelerates from zero velocity to takeoff velocity, which is typically 10% faster than the stall speed [2]. The stall speed of the Sabretooth is 150 $\frac{\text{ft}}{\text{s}}$, so the takeoff speed, V_{TO}, is 165 $\frac{\text{ft}}{\text{s}}$. To determine the distance of the ground roll, the acceleration of the aircraft can be manipulated to give the integral

$$S_G = \frac{1}{2g}\int_{V_0}^{V_{TO}} \frac{d(V^2)}{K_T + K_A V^2} = \left(\frac{1}{2gK_A}\right)\ln\left(\frac{K_T + K_A V_{TO}^2}{K_T + K_A V_0^2}\right) \tag{88}$$

where g is the acceleration due to gravity, V_0 is the initial velocity of the Sabretooth, which is 0 $\frac{\text{ft}}{\text{s}}$. The constants K_T and K_A are given by the following (89) and (90), respectively.

$$K_T = \left(\frac{T}{W}\right) - \mu \tag{89}$$

$$K_A = \frac{\rho}{2\left(W/S\right)}\left(\mu C_L - C_{D_0} - K C_L^2\right) \tag{90}$$

$\left(\frac{T}{W}\right)$ is the thrust to weight ratio during takeoff, μ is the ground rolling resistance for the runway, ρ is the density of air during takeoff, $\left(\frac{W}{S}\right)$ is the wing loading during takeoff, C_L is the coefficient of lift during takeoff, C_{D_0} is the zero-lift coefficient of drag, and K is the drag-due-to-lift factor. The thrust during takeoff varies, so it can be considered 70% of the thrust at takeoff for greater accuracy. As a function of velocity, the thrust can be determined using the engine's power and the propeller efficiency. Using equation (91) and the known takeoff weight, the thrust to weight ratio of the Sabretooth is 0.2555 during the ground roll and 0.2291 during the transition discussed later.

$$T = \frac{P\eta_p}{V} \tag{91}$$

K can be estimated using the Oswald span efficiency and the aspect ratio of the wing. The Oswald span efficiency can also be estimated as a function of the aspect ratio using Eq (93). K will also be decreased approximately 10% due to ground effect.

$$K = \frac{1}{\pi(AR)e} \tag{92}$$

$$e = 1.78(1 - 0.045(AR)^{0.68}) - 0.64 \tag{93}$$

The ground rolling resistance expected for the Sabretooth, which operates out of an austere field, can be estimated to be 0.04 with the brakes [2]. Using equation (85), the ground roll distance is estimated to be 2000 ft. After the ground roll, the Sabretooth will begin to rotate up and begin flight. Since the Sabretooth is a relatively small aircraft, it will take 1 second to rotate upwards, which will allow the Sabretooth to travel 165 ft. Once the Sabretooth has lifted from the runway, it will transition to a climb. This can be approximated as a circular arc, with a radius R and angle γ_{climb} [2]. The radius of the arc can be determined using (94).

$$R = \frac{V_{TR}^2}{0.2g} \tag{94}$$

V_{TR} is the average velocity of the aircraft during transition, which is typically 15% faster than the stall speed, or 172.5 $\frac{\text{ft}}{\text{s}}$ for the Sabretooth. The arc angle γ_{climb} can be determined using (95). This arc angle was calculated to be 9.17 degrees.

$$\gamma_{climb} = \sin^{-1}\left(\left(\frac{T}{W}\right) - \frac{1}{\left(L/D\right)}\right) \tag{95}$$

$\frac{L}{D}$ is the lift-to-drag ratio of the Sabretooth during transition. The distance traveled during the transition can be determined using (96). This distance was calculated to be 736 ft.

$$S_{TR} = R\sin\gamma_{climb} \approx R\left(\left(\frac{T}{W}\right) - \frac{1}{\left(L/D\right)}\right) \tag{96}$$

For the Sabretooth, the distance traveled during the transition is 736.3 ft. The height that the aircraft climbs can be determined using (97). This height was calculated to be 59 ft, which is higher than the obstacle expected at the end of the runway.

$$h_{TR} = R(1 - \cos\gamma_{climb}) \tag{97}$$

The obstacle at the end of the runway is cleared during the transition, so the distance traveled during the cruise segment can be considered zero because the aircraft is now considered in flight. In total, the Sabretooth needs 2,901 ft to takeoff while clearing the 50 ft obstacle. This required takeoff distance meets the 4,000 ft requirement for the design proposal [1]. A summary of all the relevant aircraft and intermediate values used for the takeoff analysis is listed in Table XXV. It is also important to note that the takeoff distance was calculated at the maximum takeoff height of 6,000 ft and was determined to be 2,896 ft.

Table XXV: Directional Static Stability Results

Parameter	Definition	Value	Unit
V_{TO}	Takeoff Velocity	165	$\frac{ft}{s}$
$\frac{T}{W}$	Thrust to Weight Ratio	0.2555 (ground roll) 0.2291 (transition)	-
μ	Ground Rolling Resistance	0.04	-
ρ	Air Density	0.002378 (sea level) 0.002048 (6,000 ft)	$\frac{slugs}{ft^3}$
$\frac{W}{S}$	Wing Loading	69.85	$\frac{lbf}{ft^2}$
C_L	Coefficient of Lift	0.756	-
C_{D_0}	Zero-lift Coefficient of Drag	0.02	-
K	Drag-due-to-lift factor, with ground effect	0.049	-
e	Oswald Span Efficiency	0.84	-
K_T	Landing Thrust Coefficient	-0.1709	-
K_A	Landing Aerodynamic Coefficient	$3.728 \cdot 10^{-6}$	-
S_G	Ground Roll Travel Distance	2000 (sea level) 1995 (6,000 ft)	ft
S_R	Rotation Travel Distance	165	ft
R	Transition Arc Radius	4620	ft
γ_{climb}	Transition Arc Angle	9.17	$degrees$
S_{TR}	Transition Travel Distance	736	ft
h_{TR}	Transition Height Distance	59	ft
S_{TO}	Total Takeoff Distance	2901 (sea level) 2896 (6000 ft)	ft

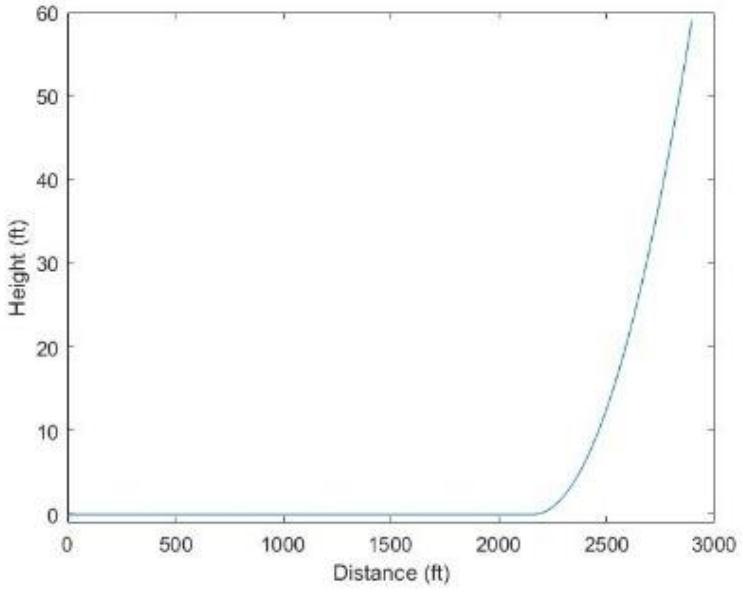

Fig. 25: Plot of the takeoff at sea level

Landing Analysis

The landing analysis includes the calculation of the distance covered between the beginning of the approach until the aircraft is stopped. It is comprised of four sections: approach, flare, free roll, and braking distance, which combined tells the total landing distance [2].

The velocity at approach, flare, and touchdown can be calculated as 1.2, 1.15, and 1.1 times the stall speed, respectively [2]. With a stall speed of 150 $\frac{ft}{s}$, this yields an approach, flare, and touchdown speed of 180 $\frac{ft}{s}$, 172.5 $\frac{ft}{s}$, and 165 $\frac{ft}{s}$ respectively. The approach angle, γ, and the radius of the transition arc, R, can be found using equations (98) and (99), respectively [2].

$$\gamma = \arcsin\left(\frac{T}{W} - \frac{1}{\frac{L}{D}}\right) * \frac{180}{\pi} \tag{98}$$

$$R = \frac{{V_{flare}}^2}{0.2g} \tag{99}$$

The acceleration due to gravity, g, is 32.2 $\frac{ft}{s^2}$. Using 0.1313 as $\frac{T}{W}$ and 14.34 as $\frac{L}{D}$, the approach angle was found to be 3.53 degrees and the radius of the transition arc was found to be 4620.5 ft. With these parameters, the flare height, h_{flare}, and distances covered during approach, $S_{approach}$, and flare, S_{flare}, can be found from equations (100), (101), and (102) [2].

$$h_{flare} = R(1 - \cos(\gamma)) \tag{100}$$

$$S_{approach} = \frac{h_{obstacle} - h_{flare}}{\tan(\gamma)} \tag{101}$$

$$S_{flare} = Rsin(\gamma) \tag{102}$$

Assuming an obstacle height at the beginning of the runway of 50 ft, the flare height is 8.76 ft, the distance covered during approach is 668.5 ft, and the distance covered during flare is 284.5 ft. The distance covered during free roll is simply the velocity at touchdown times the amount of time taken for the pilot to apply the brakes. Using 2 seconds as the delay between touchdown and braking, the free roll distance ($S_{free\ roll}$) is 330 ft [2]. To calculate the braking distance, the thrust and aerodynamic coefficients for braking, denoted as K_T and K_A respectively, must be found with equations (89) and (90). Then, the braking distance can be calculated as equation (103).

$$S_{braking} = \frac{1}{2gK_A} \ln\left(\frac{K_T + K_A V_f^{\,2}}{K_T + K_A V_i^{\,2}}\right) \quad (103)$$

Assuming the least desirable conditions of an austere field at 6,000 ft above sea level, the ground rolling resistance, μ, is 0.3, and the density, ρ, is 0.0725 lb/ft^3. The landing weight is estimated at 85% of the takeoff weight, or 9316 lbs, the coefficient of lift at landing, $C_{L,land}$, is 0.756, the zero-lift drag coefficient, $C_{D,o}$, is 0.02, and the drag due to lift factor, K, is 0.0545. The initial velocity for braking is the touchdown velocity and the final velocity after braking is 0 ft/s. K_T is -0.1687, K_A is 4.3586*10^{-9}, and the braking distance is 2506.8 ft. Combining $S_{approach}$, S_{flare}, $S_{free\ roll}$, and $S_{braking}$ yields a total landing distance of 3789.8 ft, 210.2 ft shorter than the mission requirement of 4000 ft (Table XXVI). A plot of the landing sequence is shown in Fig. 26.

Table XXVI: Landing Analysis Results

Symbol	Definition	Value	Units
$V_{approach}$	Aircraft velocity at approach	180.0	$\frac{ft}{s}$
V_{flare}	Aircraft velocity at flare	172.5	$\frac{ft}{s}$
$V_{touchdown}$	Aircraft velocity at touchdown	165.0	$\frac{ft}{s}$
γ	Approach angle	3.53	$degree$
R	Radius of transition arc	4620.5	ft
$h_{obstacle}$	Obstacle height at beginning of runway	50	ft
h_{flare}	Height at which the pilot flares	8.76	ft
K_T	Landing thrust coefficient	-0.1687	-
K_A	Landing aerodynamic coefficient	4.3586*10^{-9}	-
$S_{approach}$	Horizontal distance covered during approach	668.5	ft
S_{flare}	Horizontal distance covered during flare	284.5	ft
$S_{free\ roll}$	Horizontal distance covered during free roll	330.0	ft
$S_{braking}$	Horizontal distance covered during braking	2506.8	ft
$S_{landing}$	Total landing distance	3789.8	ft

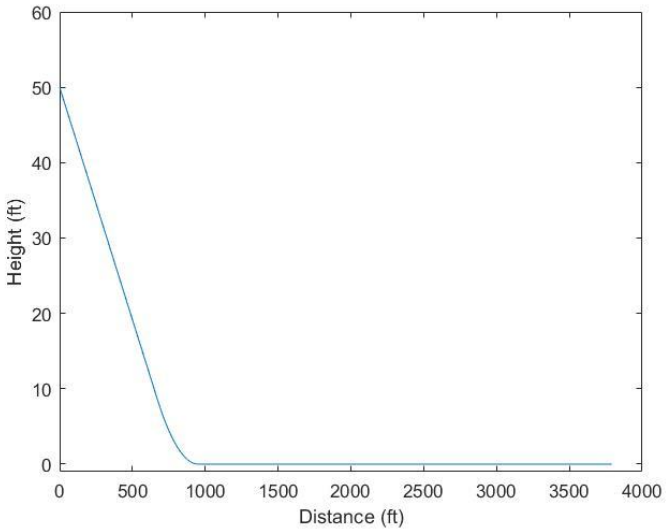

Fig. 26: Sabretooth landing plot

Operating Envelope

Developing the Operating Envelope for the UF-7 Sabretooth is necessary to understand how the plane will operate. The absolute ceiling, stall limit line, service ceiling line, and the max dynamic pressure limit was calculated.

To determine the absolute ceiling and service ceiling, it is important to consider equation (104).

$$P_s = V\left[\frac{T}{W} - \frac{qC_{D_0}}{\frac{W}{S}} - n^2\frac{k}{q}\frac{w}{s}\right] \tag{104}$$

The absolute ceiling was determined by setting $P_s = 0$. Using the equation for thrust due to power (105), the dynamic pressure equation, and the equation for pressure at a specific altitude with known air density (106), the velocity at each altitude was calculated to create the absolute ceiling line. P_{cr} and ρ_{cr} are known values from the cruise altitude of 25,000 ft.

$$T = \frac{P\eta_P}{V} \tag{105}$$

$$P_{alt} = P_{cr}\sqrt{\frac{\rho_{cr}}{\rho_{alt}}} \tag{106}$$

$$P_{cr}\sqrt{\frac{\rho_{cr}}{\rho_{alt}}}\eta_P - \frac{0.5\rho_{alt}V^3C_{D_0}}{\frac{W}{S}} - \frac{n^2KW}{0.5\rho_{alt}V^2} = 0 \tag{107}$$

The stall limit line is a line that shows what V_{stall} is at each altitude. If the plane is operating past this line, then it will not stall due to windspeed. To determine this, it is important to look at equation (108). V_{stall} was calculated

using the air density at different altitudes. The altitudes were plotted against the Mach number at that altitude, and this is what makes up the stall limit line.

$$W = L = \frac{1}{2}\rho S V_{stall}^2 C_{L_{max}} \tag{108}$$

$$V_{stall} = \sqrt{\frac{2W}{\rho S C}} \tag{109}$$

The service ceiling was calculated to be 32,339.87 ft. This was calculated by using the cruise speed of 472 ft/s and setting P_S = 0 ft/min in equation (104), because the Raymer book suggests 100 ft/min for a propeller aircraft [2] and solving for the dynamic pressure. Using the dynamic pressure, the altitude was calculated, with the result as the service ceiling. Each of the parameters used to compute this value are found in Table XXVII.

Table XXVII: Service Ceiling Calculation Parameters

Parameter	Value	Units
P_{25000}	880,000	$\frac{lbft}{s}$
ρ_{25000}	0.00107	$\frac{slugs}{ft^3}$
η_p	0.80	-
V	472 $\frac{ft}{s}$	$\frac{ft}{s}$
W	439,980.8 lbf	lbf
C_{D_0}	0.02	-
S	156.9 ft^2	ft^2
n	1	-
K	0.0545	-

The max dynamic pressure limit was calculated by determining the true airspeed at different altitudes based on the equivalent airspeed. The equivalent airspeed, EAS, is found as the maximum airspeed found in the V-N diagram, which is 660.8 ft/s. True airspeed, TAS, was calculated using equation (110). This true airspeed value was determined at different altitudes using the known air density at each altitude. This true airspeed value was then converted to Mach number using the known values for the speed of sound, a, at the specific altitude.

$$TAS = EAS\sqrt{\frac{\rho_{SL}}{\rho}} \tag{110}$$

Using each of the obtained lines, the complete operating envelope for the aircraft was plotted in Fig. 27. The absolute ceiling is the altitude for which the Ps = 0 line achieves a maximum, this happens to be at 35,560 ft. Additionally, the stall limit line approximation intersects the Ps = 0 approximation at a Mach number of 0.56 and at an altitude of 33,000 ft and intersects the maximum dynamic pressure line at a Mach number of 0.67 at an altitude of 6,000 ft.

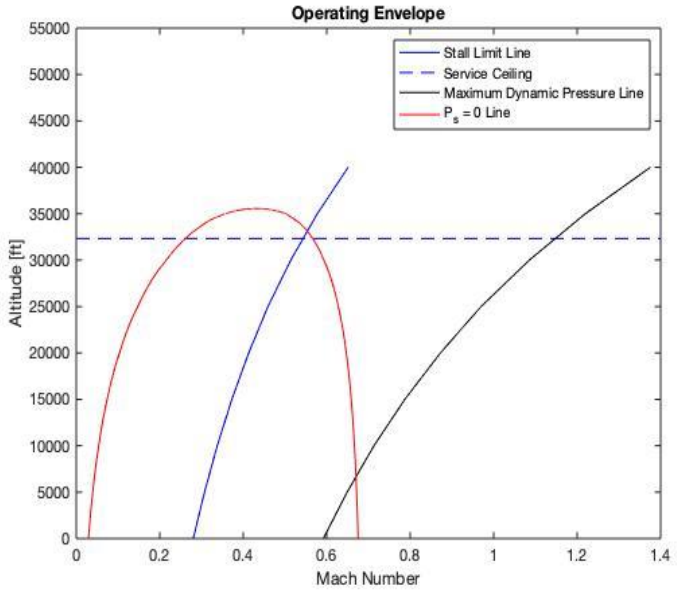

Fig. 27: Sabretooth Operating Envelope

CAD Drawings

To aid in the visualization and understanding of the vehicle, engineering drawings of the Sabretooth were generated. These drawings show areas of importance on the aircraft, such as the center of gravity, neutral point, and aerodynamic center. The moment arms for the horizontal and vertical stabilizers were also included. These drawings are included as Fig. 28 to Fig. 30 .

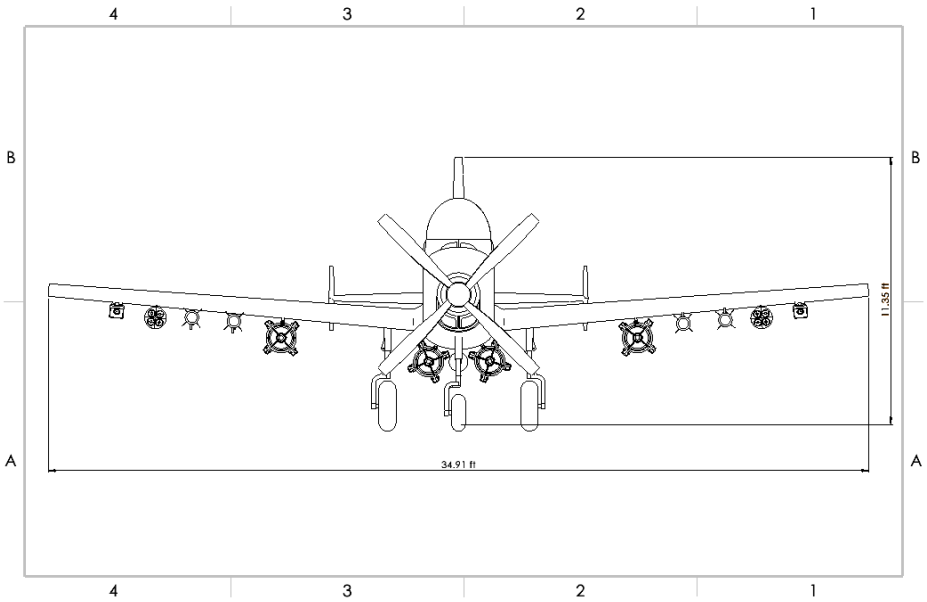

Fig. 28: Sabretooth CAD Drawing Front View

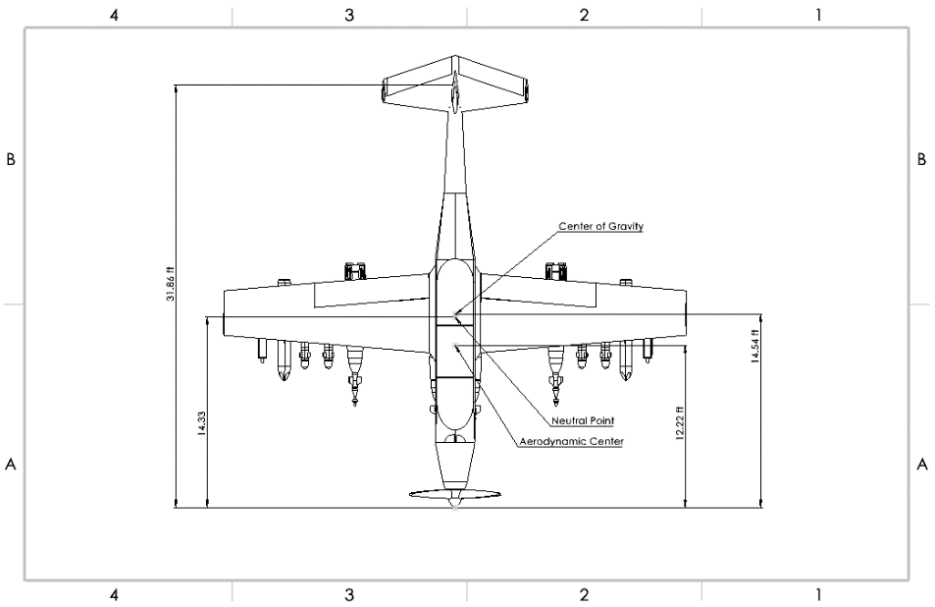

Fig. 29: Sabretooth CAD Drawing Top View

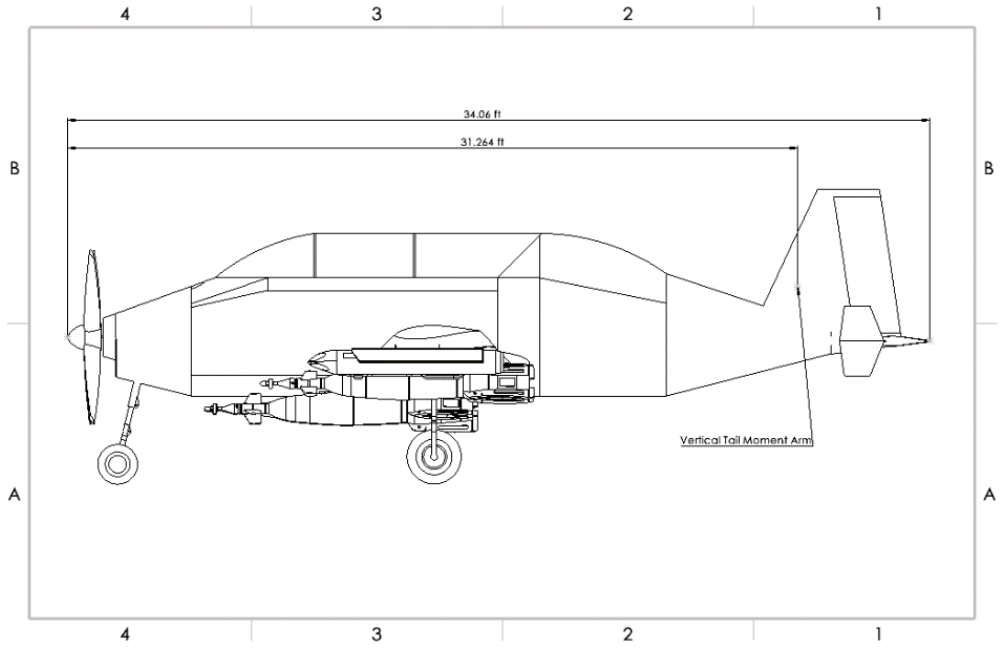

Fig. 30 : Sabretooth CAD Drawing Side View

XVI. Cost Analysis

RDT&E and Fly Away Costs

The Research, Development, Testing, & Evaluation (RDT&E) and fly away costs can be estimated using the RAND DAPCA IV cost estimation model found in the Raymer book [2]. The costs can be estimated using development hours and general development costs. This DAPCA IV cost estimation model is in 2012 dollars, so inflation was considered, and a 15% profit margin was applied to the final cost estimation value. The model was used to determine the cost of development of 50 separate units. The variables used in the equations for the model are tabulated in Table XXVIII. Turbine inlet temperature is given from the average turbine inlet temperature of the PT6A-68D and the avionics cost is estimated as $6000/lb of avionics, where the avionics is 16.18 lbs.

Table XXVIII: DAPCA IV Values

Variable	Definition	Value	Units
W_e	Empty weight	7,873.51	lbs
V	Maximum velocity	391.5133	kt
Q	Number to be produced in five years	50	-
FTA	Number of flight-test aircraft	3	-
N_{eng}	Total production quantity times number of engines per aircraft	50	-
T_{max}	Engine maximum thrust	3143.69	lbf
M_{max}	Engine maximum Mach number	.5919	-
$T_{turb_{in}} T_{turbine\ inlet}$	Turbine inlet temperature	547.83	$°R$
$C_{avionics}$	Avionics cost	$100,860	$

The equations used to estimate RDT&E and fly away costs are estimated using equations (111)-(119) using the wrap values found in Table XXIX. The wrap rates are hourly rates including direct employee salaries, employee benefits, overhead, and administrative costs. These values are in 2012 dollars, so inflation was considered in the final value. The RDT&E and flyaway costs were estimated to be $676,100,074.65 and $13,522,001.49 cost per unit.

Table XXIX: Wrap Rates

Value	Rate
R_E	$115
R_T	$118
R_Q	$108
R_M	$98

$$Engineering\ Hours = H_e = 4.86W_e^{0.777}V^{0.894}Q^{0.163} \quad (111)$$
$$Tooling\ Hours = H_T = 5.99W_e^{0.777}V^{0.696}Q^{0.263} \quad (112)$$
$$Manufacturing\ Hours = H_M = 7.37W_e^{0.82}V^{0.484}Q^{0.641} \quad (113)$$
$$Quality\ Control\ hours = H_Q = .133 \quad (114)$$
$$Development\ Support\ Cost = C_D = 91.3W_e^{0.630}V^{1.3} \quad (115)$$
$$Flight\ Test\ Cost = C_F = 2498W_e^{0.630}V^{0.822}FTA^{1.21} \quad (116)$$
$$Manufacturing\ Cost = C_M = 22.1W_e^{0.921}V^{0.621}Q^{0.799} \quad (117)$$
$$Engine\ Production\ Cost = C_{eng} = 3112[T_{max} + 243.25M_{max} + 0.969T_{turb-in} - 2228] \quad (118)$$
$$RDT\&E + flyaway = H_E R_E + H_T R_T + H_M R_M + H_Q R_Q + C_D + C_F + C_M + C_{eng} N_{eng} + C_{avionics} \quad (119)$$

Operations and Maintenance Costs

The operations and maintenance cost of the Sabretooth was based on completing 1,200 flight hours per year. The total operations and maintenance cost was estimated by adding the costs accrued in one year including the cost of fuel consumption, crew salary, and maintenance. Each of these components are an estimated percentage of the total operations and maintenance cost. Overall, fuel is assumed to total 15% of the operations and maintenance cost, whereas crew salary and maintenance total 35% and 50% of the operations and maintenance cost, respectively [2].

Fuel Costs

To begin, total fuel consumption per year was calculated which was then used to find the total cost of the fuel. To yield total fuel consumption per year, the specific fuel consumption of the engine *C*, total flight hours (1200), maximum horsepower of the engine HP_{max}, and the density of Jet A fuel at 50 degrees Fahrenheit $\rho_{Jet\ A}$, were utilized. (120). In this case, the specific fuel consumption of the engine is 0.628 $\frac{lb}{hp\ hr}$, and the density of the Jet A fuel is 6.78 $\frac{lb}{gal}$. The total cost was found simply by multiplying the total fuel consumption in gallons by the price of a gallon of Jet A fuel, $2.96 per gallon (121) [39]. Ultimately, this process yielded a total fuel cost per year of approximately $493,606.19.

$$Yearly\ Fuel\ Consumption = \frac{C * 1200 * HP_{max}}{\rho_{jet\ A}} \quad (120)$$
$$Yearly\ Fuel\ Costs = Yearly\ Fuel\ Consumption \cdot \$2.96 \quad (121)$$

Crew Salary

Several aspects were considered when determining the total cost of the Sabretooth crew. First, the ratio of crew members, *CR*, to aircraft was estimated as 1.1 [2]. Next, it was assumed the military would acquire the Sabretooth

in lots of 50. Furthermore, it was needed that each Sabretooth aircraft has two seats, therefore each aircraft will utilize two crew members while flying. To determine the total number of active crew members needed to operate the lot of 50 aircraft, each of the previous values were multiplied together (122). Overall, a total of 110 active crew members was obtained.

$$Active\ Crew = CR \cdot 50 \cdot 2 \tag{122}$$

After obtaining the number of active crew members, the total cost of the crew was obtained. To determine this cost, the total number of work hours as well as the labor wrap rate was needed. It was assumed, total working hours of the crew (including maintenance and engineering) totaled 2080 hours per year. This is 40 hours per week, for a year. Additionally, the engineering labor wrap rate was found to be $115 from Table XXIX. These values were then multiplied alongside the number of active crew members to yield the total crew cost per year (123). In the end, the cost for 110 active crew members per year yields $26,312,000.00.

$$Yearly\ Total\ Crew\ Cost = Active\ Crew \cdot 2080 \cdot \$115 \tag{123}$$

Now the crew salary was determined from the total crew cost. It was found that "employee salaries are a little less than half the wrap rate" [2]. This is, generally, because the wrap rate includes employee salary, benefits, overhead, and administrative costs [2]. As such, the combined salary of the 110 active crew members was determined to be 45% of the total crew cost. This yields a combined salary payout of approximately $11,840,400.00 per year. Additionally, dividing by the 110 active crew members yields a yearly salary of $107,640.00 per crew member.

Maintenance Costs

The final metric for determining the overall operations and maintenance cost was the total maintenance cost per year. Two values were important for this calculation: maintenance man hours per flight hour (MMH/FH) and the average hourly wage for a maintenance technician. In this case, for a military fighter aircraft, the typical value for MMH/FH was anywhere between 10 to 15. With that said, an average of 12.5 was selected for the Sabretooth. Furthermore, the average rate for a maintenance technician as of 2019 was approximately $30.92 per hour [40]. The total maintenance cost per year was obtained simply by multiplying the MMH/FH, wage rate, and total total flight hours for the service year, 1200 hours (124). This calculation yielded a total maintenance cost per year of $463,800.00.

$$Yearly\ Total\ Maintenance\ Cost = MMH/FH \cdot \$30.92 \cdot 1200 \tag{124}$$

Total Operations and Maintenance Costs

The operations and maintenance costs are a metric of how the aircraft is operated. Each of the previous costs are a roughly approximated component of the total operations and maintenance cost. To compute the total cost, 15% of the yearly fuel costs (YFC), 35% of the yearly crew salary (YCS), and 50% of the yearly maintenance costs (YMC) are summed (125). Following this process yielded a total operations and maintenance cost per year of $19,441,186.46. It is important to note, this value is for the complete lot of 50 aircraft with a total 1200 flight hours per aircraft per service year. As a result, this yields an operations and maintenance cost of $388,823.73 per year for a single Sabretooth aircraft with 1200 flight hours.

$$\textit{Yearly Operations and Maintenance Cost} = (0.15 \cdot YFC) + (0.35 \cdot YCS) + (0.50 \cdot YMC) \quad (125)$$

Miscellaneous Consumable Costs

The final components of the cost for the Sabretooth lie in consumable objects such as engine oil, tires, brakes, etc. In terms of engine oil, it was found that "oil costs average less than half a percent of total fuel costs and can be ignored" [2]. However, for the sake of accuracy, the total oil costs will be calculated. In this case, less than half a percent was taken to be 0.4 percent, or 0.004. This was then multiplied by the yearly total fuel costs to obtain the yearly total oil costs. In the end, this value came out to $2,468.00 for each Sabretooth per year. Furthermore, for the lot of 50 aircraft, the total yearly oil costs would be $123,400.00.

Aside from oil, the main consumable objects in aircraft maintenance are brake components and tires. Throughout research, very limited data was found referring to the cost of aircraft brakes and tires. It was found that, on average, aircraft brakes are replaced every 1,000 to 2,000 landings [41]. An estimate for the length of time it takes to complete the design mission with the Sabretooth aircraft is approximately 5.63 hours. If a service year consists of 1,200 flight hours, then approximately 213 flights are completed per year. This would mean each aircraft only utilizes one set of brakes per service year. In terms of cost, a complete set of brakes (12-piece set) for a Boeing 777 totals roughly $100,000. As a very rough approximation, given the much smaller scale of the Sabretooth compared to a Boeing 777 a value of $10,000 for each set of landing gear is an appropriate estimation. As such, the total cost of brakes for the lot of 50 aircraft is approximately $500,000.

Finally, the estimated cost for aircraft tires is needed. On average, aircraft tires cost between $15 and $5500 [42]. Using this estimation, one tire for the Sabretooth costs approximately $2,750.00 and three tires are used, totaling

$8,250.00 per aircraft per year. For the lot of 50 aircraft, tires will cost approximately $412,500.00. Furthermore, aircraft tires are typically replaced anywhere from 120 to 400 landings [43]. Previously assuming the Sabretooth runs a total of 213 flights per service year means two sets of tires will be needed per aircraft per year. This brings the total cost of tires to $825,000.00 per year for the lot of 50 aircraft.

Trade Studies

Trade studies allow engineers to compare different designs and see which design choice is best for the given application. In this report, trade studies were performed for the airfoil selection, engine selection, and material selection for the aircraft structure. The airfoil trade study, detailed in Table V, indicated that the NACA 63A415 would be the ideal airfoil for the Sabretooth, while the trade study performed in Table VII confirmed that the PT6A-68D is the best powerplant for the Sabretooth. The materials trade study, shown in Table XVIII, allowed the team to choose which sections of the plane should use a given material, such as AL-2024 for the wing box rather than composites.

Other aspects of the Sabretooth's design, such as propeller selection, wing vertical location selection, and tail geometry, were chosen as design parameters that shape the rest of the aircraft's design. The propeller in particular was chosen to be aluminum and made of 5 blades to be more resistant to potential damage than composites, with a diameter determined by the tip speed calculations (Eq. (24)) [2]. Tail selection was heavily influenced by the Raymer textbook. A conventional tail was chosen because it did not have any drawbacks in terms of clean air to the rear or weight compared to other tail designs. It was also chosen simply because "70% or more of the aircraft in service have such a tail arrangement" [2]. The conventional tail provides adequate stability and control at the lightest weight.

Sizing Matrix and Carpet Plots

A sizing matrix shows the effect of the variance of two parameters on other parts of the aircraft [2]. For the Sabretooth, the gross takeoff weight (W_o), excess power (P_s), and takeoff distance (S_{to}) were observed for changes in T/W and W/S of ±10%. As T/W and W/S were increased, so were the observed values (Table XXX). One of the effects of a sizing matrix is the determination of the lightest possible takeoff weight for a particular aircraft. For the UF-7 Sabretooth, it was found that a variant of the aircraft could theoretically weigh 8878 lbs at takeoff with an excess thrust of 24.1 ft/s and a takeoff distance of 1691 ft. Conversely, the heaviest configuration of the Sabretooth would weigh 13262 lbs, have 36.7 ft/s of excess thrust, and have a takeoff distance of 12069 ft.

Table XXX: Sizing Matrix

	W/S = 62.87 lb/ft^2	69.85	76.84
T/W = 0.114826	W_o = 8878 lbs P_s = 24.0984 fps S_{to} = 1691 ft	W_o = 9864 lbs P_s = 24.5177 fps S_{to} = 2309 ft	W_o = 10851 lbs P_s = 24.6132 fps S_{to} = 3129 ft
0.127585	W_o = 9865 lbs P_s = 30.1204 fps S_{to} = 2327 ft	W_o = 10960 lbs P_s = 30.5397 fps S_{to} = 2901 ft	W_o = 12057 lbs P_s = 30.6352 S_{to} = 4605 ft
0.140343	W_o = 10851 lbs P_s = 36.1424 fps S_{to} = 3148 ft	W_o = 12056 lbs P_s = 36.5617 fps S_{to} = 4641 ft	W_o = 13262 lbs P_s = 36.6572 fps S_{to} = 12069 ft

Using this information, a set of carpet plots can be formed. Carpet plots are created by plotting each data point to its respective W/S value, then connecting the values that have the same T/W. They can be used for visualizing the performance of the aircraft at different T/W and W/S settings (Fig. 31 to Fig. 33).

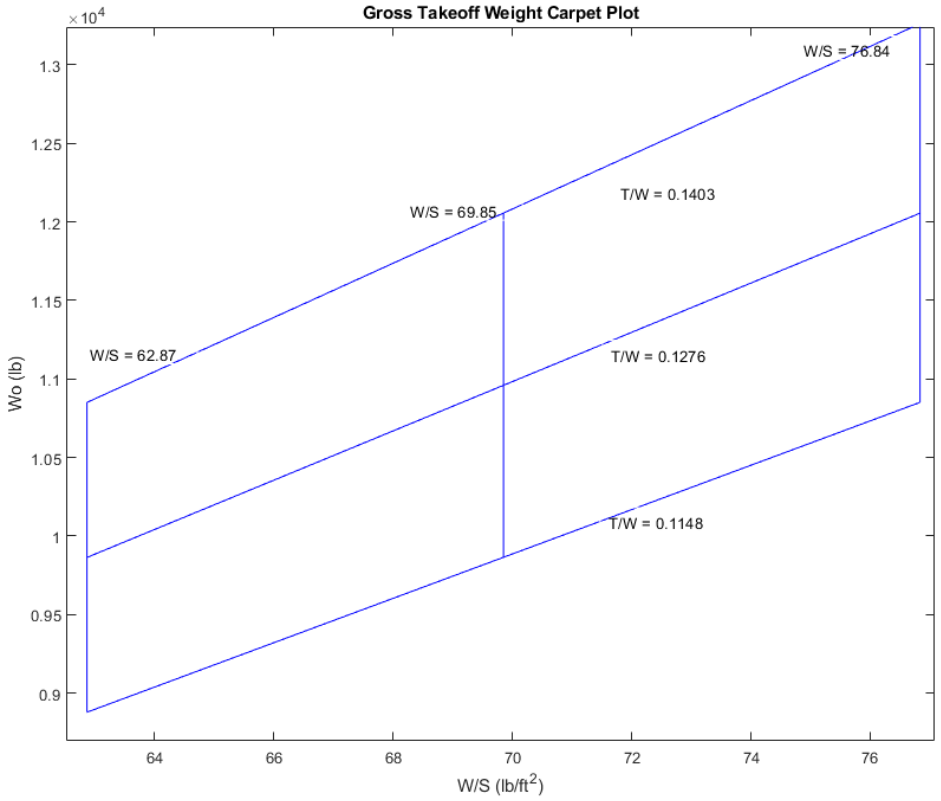

Fig. 31: Carpet plot of the Sabretooth for gross takeoff weight

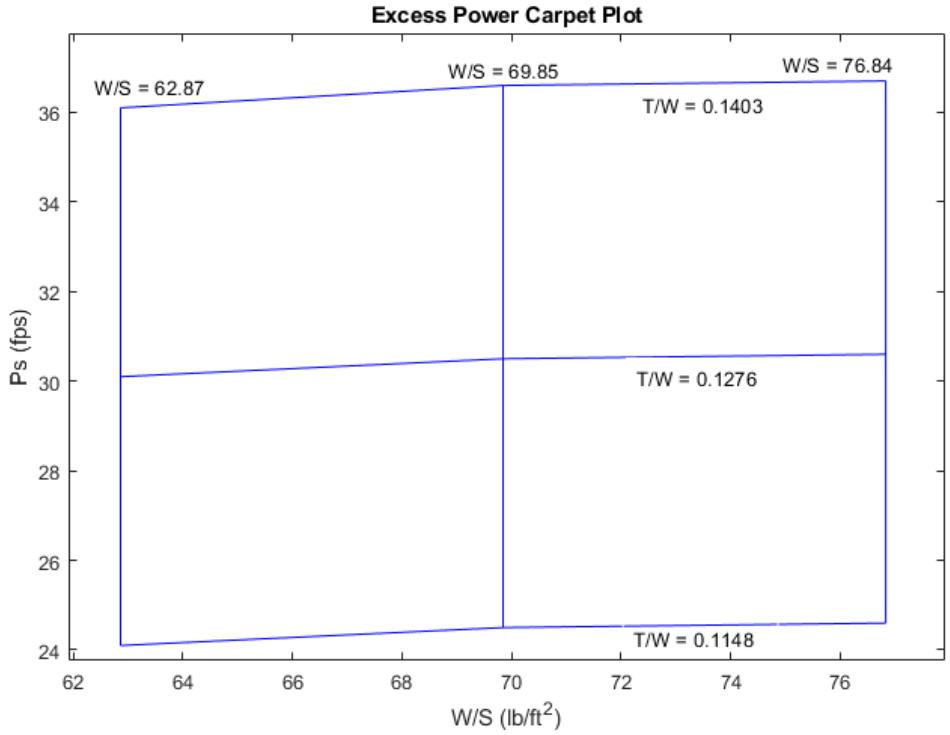

Fig. 32: Carpet plot of the Sabretooth for excess power

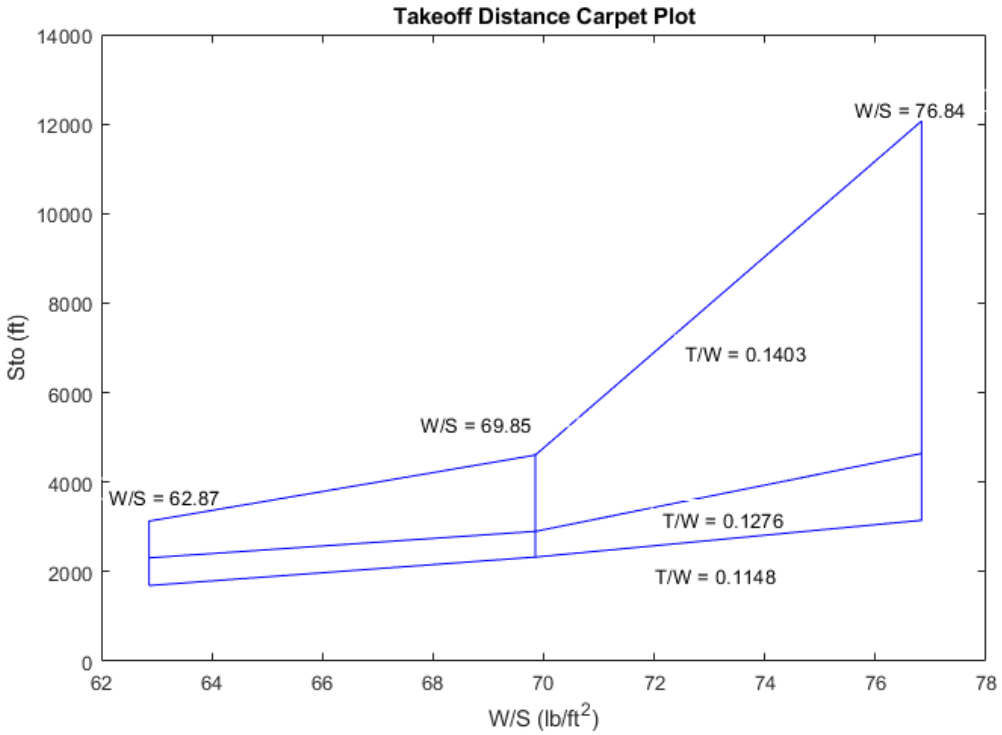

Fig. 33: Carpet plot of the Sabretooth for takeoff distance

XVII. References

[1] AIAA. (2021) *AIAA Undergraduate Team Aircraft Design RFP 2021* https://www.aiaa.org/get-involved/students-educators/Design-Competitions

[2] Raymer, Daniel P. *Aircraft Design: A Conceptual Approach Sixth Edition.* Playa del Ray, American Institute of Aeronautics and Astronautics, 2018.

[3] Beechcraft. (2021). *AT-6 Wolverine Light Attack.* Textron Aviation. https://defense.txtav.com/en/at-6

[4] Embraer. (2018). *Built For The Mission A-29 Specifications.* A-29. https://www.builtforthemission.com/a-29-super-tucano/a-29-specs/

[5] Federal Aviation Administration. (2018). *Volume 4 Aircraft Equipment and Operational Authorization, Chapter 3 Airplane Performance and Airport Data, Section 1 Safety Assurance System: Airplane Performance Computation Rules.* https://fsims.faa.gov/wdocs/8900.1/v04 ac equip & auth/chapter 03/04_003_001.htm

[6] "NACA 63A415 (naca63415-il)," Airfoil Tools. [Online]. Available: http://airfoiltools.com/airfoil/details?airfoil=n63415-il#polars. [Accessed: 01-Feb-2021].

[7] Engineering ToolBox, (2003). U.S. Standard Atmosphere. [online] Available at: https://www.engineeringtoolbox.com/standard-atmosphere-d_604.html [Accessed 25 Jan. 2021].

[8] Pratt and Whitney Canada Corp., Type Certification Data Sheet. Pratt and Whitney Canada Corp., Longueuil, Quebec, 2007. https://web.archive.org/web/20090910012845/http://www.tc.gc.ca/aviation/applications/nico-celn/en/getfile_inc.asp?x_lang=e&AFCflag=Y&doc_type=pdf&aprv_num=E-19&isu_num=44&isu_dt_start=2007-12-07+00%3A00%3A00&proj_num=070034 [Accessed 5 Feb. 2021].

[9] Teal Group Corporation (2020) *General Electric Catalyst.* [online] Available at: http://tealgroup.com/images/TGCTOC/sample-wpsba.pdf [Accessed 5 Feb. 2021].

[10] "Type Certificate Data Sheet EASA.IM.A.636 Textron Model 3000," European Aviation Safety Agency. [Online] Available at:

http://web.archive.org/web/20171220162942/https://www.easa.europa.eu/system/files/dfu/TCDS%20EASA%20IM%20A%20636%20Issue%201.pdf [Accessed 5 Feb. 2021]

[11] Pochari, Christophe. GrabCAD Community (2019) *Turboshaft/Turboprop* [online] Available at: https://grabcad.com/library/turboshaft-turboprop-1 [Accessed 7 Feb. 2021].

[12] "Data Section - Tires," *Goodyear Aviation*. [Online]. Available: https://www.goodyearaviation.com/resources/pdf/tire-specifications-6-2018.pdf. [Accessed: 17-Feb-2021].

[13] J. Roskam and C.-T. E. Lan, "Airplane Aerodynamics and Performance," Google Books. [Online]. Available: https://books.google.com/books?id=_FBLtC3qpr4C&pg=PA36&dq=fineness%2Bratio#v=onepage&q=fineness%20ratio&f=false. [Accessed: 25-Feb-2021].

[14] "Mk16 ejection seat For T-6 Texan II - MARTIN-BAKER," 09-Jun-2017. [Online]. Available: https://martin-baker.com/products/mk16-ejection-seat-for-t-6-texan-ii/. [Accessed: 27-Feb-2021].

[15] Through-canopy, For & Egress, Crew & Bement, Laurence. (2000). *Explosive Fracturing Of An F-16 Canopy For Through-Canopy Crew Egress.*

[16] E. Torenbeek, *Synthesis of subsonic airplane design: an introduction to the preliminary design of subsonic general aviation and transport aircraft, with emphasis on layout, aerodynamic design, propulsion and performance*. Dordrecht: Kluwer, 2010.

[17] "20mm Giat M621," Weaponsystems.net. [Online]. Available: https://weaponsystems.net/system/1009-20mm+Giat+M621. [Accessed: 27-Feb-2021].

[18] "Works 11: 20 mm Gun Offered for the Helicopters," Defence24.com. [Online]. Available: https://www.defence24.com/works-11-20-mm-gun-offered-for-the-helicopters. [Accessed: 27-Feb-2021].

[19] "M61A1/M61A2 20mm Gatling Gun Systems," General Dynamics Ordnance and Tactical Systems, 20-Jul-2018. [Online]. Available: https://www.gd-ots.com/armaments/aircraft-guns-gun-systems/m61a1/. [Accessed: 27-Feb-2021].

[20] “GAU-4 20mm Vulcan M61A1/M61A2 20mm Automatic Gun,” M61 20mm cannon. [Online]. Available: https://fas.org/man/dod-101/sys/ac/equip/m61.htm. [Accessed: 27-Feb-2021].

[21] Factsheets: GAU-8/A Avenger. [Online]. Available: https://web.archive.org/web/20100416063452/http:/www.nationalmuseum.af.mil/factsheets/factsheet.asp?id=1019. [Accessed: 27-Feb-2021].

[22] “Machine Gun Pods,” Machine Gun Pods | FN HERSTAL. [Online]. Available: https://www.fnherstal.com/en/product/machine-gun-pods. [Accessed: 27-Feb-2021].

[23] “FN® HMP400 Pod,” FN®. [Online]. Available: https://fnamerica.com/products/fn-airborne-pod-systems/fn-hmp400-pod/. [Accessed: 27-Feb-2021].

[24] “General Dynamics M134 Minigun,” Military Factory - Global Defense Reference. [Online]. Available: https://www.militaryfactory.com/smallarms/detail.asp?smallarms_id=243. [Accessed: 27-Feb-2021].

[25] A. Parsch, “Raytheon (Texas Instruments) Paveway II (GBU-10/B, GBU-12/B, GBU-16/B, GBU-17/B, GBU-48/B, GBU-49/B, GBU-50/B, GBU-51/B),” *Raytheon Paveway II*, 2006. [Online]. Available: https://www.designation-systems.net/dusrm/app5/paveway-2.html. [Accessed: 24-Feb-2021].

[26] “AGM-114 Hellfire,” *Military.com*, 2021. [Online]. Available: https://www.military.com/equipment/agm-114-hellfire. [Accessed: 24-Feb-2021].

[27] “Laser Guided Rockets”, 2021. [Online]. Available: https://elbitsystems.com/product/laser-guided-rockets/. [Accessed: 24-Feb-2021].

[28] Niu, M. C.-Y., Airframe structural design, SAE International, 1998

[29] S. Gudmundsson, “Chapter 4 - Aircraft Conceptual Layout.” 2014.

[30] “Aircraft Structure,” in *Pilot's Handbook of Aeronautical Knowledge*, *Federal Aviation Administration.* 24-Oct-2003. [Online]. Available: http://home.iitk.ac.in/~mohite/Aircraft_components.pdf. [Accessed 09-Mar-2021].

[31] "Types of Aircraft Construction (Part One)," *Flight Literacy*, 03-Apr-2020. [Online]. Available: https://www.flightliteracy.com/types-of-aircraft-construction-part-one/. [Accessed: 09-Mar-2021].

[32] "Aluminum Properties," EAI. [Online]. Available: https://www.experimentalaircraft.info/articles/aircraft-aluminum.php. [Accessed: 07-Mar-2021].

[33] "What Are the Benefits of Composite Propellers?," Hartzell Propeller, 19-Apr-2018. [Online]. Available: https://hartzellprop.com/benefits-of-composite-propellers/. [Accessed: 09-Mar-2021].

[34] A. A. D. Sarhan, "Research Gate," ResearchGate. [Online]. Available: https://www.researchgate.net/figure/S-N-curve-of-plain-fatigue-for-AL7075-T6_fig1_281624274. [Accessed: 09-Mar-2021].

[35] "GOE 411 Airfoil (goe411-il)," Airfoil Tools. [Online]. Available: http://airfoiltools.com/airfoil/details?airfoil=goe411-il . [Accessed: 12-Mar-2021].

[36] "Mission & Flight Critical Processors," Lockheed Martin. [Online]. Available: https://www.lockheedmartin.com/en-us/products/avionics-aircraft-modernization/mission-flight-critical-processors.html [Accessed: 15-Mar-2021].

[37] "What are fly-by-wire systems?," *BAE Systems | United States*. [Online]. Available: https://www.baesystems.com/en-us/definition/what-are-fly-by-wire-systems. [Accessed: 12-Mar-2021].

[38] C. McBaine, "Estimating Weight of Aircraft Electrical Wiring Systems" in *Society of Allied Weight Engineers*: *Procession of the 10th National Conference, St. Louis, Missouri, USA, May 21-24.*

[39] E. McCusker, "Memorandum for Under Secretary of Defense For Acquisition and Sustainment," Under Secretary of Defense. [Online]. Available: https://www.dla.mil/Portals/104/Documents/Energy/Standard%20Prices/Petroleum%20Prices/E_2019Oct1PetroleumStandardPrices_190928.pdf?ver=2019-09-30-072433-663 . [Accessed: 07-Apr-2021].

[40] "Aircraft and Avionics Equipment Mechanics and Technicians : Occupational Outlook Handbook," U.S. Bureau of Labor Statistics, 01-Sep-2020. [Online]. Available: https://www.bls.gov/ooh/installation-maintenance-and-repair/aircraft-and-avionics-equipment-mechanics-and-technicians.htm. [Accessed: 07-Apr-2021].

[41] "What You Should Know About… Aircraft Brakes". HYDRO, 28 Mar. 2019. [Online]. Available: www.hydro.aero/en/newsletter-details/what-you-should-know about aircraft-brakes.html. [Accessed: 07-Apr-2021].

[42] Odukoya, James, et al. "How Much Do Airplane Tires Cost? General, Commercial, and Military Aviation Tires." HighSkyFlying, 10 Apr. 2020, www.highskyflying.com/how-much-do-airplane-tires-cost-general-commercial-and-military-aviation tires/#:~:text=All%20airplane%20tires%20are%20sold, range%20from%20%2415%20to%20%245500.

[43] "What You Should Know About… Aircraft Wheels". HYDRO, 11 Dec. 2018, www.hydro.aero/en/newsletter-details/what-you-should-know-aboutaircraft-wheels.html#:~:text=Tires%20are%20changed%20every%20120,in%20the %20world's %20hottest %20regions.

[44] C.E. Lan and J. Roskam, *Airplane Aerodynamics and Performance.* Lawrence (Kan.): Design Analysis and Research Corporation, 2016.